2020

LANDSCAPE ECOLOGY AND POPULATION GENOMICS OF TWO SYMPATRIC PITVIPER SPECIES ACROSS A FRAGMENTED APPALACHIAN LANDSCAPE

Thomas Maigret

STUDENT AGREEMENT:

I represent that my thesis or dissertation and abstract are my original work. Proper attribution has been given to all outside sources. I understand that I am solely responsible for obtaining any needed copyright permissions. I have obtained needed written permission statement(s) from the owner(s) of each third-party copyrighted matter to be included in my work, allowing electronic distribution (if such use is not permitted by the fair use doctrine) which will be submitted to UKnowledge as Additional File.

I hereby grant to The University of Kentucky and its agents the irrevocable, non-exclusive, and royalty-free license to archive and make accessible my work in whole or in part in all forms of media, now or hereafter known. I agree that the document mentioned above may be made available immediately for worldwide access unless an embargo applies.

I retain all other ownership rights to the copyright of my work. I also retain the right to use in future works (such as articles or books) all or part of my work. I understand that I am free to register the copyright to my work.

REVIEW, APPROVAL AND ACCEPTANCE

The document mentioned above has been reviewed and accepted by the student's advisor, on behalf of the advisory committee, and by the Director of Graduate Studies (DGS), on behalf of the program; we verify that this is the final, approved version of the student's thesis including all changes required by the advisory committee. The undersigned agree to abide by the statements above.

Thomas Maigret, Student

Dr. David Weisrock, Major Professor

Dr. David Weisrock, Director of Graduate Studies

LANDSCAPE ECOLOGY AND POPULATION GENOMICS OF TWO SYMPATRIC PITVIPER SPECIES ACROSS A FRAGMENTED APPALACHIAN LANDSCAPE

DISSERTATION

A dissertation submitted in partial fulfillment of the
requirements for the degree of Doctor of Philosophy in the
College of Arts and Sciences
at the University of Kentucky

By

Thomas Arthur Maigret

Lexington, Kentucky

Co-Directors: Dr. David W. Weisrock, Professor of Biology

and Dr. John J. Cox, Professor of Forestry and Natural Resources

Lexington, Kentucky

https://orcid.org/0000-0002-6193-0207

ABSTRACT OF DISSERTATION

LANDSCAPE ECOLOGY AND POPULATION GENOMICS OF TWO SYMPATRIC PITVIPER SPECIES ACROSS A FRAGMENTED APPALACHIAN LANDSCAPE

Understanding the link between landscape patterns and ecological and evolutionary processes is an important prerequisite for informed wildlife conservation and management, especially in rapidly changing landscapes. Until recently, the inaccessibility of spatial and genomic data sets of sufficient resolution limited our ability to incorporate the impacts of landscape patterns into predictions of ecological and environmental outcomes. In this dissertation, I utilized several high-resolution spatial and genomic data sets to address ecological questions in a rapidly fragmenting landscape in southeastern Kentucky. Overall, my results indicate that large-scale surface coal mining is causing widespread homogenization of landforms, resulting in a uniquely permanent form of habitat loss. This is likely causing significant fragmentation of remain forested habitat in many portions of the Cumberland Plateau of Kentucky, as evidenced by reductions in suitable overwintering habitat for the timber rattlesnake (*Crotalus horridus*). At the level of the individual, the high resolution and three-dimensional imagery provided by lidar remote sensing systems allows for a much more accurate assessment of the drivers of individual movement in *C. horridus* than using coarse topographic data sets alone. While this fragmentation might be expected to limit migration and increase genetic differentiation among population, patterns of genomic diversity in another common pit viper, the copperhead (*Agkistrodon contortrix*), suggest that contemporary surface mining is not associated with spatial patterns of genomic diversity. However, using a 2,140 SNP data set, I did find significant associations between a historic highway path and divergent genomic patterns, suggesting a time lag may be responsible for contemporary genomic patterns associated with a historic barrier to movement. When examining the landscape at broad spatial scales, the topographic rearrangement of land after mining followed steady patterns until approximately 2011. At this point, coinciding with federal policy shifts aimed at reducing the frequency of valley fill operations, mining impacts in stream bottoms decreased markedly, but ridgetops and upper slopes continued to be impacted at rates equal to or greater than before 2011. I recommend topographic restoration be highlighted as a worthy goal of reclamation, on par with vegetation establishment and erosion control.

KEYWORDS: gene flow, mountaintop mining, habitat fragmentation, Crotalinae, lidar

Thomas A. Maigret

27 April 2020

Date

LANDSCAPE ECOLOGY AND POPULATION GENOMICS OF TWO SYMPATRIC PITVIPER SPECIES ACROSS A FRAGMENTED APPALACHIAN LANDSCAPE

By

Thomas Arthur Maigret

Dr. David W. Weisrock
Co-Director of Dissertation

Dr. John J. Cox
Co-Director of Dissertation

Dr. David W. Weisrock
Director of Graduate Studies

27 April 2020
Date

ACKNOWLEDGMENTS

This work was only possible through the assistance of many individuals, to whom I am very grateful. Certainly, I owe the greatest debt to my very patient wife Hillary, and next to my parents and siblings. Together they provided me with a solid foundation.

My co-advisors, Dr. John Cox, and Dr. David Weisrock should be lauded for the critiques, advice, and unrelenting support they offered across six years. The comments and encouragement of my dissertation committee members, including Dr. Catherine Linnen and Dr. Steven Price, was likewise critical, as was the input of other professors, most notably Dr. Jian Yang. Encouragement along the way from Dr. Carol Baskin, Dr. Nicholas McLetchie, Dr. Jeremiah Smith, Dr. Robin Cooper, and others is also appreciated. Along similar lines, the critiques and assistance of my fellow graduate students and postdocs was indispensable. This group includes but is not limited to Robin Bagley, Emily Bendall, Kim Vertacnik, Paul Hime, Kara Jones, Mason Murphy, Scott Hotaling, Mary Foley, Schyler Nunziata, Levi Gray, Katie Everson, Jim Shaffer, Brittany Slabach, Ben Cloud, Luc Dunoyer, Jacqueline Dillard, Derek Filipek, Kenton Sena, Zach Hackworth, Aviv Brokman, Jonathan Moore, and many others. Furthermore, field and lab assistance from Andrea Drayer, Nicolette Lawrence, Ricky Grewelle, Wendy Leuenberger, Allison Davis, Chris Osborne, and Cameron Bate was essential.

Another group of individuals also played an important role. My fieldwork was only possible due to the immeasurable depth of hospitality provided by residents of Breathitt, Perry, Knott, and Leslie counties. Though too numerous to fully list here, at a minimum this includes Erwin and Neva Williams, Ted and Flora Sizemore, David Collett, Grover Napier, Doran Howard, and RB and Anna Lee Combs. I cherish the time I've been able to spend with them. My experiences in eastern Kentucky between 2011 and 2020 transformed my worldview in ways I could not control and could not have possibly foreseen. I was led to a place I did not intend to visit.

TABLE OF CONTENTS

LIST OF TABLES

LIST OF FIGURES

CHAPTER 1: INTRODUCTION

1.1 Fragmented landscapes, evolutionary processes, and biodiversity conservation

Habitat loss is the most important driver of global biodiversity declines, and habitat loss is expected to accelerate in the 21st century (Wilcove et al. 1998, Haddad et al. 2015, Jantz et al. 2015). The process by which habitat suitable for a given species is replaced by unsuitable habitat typically occurs piecemeal, producing a mosaic of habitat and nonhabitat (Fahrig 2003). Thus while only a fraction of the total landscape may experience shifts in land cover or habitat quality, fragmentation of the habitat at the landscape scale may interfere with ecological and evolutionary processes that are important for populations to persist within remaining habitat fragments (Fahrig and Merrian 1994, Fahrig 2003). Discontinuities between patches of habitat often create interruptions in migration, which may subsequently reduce individual fitness within patches of remaining habitat (Keyghobadi et al. 2007). Even when patches of suitable habitat are structurally connected, movement of individuals and their alleles may be hampered due to behavioral, demographic, or ecological factors which affect mating, flowering, or movement of mature individuals. In this way, connectivity which is purely structural might be differentiated from connectivity which is functional and thus permits gene flow (Baudry and Merriam 1988, Taylor et al. 1993).

Testing for functional connectivity using traditional ecological field studies is not straightforward. Mark-recapture or telemetry studies can be informative, but may miss scant individuals that cross putatively suboptimal habitat. Quantifying functional connectivity amongst patches of habitat using neutral genetic markers can more

thoroughly inform management of fragmented populations and has become a major application of evolutionary biology though the recently developed sub-discipline of "landscape genetics" (Manel et al. 2003, Manel and Holderegger 2013). An amalgamation of landscape ecology and population genetics, landscape genetics seeks to understand how evolutionary processes affect wild populations by relating patterns of genetic differentiation and gene flow to landscape structure (Manel et al. 2003, Holderegger and Wagner 2008). Measuring genetic structuring in a fragmented landscape can shed light on important factors such as population subdivision, relative permeability of landscape features, and genetic diversity among habitat fragments. This information can subsequently be incorporated into management plans or placed within the framework of deeper empirical research (Segelbacher et al. 2010).

The loss of genetic diversity in small and isolated populations is a major concern for conservation biologists (Reed and Frankham 2003, Spielman et al. 2004, Frankham 2005). Traditionally, it has been thought that as large and contiguous populations are broken up into smaller isolated populations due to habitat fragmentation, genetic diversity is likely to be lost due to counteracting effects of inbreeding and genetic drift (Soule et al. 1987, Willi et al. 2006). Inbreeding increases homozygosity, which allows previously hidden deleterious recessive traits to undergo purifying selection, which further reduce population size and presumably increases the likelihood of future inbreeding on top of increased effects of drift due to the shrunken population size (Gilpin and Soule 1986). Increasing gene flow into these small populations can move populations off this pathway to potential extinction by replacing genetic diversity, in addition to other demographic benefits of higher population size such as buffering against stochastic events (Lande

1988). However, selection is known to overpower drift in very small populations (Koskinen et al. 2002), at times preserving genetic diversity through putative balancing selection in both wild and experimental populations (Aguilar et al. 2004, Fraser et al. 2014, Schou et al. 2017). Furthermore, while gene flow is often taken as universally beneficial in landscape genetics literature (Richardson et al. 2016), genetic connectivity may be burdensome for some populations due to migration of maladaptive alleles and the potential for disease or invasive species to spread via movement corridors (Frankham et al. 2011, Simberloff et al. 1992).

Regardless of the effect, however, quantifying functional connectivity remains a major application of evolutionary biology and landscape ecology. Properly identifying drivers of gene flow, mechanisms which reduce functional connectivity, and the landscape-level genetic implications of connectivity loss is an important perquisite for the development of informed wildlife conservation strategies (Frankham et al. 2017), and is likely to only become more important as habitat loss appears poised to accelerate throughout the 21st century (Jantz et al. 2015).

1.2 Advances in data generation and the future of landscape genetics

New tools and technologies have been key to the rise of landscape genetics (Manel et al. 2003, Holderegger and Wagner 2008). With the advent of molecular techniques, much more accurate estimates of migration, genetic differentiation, and genetic diversity became possible, immensely increasing the potential for evolutionary

principles to inform conservation and management of wild populations (Koenig et al. 1996, Gibbs and Weatherhead 2001, Manel et al. 2003, Manel and Holderegger 2013). However, our ability to use genetic information for purposes such as population delineation and assignment of individuals to putative populations is highly dependent on the type and number of genetic markers employed in the analysis. Recent developments in reduced-representation sequencing, especially methods which can be applied to nonmodel organisms (e.g., Peterson et al. 2012), have greatly improved our ability to quantify genetic differentiation and to thus examine the associations between landscape and ecological factors and genetic structure of wild populations. Parallel to the advances in generating genetic data sets has been the rapidly expanding accessibility of geospatial data (Porter et al. 2012, Neumann et al. 2015). The development of accurate, high-resolution elevation, vegetation, and landcover data sets via satellite and aircraft-mounted equipment has permitted the testing of a broad array of hypotheses regarding landscape effects on gene flow, and has allowed for the formulation of proactive management planning across a variety of landscapes (e.g., Milanesi et al. 2017).

While rapidly increasing genetic and geospatial data sets have aided our ability to answer fundamental questions about the geographic arrangement of genetic diversity, many key areas have yet to be thoroughly examined (Balkenhol et al. 2016). These unexplored topics include temporal factors surrounding habitat fragmentation and genetic differentiation, the three-dimensional nature of habitat suitability and habitat loss, and potential strategies for understanding and mitigating habitat loss using newly accessible data sets. The landscape of central Appalachia in the eastern US is an optimal location for exploring these issues.

1.3 Surface mining and forest fragmentation in central Appalachia

Central Appalachia contains one of the most biodiverse temperate forests on Earth (Ricketts et al. 1999, Hinkle et al. 2003), and has been a major source of coal for the eastern US since the early 20th century (Bernhardt and Palmer 2011). Since c. 1975, surface mining has gradually replaced underground methods of coal extraction, and today the majority of coal reserves in central Appalachia are recoverable only by surface mining (US EIA 2015). Surface coal mining, which often takes the form of so-called "mountaintop removal", involves the removal of all flora, fauna, soil, subsoil, and bedrock strata overlying the targeted coal seam. The material which is removed, termed "overburden", is deposited into nearby stream valleys creating what are often called "valley fills". As a result, the surface mining process typically replaces mature forest with a flattened, denuded landscape devoid of the preexisting soil, subsurface structure, native vegetation, and hydrologic networks (Zipper et al. 2011). While only a fraction of the landscape is typically mined, the horizontal stratigraphic layout of coal seams, especially in high relief terrain, results in a patchwork of minelands separated by blocks of largely undisturbed forest, which increases the fragmentation of remaining forest even when a relatively small proportion of the land surface is mined (Wickham et al. 2007)..

Beyond Appalachia, surface mining is becoming an increasingly popular method of resource extraction, with major consequences for habitat loss (Palmer et al. 2010, Yang 2013). The effects of surface mining and reclamation on aquatic fauna are serious and well-documented (e.g. Lindberg et al. 2011), but the effects on terrestrial fauna, in

Appalachia or elsewhere, are poorly understood (Wickham et al. 2013). This is especially true from a habitat fragmentation perspective: despite surface mines occupying more than 20% of the land surface in some eastern Kentucky counties, the effects on gene flow among forest fragments has never been examined (US GAO 2009, Wickham et al. 2013).

1.4 Relevant life history traits of the two study species

To study the consequences of this rapidly changing landscape on ecological and evolutionary processes, I am focusing on the spatial ecology of two sympatric pitviper species, *Agkistrodon contortrix* and *Crotalus horridus*, inhabiting a formerly continuously forested Appalachian landscape now punctuated by large-scale surface coal mines and related infrastructure. Both species are well-suited study organisms for understanding the effects of habitat fragmentation. Both *A. contortrix* and *C. horridus* are forest-associated predators that require large territories for foraging, characteristics associated with sensitivity to habitat fragmentation (Holt et al. 1999, Davies et al. 2000, Ewers and Didham 2006, Keinath et al 2017). Moreover, their low dispersal capabilities, general philopatry, and site fidelity to thermal resources important for overwintering predispose them to fine-scale genetic structuring and have made them attractive study systems for landscape genetics research (Reinert 1993, Gibbs and Weatherhead 2001, Clark et al. 2008, Clark et al. 2010). Specific to my research goals, *A. contortrix* and *C. horridus* exhibit a strong association with undisturbed, mature deciduous forest, and both have been shown to be susceptible to habitat loss elsewhere in their range (Ernst and Ernst 2003, Clark et al. 2010, Steen et al. 2014, Bushar et al. 2015, Carter et al. 2015).

1.5 Overview of empirical chapters

In the first empirical chapter of my dissertation, I explore the three-dimensional effects of surface coal mining on the topographically-influenced ecological communities of the Cumberland Plateau of Kentucky. By modeling the overwintering habitat preferences of a native pit viper, the timber rattlesnake, *Crotalus horridus*. I examine how surface mining is causing habitat loss not only directly through deforestation, but also through topographic homogenization. I further explore how landcover has shifted between 1992 and 2011 across different topographic positions. This chapter was recently published in Frontiers in Ecology and the Environment, and therefore is formatted according to that journal's guidelines.

In the next chapter, I use a genomic data set to assess the influence of landscape features on genetic dissimilarity in a different native pit viper, the copperhead, *Agkistrodon contortrix*. Here, while I found no evidence for genetic isolation resulting from spatial patterns of surface mining or contemporary highway networks, I did find that the path of a historic highway corresponded remarkably well with patterns of genomic differentiation. By subsampling my data set, I explored effects of data set size and data quality on my results. This chapter was recently published in the journal Molecular Ecology, and is formatted accordingly.

I also tested for the influence of a major federal policy shift on the topographic patterns of surface mining in the Cumberland Plateau of Kentucky. By examining annual patterns of new mining between 1986 and 2018 in conjunction with historic and recently

developed elevation data sets, I found a significant decrease in valley fills coinciding with a 2010 Obama administration federal policy reformulation. Despite reduced impacts of mining on stream valleys, my results indicate that, as an unintended consequence, ridgetops may be absorbing more mining activity as a result. This chapter is formatted for submission to a Nature Group journal.

In my final empirical chapter, I use high-resolution remote sensing imagery to test for fine-scale factors affecting thermoregulation in *Crotalus horridus*. Using linear mixed models, I found support for a strong, negative effect of vegetation height on the difference between air and internal body temperatures in *C. horridus*. My results suggest that a natural buffering capacity present in complex, three-dimensional forest habitats may allow some ectotherms to thermoregulate efficiently under diverse thermal regimes. This chapter is not yet formatted for any specific journal.

CHAPTER 2:

PERSISTENT GEOPHYSICAL EFFECTS OF MINING THREATEN RIDGETOP BIOTA OF APPALACHIAN FORESTS

2.1 Abstract

Surface coal mining can permanently alter the rugged topography of Appalachia, which plays an important role in creating and maintaining the structure, composition, and diversity of the region's ecological communities. We used remote-sensing datasets to characterize the past and future topographic impacts of surface coal mining on the mixed-mesophytic forests of eastern Kentucky. To provide context, we examined the consequences of widespread topographic rearrangement for an imperiled ridgetop-associated predator, the timber rattlesnake (*Crotalus horridus*). We found that surface mining disproportionately impacts ridgetop habitats, causing large reductions in the suitable habitat for *C. horridus* and likely other ridgetop- dependent biota. Land permitted for surface mining is also concentrated in high topographic positions, thus patterns of habitat loss are likely to remain concentrated in these ecosystems. These permanent topographic shifts complicate restoration of preexisting microhabitats, creating homogenized landscapes, threatening long-term ecosystem health, and charting a new course towards less diverse ecological communities.

2.2 Introduction

For over a century, coal mining has provided a source of income for many communities in the Appalachian region of the eastern US. However, this process has caused landscape-level habitat loss and fragmentation of the forests that cover the

region's mountains and foothills (Wickham et al. 2007). Mixed-mesophytic forests of central Appalachia display striking complexity, and are among the most biodiverse temperate forests on Earth (Hinkle et al. 1993, Ricketts et al. 1999). Much of this diversity is owed to a number of topographically-driven gradients which promote unique microhabitats and associated forest communities (Braun 1950, Whittaker 1956, Overstreet 1984). Narrow ridgetops, steep-sided slopes, and narrow, low-order stream valleys create a highly dissected landscape of tightly packed ridges and hollows, where interactions among aspect, slope, topographic position, and other factors result in variation among temperature, moisture, solar radiation, soils, and coarse woody debris density (Muller 2003). The commensurate rapid turnover of species across short spatial scales elevates beta diversity in canopy trees (Muller 1982), herbaceous flora (McEwan and Muller 2011), and a wide collection of fauna (Kiser and Meade 1993, Ford et al. 2002, Krupa and Lacki 2002, Wood et al. 2006, Newell and Rodewald 2011).

Although recently in decline due to increased competition from alternative energy sources, surface coal mining remains a popular method of coal extraction in central Appalachia and elsewhere. Much of the remaining Appalachian coal reserves, and a majority of the coal reserves in eastern Kentucky, are only accessible by surface mining (US EIA 2015). The surface mining process begins with the clearing of all vegetation, typically mature forest, in addition to topsoil and subsoil. Explosives are used to remove any overlying bedrock, providing direct access to the coal seams. The overlying rock, vegetation, and soil are disposed of by reconstructing local topography or by filling adjacent headwater stream valleys. Compliance with the 1977 Surface Mine Control and Reclamation Act (SMCRA) requires the "approximate original contours" (AOC) be

reestablished after mining has ceased. However reproducing AOC are often difficult due to stability issues and volume differences between fragmented and intact rock (Copeland 2015). In addition, SMCRA allows for exceptions from this requirement in situations where beneficial post-mining land uses could compensate for the adverse effects of not returning the land to AOC (OSM 2000). Such waivers are often granted to "mountaintop removal mining", a specific form of surface mining at or near ridge or mountain peaks. Other types of surface coal mining (such as contour mining) occurring on steep slopes have also taken the advantage of this AOC variance, and while not strictly defined as "mountaintop removal", these forms of mining may also result in significant changes to topography. After mining, land is typically reclaimed by tightly packing remaining rock fragments using heavy equipment and sowing of alien (primarily) and native grasses, legumes, and sometimes planting trees and shrubs to immediately establish vegetative cover and reduce erosion. Consequently, reclaimed minelands are usually dominated by non-native vegetation, and lack the soil and substrate heterogeneity which typified the previous environment. Natural succession is often severely arrested due to soil compaction, and regrowth of native forest without significant restoration is unlikely (Zipper et al. 2011). As of 2005, approximately 5700 km^2 of forest had been converted to surface mine, and over 3200 km of streams had been buried throughout Appalachia (EPA 2005, Bernhardt and Palmer 2011)

While the impacts of surface coal mining on aquatic ecosystem function and biodiversity have been studied, the terrestrial implications remain less well understood. Wickham et al. (2007) found large decreases in interior forest as a result of mining, and Wickham et al. (2013) speculated that impacts could be major for terrestrial biodiversity,

especially for ecological communities occupying upper slopes and ridgetops. Recent research on 3-dimensional topographic effects of mining on aquatic ecosystems has documented changes in slope distributions across wide areas, driven by the lowering of mountain peaks and filling of headwater stream valleys (Ross et al. 2016). These deep and lasting topographic impacts are markedly different from more common drivers of habitat loss such as deforestation or urbanization, and require very different approaches for restoration.

This homogenization of topographically-driven microhabitats is a major obstacle to ecological restoration efforts, notwithstanding more localized soil remediation and reforestation efforts. The extent and specific consequences of mining for the topographically-driven biodiversity of central Appalachia, however, remains unexamined. We examined patterns of surface coal mining and consequences for terrestrial biodiversity across the Cumberland Plateau (CP) of eastern Kentucky in three ways: (1) by comparing newly constructed pre-mining and post-mining geospatial datasets to quantify impacts on topographically-restricted terrestrial ecological communities, (2) by examining similar patterns in land permitted for surface mining, and (3) by estimating the impact of past and future mining on overwintering habitat of the timber rattlesnake (*Crotalus horridus*), a focal species we used to demonstrate the potential consequences for an imperiled ridgetop-dependent species. Our results allow for speculation and further analyses into the persistent effects of mining and suggestions for policy development, and for future projections based on mine permitting trends.

2.3 Methods

2.3.1 Study Area

Our study focused on the 14,021 km^2 Cumberland Plateau (CP) in eastern Kentucky. Both a physiographic province and an ecoregion, the CP in Kentucky is characterized by horizontal Pennsylvanian sandstone, shale, and coal bedrock, steep-sided low hills, narrow ridgetops and narrow headwater stream bottoms. Specifically for our *C. horridus* habitat modeling, we relied on hibernacula obtained through radio-telemetry conducted in the University of Kentucky's Robinson Forest (RF, 5267 ha) located in Breathitt, Knott, and Perry counties, Kentucky. Elevations at RF varied from 243–500 m, and the topography and vegetation is typical of the CP (Overstreet 1984).

2.3.2 Spatial Analyses of Mining

We analyzed patterns of surface coal mining across the CP using a number of independent spatial datasets. No map displaying active and reclaimed surface mines in the CP is available publicly, thus we constructed one using USGS National Landcover Datasets (NLCD) from 1992 and 2011 in concert with satellite imagery and mining permit data (Vogelmann et al. 1992, Homer et al. 2015). Specifically, we focused on land within permit boundaries falling into landcover classes which are common among reclaimed minelands. These included bare rock, strip mines, open water, and transitional land for the 1992 NLCD dataset, and barren land, grassland/herbaceous classes, and open water when we examined the 2011 NLCD dataset. Landcover classes which were uncommon among reclaimed minelands, such as urbanized lands, row crops, or shrubland, were not included in our analysis. This resulted in a layer of mined (mines >

10 ha) and unmined land surface across the study area, which was used as a dichotomous mined/unmined filter for later analyses. We examined patterns of mining related to topographic position index (TPI), defined as a value based on proximity to the lowest or highest point with a local (1 km, circular) window. Using TPI instead of elevation allows for consistent comparisons between local ridgetops and valley floors regardless of gradual elevation changes across the study area by generating values tied to local topography. We generated TPI values using the Land Facet Analysis extension (Jenness Enterprises, Flagstaff, AZ) based on a pre-mining (c. 1980) USGS DEM raster and a post-mining (2013-2015) DEM raster created by the Kentucky Division of Geographic Information. Since the DEMs we used to generate TPI values were collected at different times and with different methods, we standardized TPI values using z-scores by using the formula:

$$z = \frac{x - \mu}{\sigma}$$

where z equals the standardized TPI z-score, x represents each TPI measurement, and μ and σ represent the mean and standard deviation of each TPI grid, respectively (Jenness 2006). Conversion to z-scores creates a common scale of measurement whereby the mean is zero and standard deviation is 1. However, the distribution of the data remain unchanged, thus z-scores are useful for comparing the distributions of datasets where the measurement scales may differ. We topographically categorized the output TPI raster values as valley floor, lower slope, middle slope, upper slope or ridgetop based on pre-mining one-fifth quantiles, and then conducted a likelihood ratio test (G-test) in JMP 10

(SAS Institute, Inc, Cary, NC, USA) to test whether certain topographic classes were mined or permitted for mining more frequently than expected due to chance. We augmented our mining analyses by using a dataset of active surface mining permits obtained from the Kentucky Division of Mine Permits (KDMP), current as of January 2017. Lands under active permit are currently being mined, approved for mining, or currently being reclaimed. We filtered land undergoing secondary mining ("re-mining") out of our permit-focused analyses.

We also quantified land subjected to elevation reduction associated with surface mining. We compared historic USGS DEMs from c. 1980 to a recently developed (2013-2015) DEM layer created by Kentucky's Aerial Photography and Elevation Data (KYAPED) program generated from LiDAR remote sensing imagery, similar to the methods of Ross et al. (2016). This LiDAR dataset covered 66.1% of the study area, and cell size was converted from 1.5m resolution to 30m to match the historic USGS data resolution. We then subtracted the 2013-15 layer from the pre-mining raster and filtered this surface for elevation losses >10 m within mined land only, thus removing small and/or confounding sources of elevation loss (e.g., highway construction). To quantify changes in landscape position and forest cover, we created temporal transition matrices between both our five topographic classes and relevant NLCD cover classes. We used our pre- and post-mining elevation datasets to quantify topographic changes, and compared 1992 and 2011 NLCD datasets to compare landcover class changes. Due to changes in how NLCD classified forest types between the 1992 and 2011 datasets, we pooled Mixed Forest, Deciduous Forest, and Evergreen Forest into a single "All Forest" category.

2.3.3 Focal Species

To give context to the impacts of ridgetop habitat loss, we examined consequences for the timber rattlesnake (*Crotalus horridus*). A large-bodied pitviper native to the eastern U.S. and southern Ontario, populations of *C. horridus* are believed to be decreasing (Hammerson 2007). *C. horridus* was extirpated from four states and provinces in the 20th century, and is endangered or threatened in 13 US States. In Kentucky, *C. horridus* is under no state protection, but is listed as a "species of greatest conservation need (SGCN)". *C. horridus* plays an important predatory role in forest ecosystems, having the potential to control small mammal populations and perhaps subsequently influence disease dynamics (Clark et al. 2002, Kabay et al. 2013). Though loss of mature forest habitat imperils *C. horridus* populations generally, management is often focused on conservation of hibernacula, where snakes overwinter and to which individuals display intense site fidelity (Brown 1993). Especially in regions where *C. horridus* and other pitvipers overwinter communally, destruction of hibernacula can be expected to result in the instant elimination of whole populations, often by directly killing hibernating individuals.

Between 2012 and 2015, we individually captured 17 adult *C. horridus* at RF. All snakes were transported to a nearby veterinary facility for surgery, which largely followed the methods of Reinert and Cundall (1982). We first used L.L. Electronics model LF1 transmitters but later switched to Advanced Telemetry Systems (ATS, Isanti, MN, USA) models R1535, R1540, and R1680. Animals were held briefly after surgery to ensure wound closure prior to being released at the precise point of capture, upon which tracking began immediately. Snakes were tracked continuously until they entered their

hibernacula in the fall, after which they were immobile until emerging in spring. Hibernacula sites generally consisted of rock crevices and small talus piles, typically encompassing between 0.5 and 10 m^2. Snake handling and processing were approved under University of Kentucky IACUC Protocol 2012-0954.

We used a Mahalanobis (D^2) statistic to model potential hibernacula sites for *C. horridus* across the CP. D^2 approaches are frequently used for habitat modeling with presence-only data, and have been used to quantify habitat suitability and separate suitable habitat from non-habitat for numerous taxa based on recent or historical presence records (Clark et al. 1993, Buehler et al. 2006). We relied on both natural history literature (Brown 1993) and previous partitioned D^2 model-based findings for *C. horridus* (Browning et al. 2005) to select relevant predictor variables of occupancy; thus we used slope (deg), topographic position index (TPI), winter solar radiation (Wh/m^2), and aspect (degrees from south, 0-180) as our inputs. Slope, aspect, and winter solar radiation values were generated via the appropriate tools in ArcMap 10.1 using a pre-mining 30m resolution USGS DEM. After creating our input variable layers, we generated our D^2 raster surface again using the Land Facet Analysis extension and our 17 hibernacula locations. We then obtained the 17 D^2 values of our hibernacula locations from our raster surface and bootstrapped to create 90%, 95%, and 99% confidence intervals using R.3.3.0 (boot library, R statistical language, Canty 2005).

2.4 Results

Approximately 963 km^2 (6.9%) of the CP in Kentucky was classified as mined as of 2011, and a further 709 km^2 (5.1%) was unmined as of 2011 but is under active mining

permits as of January 2017 (WebTable 1(a)). Across the entire study area, mining removed disproportionately more ridgetop (281 km^2, 29.2% of total mined, 10.0% of total ridgetop habitat in CP) than other topographic positions, a highly significant difference ($G = 637.9$, $p < 0.0001$) (WebTable 1(a), Figure 1 (a)). Accordingly, permits covered substantially more ridgetop (191 km^2, 6.8% of total ridgetop habitat in CP) than other topographic positions ($G = 287.8$, 26.9% of permitted land, $p < 0.0001$) (Figure 1(b)). Our transition matrices show substantial shifting of topographic classes and landcover (WebTable 1(b), (c)). Roughly half of mined land was moved to different topographic positions than their pre-mining topographic position classes, though much of this movement was to adjacent classes. Middle and upper slopes were most likely to retain their position, whereas lower slopes and valley floors shifted classes most frequently. Areas which experienced elevation reduction had elevated TPI compared to the CP as a whole (WebFigure1). In terms of landcover transition, the vast majority of land (93.5%) classified as strip mines in 1992 remained strip mines or became classified as grassland in 2011. Only 7.3% of 1992 surface mines had returned to forest class by 2011 (WebTable 1(c)). However, areas classified as various "forest" types by the NLCD due to canopy closure since mining ceased may not be similar to the preexisting mixed-mesophytic forest community. While 11.6% of forested land was classified as forest in both 1992 and 2011, these raster cells are located around the periphery of irregularly-shaped mine polygons, and most likely represent boundary fluctuations between our raster and shapefile layers.

Mean input variable statistics for our 17 *C. horridus* hibernacula sites (WebTable4) were substantially though not significantly different from the mean values

for the study area at large. Hibernacula sites had higher mean TPI (26.8 m above local mean) and winter solar radiation (5.5 x 10^5 Wh/m^2) than the CP in general (-0.07, solar radiation = 5.1 x 10^5 Wh/m^2), but had similar slope (CP = 20.4 deg, hibernacula = 19.7 deg) and aspect (CP = 183.0 deg, hibernacula = 195.4 deg). Mined lands also showed elevated mean TPI (5.8 m) and solar radiation (5.3 x 10^5 WH/m^2) compared to the CP in general, while slope (20.3 deg) and aspect (181.6 deg) were similar. We found that across the entire CP, a large amount of habitat suitable for hibernacula exists (38.3%-40.3% of the CP, WebTable2). Our model also estimated that 7.8-7.9% of suitable habitat in the CP region of Kentucky had been surface mined as of 2011 and a further 5.5% was currently permitted for surface mining, a substantially higher proportion than mined land across the CP generally. This disproportionate loss of habitat is principally driven by overlapping preferences of *C. horridus* and mining for high topographic positions, as maps of permitting and extant mines clearly show (WebFigure1, WebFigure2).

Kernel density histograms show the homogenizing effect of mining on topography and topographically-driven abiotic variables (Figure 2, Figure 3). Slope in mined lands is driven sharply lower, whereas distributions of TPI and winter solar radiation are compressed to middle values at the expense of both high and low values; aspect is less affected. The homogenizing effect on solar radiation, a factor critically important to moisture and soil qualities, is particularly apparent.

2.5 Discussion

Although market forces have reduced use of coal for electricity generation in the US, surface coal mining will continue in Appalachia for the near future and cause further loss of topographically-driven forest communities. In the short term, reclaimed sites are woefully poor replacements in terms of soil conditions (Haering et al. 2004), vegetation reestablishment (Simmons et al. 2008), and the frequency of invasive species (Oliphant et al. 2017). Indeed, our landcover transition analyses show that only a small amount of reclaimed minelands returned to forest or forest-like conditions between 1992 and 2011, a portion of which is accounted for by University of Kentucky experimental tree plots. Land surfaces constructed during the process of mine reclamation are seldom as hospitable to subsurface biota as those which existed before mining (Wood et al. 2017). For example, the compacted substrate typical of many reclaimed minelands has been associated with lower abundances of small mammals and salamanders (Larkin et al. 2008, Wood and Williams 2013). While some studies have documented use of boulders and other uncompacted substrates by native wildlife (e.g. Chamblin et al. 2004, Gess et al. 2013), more research is needed to test the effectiveness of specific mine reclamation practices in regards to restoration of subsurface habitats important to native flora and fauna, including *C. horridus*.

Our topographic analyses suggest that the long-term outlook for ecological restoration of surface mines will prove extremely challenging. Despite the planting of native flora and recovery of soils, topographic changes appear to prohibit reclaimed sites from harboring ecological communities similar to the preexisting topographically-defined

biota. When the entire CP is considered, density histograms reveal tangible impacts of pre-2011 mining on these topographic variables across the entire region (Figure 3). This suggests that, at a regional scale, surface mining is substantially altering the very topographic gradients which provide the foundation for elevated beta diversity in the mixed-mesophytic forest. In the case of *C. horridus*, mining appears to be pressuring slope, TPI, and solar radiation values away from preferred ranges, thereby altering critically important winter habitats.

Habitat loss as a result of altered topographic position is especially consequential for the disproportionately affected ridgetop habitats, which host a unique suite of flora and fauna, including many threatened taxa (Jones 2004, WebTable 5). The causes of this outsized impact are likely cost-benefit driven: mineral deposits with less overburden are more economically desirable, thus high TPI habitats are the most endangered, a phenomenon mirrored in other mountainous parts of the world where surface mining is common (Yang et al. 2013). While ridgetops are almost twice as likely to be mined as other topographic positions, a sizeable portion of ridgetops remain in their original topographic class. Critically absent is research into the possibility of reestablishing topographically-restricted communities in the increasingly large swathes of reclaimed mineland which retain their topographic position. Indeed, simply reestablishing tree growth to any extent in these ecologically denatured areas has been challenging (Zipper et al. 2011). Likewise, impacts of habitat loss on genetic connectivity of native flora or terrestrial fauna have not been investigated. Considering that 16.8% of ridgetops across the CP are already mined or permitted for mining, landscape-scale forest fragmentation is doubtless already common, especially considering the uneven distribution of mining

across the CP whereby some watersheds have seen >20% of their total land surface mined or permitted for mining (WebTable 3). Furthermore, local and regional-scale microclimatic effects of surface mining are poorly understood, and our analyses underscore the potential for major influences at multiple scales (e.g. Wickham et al. 2013).

Our analyses are among the first efforts to quantify the aggregate current and future impacts of mountaintop removal mining on the topographic complexity of Appalachian ecosystems from c. 1980 to 2011. Our estimates are conservative for several reasons: we omitted early surface mining effects, as our "pre-mining" DEM datasets were collected c. 1980 and did not account for large, early surface mines (e.g., Starfire Mine in Knott County, KY). We also omitted isolated mines <10 ha in size, mines which opened and were reclaimed between 2011 and 2017 thus escaping both our mining and permit analyses, and any surface mines which operated outside of mining permit boundaries. By using NLCD to identify mined land, we may have missed land converted to atypical uses after mining, such as housing or row crops, instead of the more conventional barren, transitional, and herbaceous landcover classes we targeted. Accounting for these factors may substantially increase the total area of the CP mined since surface mining techniques became popular. While our reliance on grassland to delineate mined areas might have included grassland unrelated to mining, we believe this to be insignificant because (1) grasslands >10 ha in size are generally rare on unmined landscapes in the CP, and (2) such lands would need to fall within surface mining permit boundaries to be counted; indeed, only 1.7% of land we identified as mined was classified as agricultural fields or pastures in 1992 (WebTable1(c)). Two caveats pertaining to our *C. horridus* habitat

modeling deserve mention. First, our goal was not to construct the most parsimonious habitat suitability model but to apply previously established model selection findings to our region, and inclusion of fine-scale features may improve suitability estimation over small extents. Based on available literature (Brown et al. 1993, Browning et al. 2005), however, we feel that deviations from our model will have limited impact on our conclusions given the scale and patterns of surface mining in the CP. A second caveat involves the broad application of our model, which is based on hibernacula from a small (80 km^2) area, onto the entire CP (14,021 km^2). Nevertheless, topographic consistency within the ecoregion and our reliance on TPI instead of elevation may mitigate this concern.

If coal from Appalachian surface mines continues to play a significant role in energy production, our data suggest that sacrificing the topographic drivers of biodiversity in Appalachian forests could be a major tradeoff. The homogenization of physical factors is setting reclaimed lands on a new geophysical trajectory (Ross et al. 2016), and certain habitats seem unlikely to appear through natural processes on reclaimed land given major topographic shifts. While new reclamation methods may prove effective at mitigating this long-term mining-related habitat loss for *C. horridus*, much more research is needed to address gaps regarding the impacts of mining on other terrestrial biodiversity and the potential for reestablishment of topographically-restricted communities. Ridgetop communities in particular, including taxa associated with exposed ancient capstones and surrounding oak-pine forests, appear to be under threat of widespread destruction. Despite this, opportunities remain to minimize future losses. The majority of Appalachian ridgetop habitats in the CP remain intact, and improved

reclamation practices focused on preserving topographic complexity, such as research-informed reconstruction of exposed ridgetop rock outcrops on reclaimed land or discouraging the filling of stream valleys, might mitigate losses (Copeland 2015). In terms of specific mining practices, to prevent instant elimination of uncommon or imperiled populations of ridgetop-associated flora or fauna such as those of *C. horridus*, mining in high TPI habitats should be discouraged especially during seasons when at-risk fauna are known to be vulnerable. Yet to preserve the biodiversity of mixed-mesophytic forests in the CP, our research suggests that avoiding deep, permanent geophysical rearrangement like that which has defined contemporary surface mining is the most important action to be taken.

2.6 Acknowledgments

We are grateful for funding provided by the University of Kentucky and by the USDA National Institute of Food and Agriculture, McIntire Stennis project 1014537, and the approval of IACUC protocol 2012-0954. We are also grateful for the help of Dr. Ashley Keith, DVM, the Kentucky Division of Geographic Information, J. Hutton for his photography, and the field assistance of D. Collett, C. Osborne, T. Sizemore, E. Williams, and N. Williams.

Table 2.1. Total land impacted by surface mining organized by topographic position, with percent of each class mined as of 2011 and not mined as of 2011 but permitted for mining as of 2017, and results of our likelihood ratio test (G-test) which we used to test for differences in the frequency of mining and permitting among topographic positions.

Slope position class	Total area in CP (km^2)	Total area mined (km^2)	Total area permitted (km^2)	Percent of class area mined, 2011	Percent of class area permitted, 2017
Valley Floor	2802	171	143	6.1	5.1
Lower Slope	2837	140	109	4.9	3.8
Middle Slope	2783	156	116	5.6	4.2
Upper Slope	2798	215	149	7.7	5.3
Ridgetop	2799	281	191	10.0	6.8
Total	14020	963	709		
G-test results		$p<0.0001$ $G = 637.9$	$p<0.0001$ $G = 287.8$		

Table 2.2. Transition matrix of topographic position, before (c. 1980) and after (2013) surface mining. Numbers refer to percent of c. 1980 totals whereas totals refer to total land area per class per year in km^2.

	c. 1980	Valley Floor	Lower Slope	Middle Slope	Upper Slope	Ridgetop	Totals (km^2)
2013-15	Valley Floor	47.70	11.99	1.18	0.20	0.12	78
	Lower Slope	27.12	40.28	16.47	2.69	0.97	108
	Middle Slope	19.42	36.09	52.63	25.99	9.53	198
	Upper Slope	5.57	11.30	28.45	58.59	35.42	231
	Ridgetop	0.19	0.35	1.28	12.53	53.96	137
	Totals (km^2)	130	113	128	170	211	752

Table 2.3. Transition matrix of major landcover classes within the boundaries of 2011 surface mines, 1992-2011. Numbers refer to percent of 1992 totals, whereas totals refer to total land area per class per year in km^2.

	1992	Open Water	Strip Mines	All Forest	Grassland	Totals (km^2)
2011	Open Water	5.11	0.19	0.14	1.25	2
	Strip Mines	45.58	18.57	27.36	21.08	245
	All Forest	4.83	7.29	11.57	9.36	104
	Grassland	44.49	73.89	60.85	68.18	581
	Totals (km^2)	3	103	810	16	932

Table 2.4. Total *C. horridus* winter habitat, winter habitat mined as of 2011, and winter habitat permitted for surface mining as of 2017 under three confidence intervals.

Confidence Interval	Total Suitable Habitat (km^2)	Percent of Study Area Suitable	Total Habitat Mined (km^2)	Percent of Habitat Mined	Total Habitat Permitted (km^2)	Percent of Habitat Permitted
90%	5377	38.3%	423	7.9%	297	5.5%
95%	5527	39.4%	434	7.8%	306	5.5%
99%	5647	40.3%	443	7.8%	313	5.5%

Table 2.5. Total area, percent area surfaced mined as of 2011, and percent area under active permits for surface mining as of January 2017 for each USGS 8-digit Hydrologic Unit in the study area.

Watershed	Area (km^2)	Area mined (km^2)	Percent mined	Area permitted (km^2)	Percent permitted
Licking River	665	50	7.5	39	5.9
Tug River	1232	196	15.9	137	11.1
Big Sandy River	137	3	2.2	2	1.5
Upper Kentucky River	20	1	5.0	2	10.0
Lower Levisa Fork	2816	203	7.2	201	7.1
North Fork Kentucky River	3169	385	12.1	245	7.7
Middle Fork Kentucky River	1410	103	7.3	174	12.3
South Fork Kentucky River	1695	36	2.1	121	7.1
Upper Levisa Fork	928	122	13.1	107	11.5
Upper Cumberland River	1949	75	3.8	150	7.7

Table 2.6. Mean and standard deviations (italicized) of *C. horridus* overwintering habitat model parameters for the entire CP, hibernacula sites (n=17), for suitable habitat as determined by varying confidence intervals, for land classified as mined and for unmined land with active mining permits.

		Area [km^2]	Slope [deg]	Aspect [deg]	TPI [ft]	Winter Solar Radiation [WH/m^2]
Cumberland Plateau		14021	20.4 (*8.2*)	183.0 (*103.1*)	-0.07 (*86.7*)	512153.6 (*98741.3*)
Hibernacula		-	19.7 (*6.1*)	195.4 (*84.1*)	88.0 (*70.5*)	549631.3 (*79386.7*)
Habitat	90% CI	5377	22.2 (*5.4*)	196.6 (*74.9*)	48.0 (*62.4*)	562893.2 (*74348.5*)
	95% CI	5527	22.2 (*5.5*)	196.7 (*75.5*)	47.5 (*62.9*)	561820.1 (*75217.6*)
	99% CI	5647	22.2 (*5.5*)	196.7 (*76.0*)	47.1 (*63.3*)	560965.2 (*75903.8*)
Mined Land, 2011		963	20.3 (*8.0*)	181.6 (*98.9*)	18.9 (*93.7*)	527214.2 (*97064.4*)
Permitted Land, 2017		709	22.6 (*7.3*)	184.7 (*104.3*)	11.9 (*95.5*)	507876.2 (*106177.6*)

Table 2.7. Rare and threatened taxa associated with high TPI habitats in the Cumberland Plateau of Kentucky. Global status for animals is from IUCN, for plants from Kentucky State Nature Preserves Commission. NL = not listed, NT= near threatened, VU= vulnerable, T= threatened, FSC = federal species of concern, and E= endangered. Source refers to literature associating the species with ridgetops in the study area.

Common Name	Global Status	US Federal Status	Source
Red-cockaded woodpecker	NT	T	Kalisz and Boechtter 1991
Allegheny woodrat	NT	FSC	Lacki and Krupa 2001
Cerulean warbler	VU	FSC	Buehler et al. 2007
Indiana bat	NT	E	Kiser and Elliott 1996
Sweet pinesap	G3	FSC	KSPNC 2012
Ovate catchyfly	G3	NL	KSPNC 2012
Soft-haired thermopsis	G3	NL	KSPNC 2012

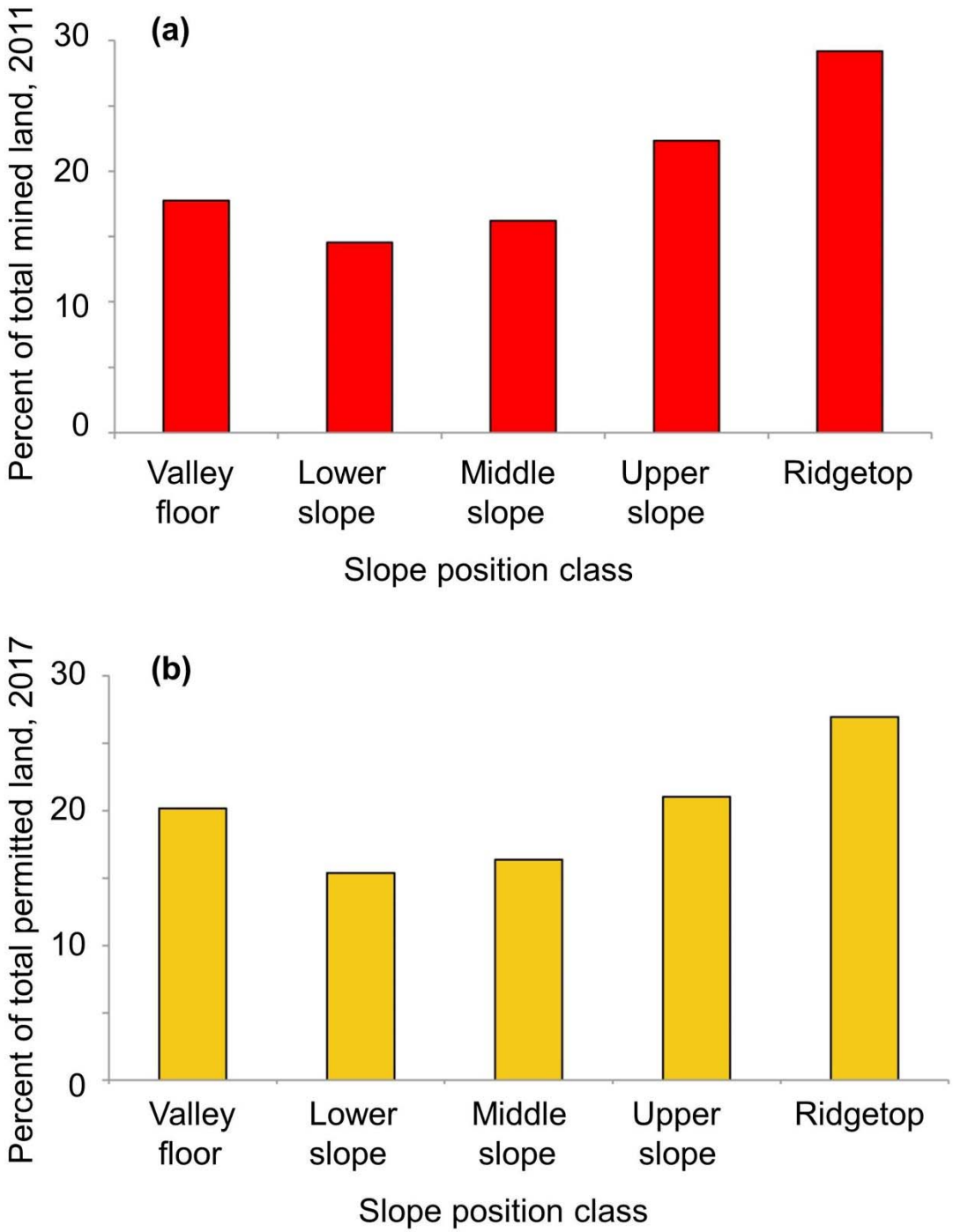

Figure 2.1. Percent of the total land area within each one-fifth quantile based slope position class (valley floor, upper, middle, and lower slope, and ridgetop) in the Cumberland Plateau (a) mined as of 2011 or (b) not mined as of 2011, but permitted for mining as of 2017.

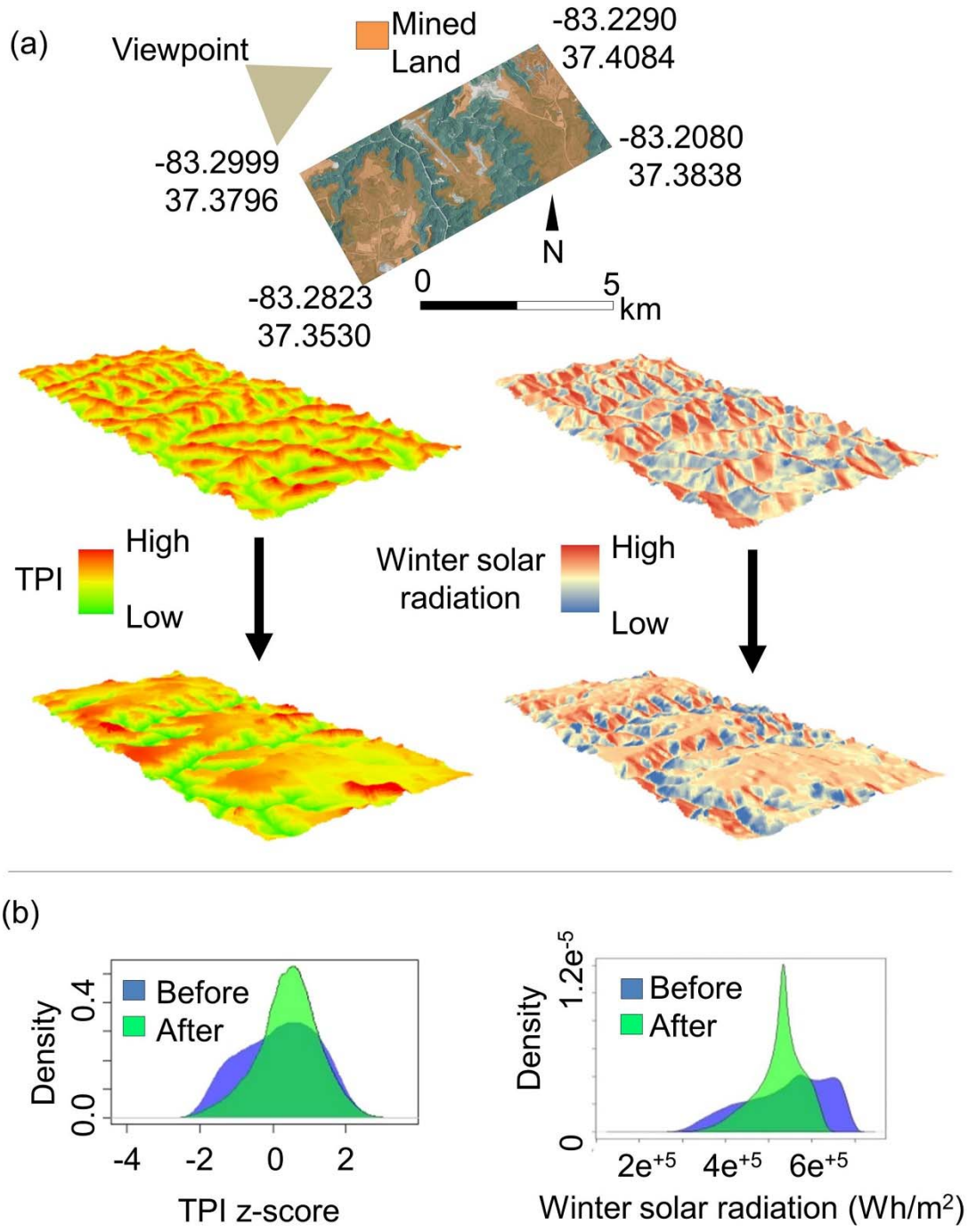

Figure 2.2. Visual representation of fine-scale geophysical changes after mining. Above, a National Agriculture Imagery Program (NAIP) image of the area of interest in 2014, with mined areas overlaid in orange. Middle, the distribution of TPI and winter solar radiation before and after mining. Bottom, density plots for standardized topographic position index (TPI) and winter solar radiation before and after mining across all mined lands in the study area.

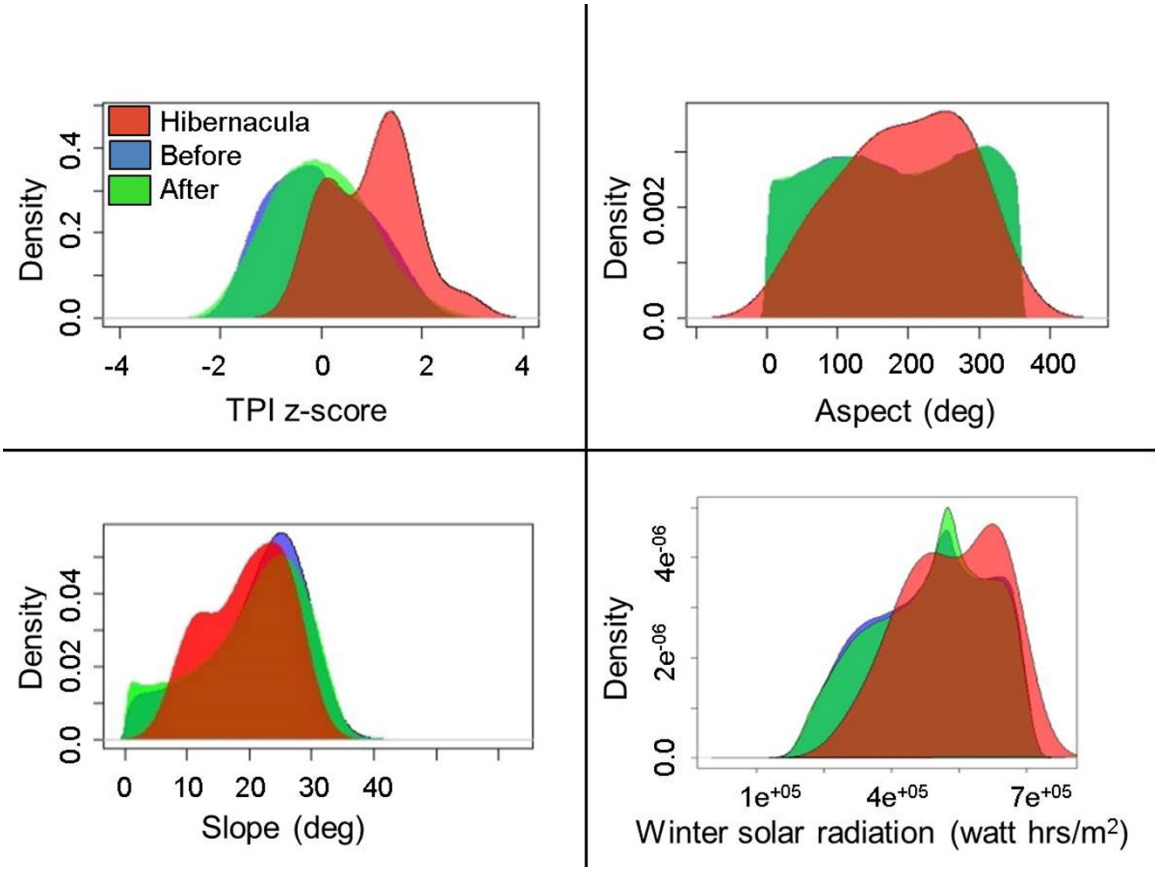

Figure 2.3. Kernel density plots for TPI, slope, aspect, and winter solar radiation for our hibernacula sites superimposed on each variable's distribution across the entire 14,021 km2 Cumberland Plateau of Kentucky before and after mining. TPI values have been standardized to z-scores.

Figure 2.4. Photograph of an adult *C. horridus* in the study area, credit Jake Hutton.

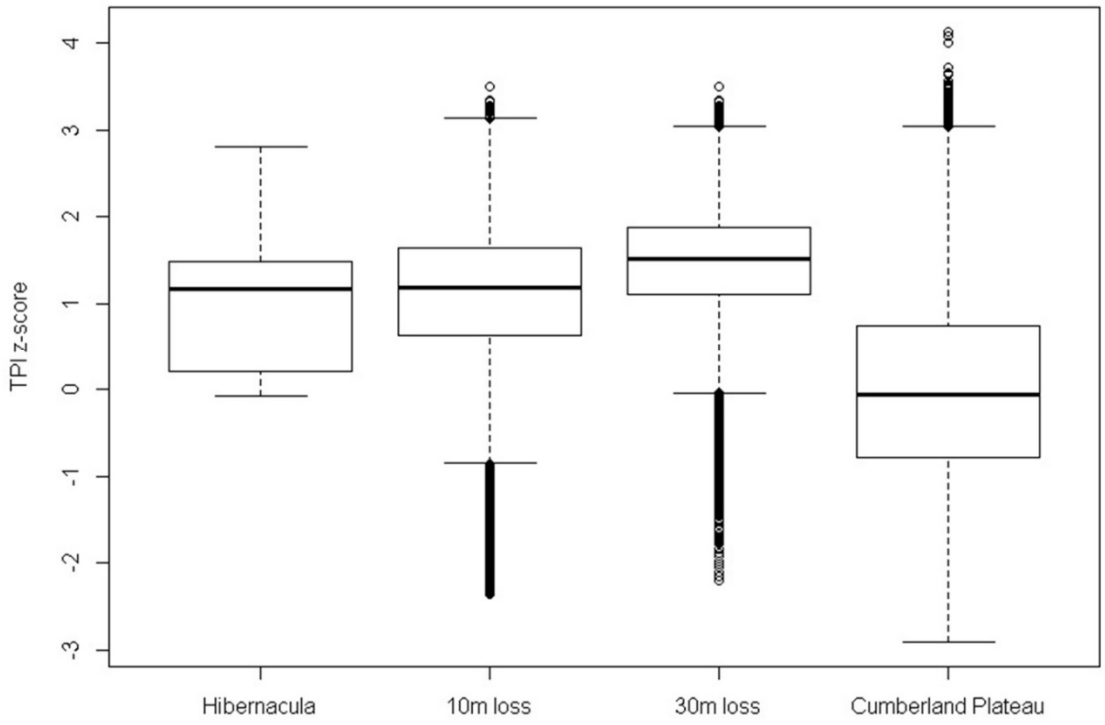

Figure 2.5. Boxplot of topographic position index (TPI) z-scores for *C. horridus* hibernacula (mean=1.02, sd=0.81), areas of >10m (mean=1.08, sd=0.79) and >30m (mean=1.47, sd=0.62) elevation loss from mining, and the entire Cumberland Plateau (mean=0.00, sd=1.00). Individual data points represent 30m raster cells.

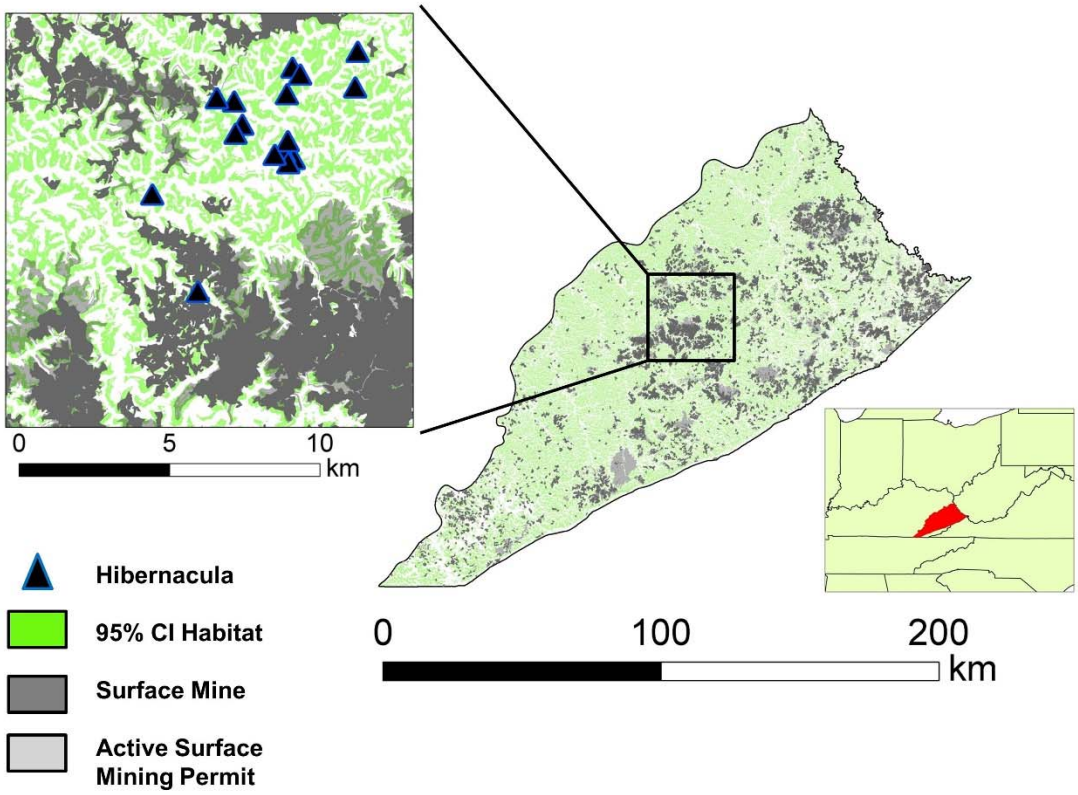

Figure 2.6. Suitable *C. horridus* overwintering habitat (95% confidence) across the Cumberland Plateau, with surface mines and areas permitted for mining denoted. Inset refers to telemetry study area.

CHAPTER 3:

A SPATIAL GENOMIC APPROACH IDENTIFIES TIME LAGS AND HISTORIC BARRIERS TO GENE FLOW IN A RAPIDLY FRAGMENTING APPALACHIAN LANDSCAPE

3.1 Abstract

The resolution offered by genomic data sets coupled with recently developed spatially informed analyses are allowing researchers to quantify population structure at increasingly fine temporal and spatial scales. However, both empirical research and conservation measures have been limited by questions regarding the impacts of data set size, data quality thresholds, and the time scale at which barriers to gene flow become detectable. Here, we used restriction site associated DNA sequencing to generate a 2,140 SNP data set for the copperhead snake (*Agkistrodon contortrix*) and address the population genomic impacts of recent and widespread landscape modification across an approximately 1000 km^2 region of eastern Kentucky, USA. Nonspatial population-based assignment and clustering methods supported little to no population structure. However, using individual-based spatial autocorrelation approaches we found evidence for genetic structuring which closely follows the path of a historically important highway which experienced high traffic volumes from ca. 1920 to 1970 before losing most traffic to a newly constructed alternate route. We found no similar spatial genomic signatures associated with more recently constructed highways or surface mining activity, though a time lag effect may be responsible for the lack of any emergent spatial genetic patterns. Subsampling of our SNP data set suggested that similar results could be obtained with as few as 250 SNPs, and a range of thresholds for missing data exhibited limited impacts on the spatial patterns we detected. While we were not able to estimate relative effects of

land uses or precise time lags, our findings highlight the importance of temporal factors in landscape genetics approaches, and suggest the potential advantages of genomic data sets and fine-scale, spatially informed approaches for quantifying subtle genetic patterns in temporally complex landscapes.

3.2 Introduction

Habitat loss and fragmentation resulting from natural resource extraction, agriculture, and urbanization is setting some populations on new demographic trajectories, with increasing and persistent genetic diversity loss (Haddad et al. 2015). Understanding the effects of this rapid landscape change on population structure and genetic diversity is critical for informing science-based conservation and management (Hilty et al. 2012, Keller et al. 2015, Waits et al. 2016). However, a variety of geographic and ecological factors can affect the amount and rate at which spatial genetic structuring builds in a given system, creating challenges for the development of proactive management plans (Epps and Keyghobadi 2015, Balkenhol et al. 2016, Richardson et al. 2016). Thus, while migration may be limited by contemporary landscape factors, genetic structure may not be detectable until many generations after a barrier forms, especially if the power to detect such patterns is limited by the quantity or quality of genetic data available (Landguth et al. 2010, McCartney-Melstad et al. 2018).

The use of large single nucleotide polymorphism (SNP) data sets has improved the detection of recent habitat fragmentation in several ways. First, increased genome-wide sampling reduces the number of individuals needed to quantify differentiation among sampling locations (Willing et al. 2012, Nazareno et al. 2017). With this lower

threshold for per-locale individual sampling, genomic data can permit sampling schemes encompassing a broader geographic area and a more hierarchical design, thus allowing for more robust resolution of patterns at multiple spatial scales (Anderson et al. 2010, Balkenhol and Fortin 2016). Furthermore, while the relatively high mutation rate of microsatellites is advantageous for detecting recent genetic change (Epps and Keyghobadi 2015), the greater genome-wide sampling of large SNP data sets can potentially detect weaker spatial genetic patterns resulting from relatively recent or porous barriers to gene flow (Landguth et al. 2012). For example, McCartney-Melstad et al. (2018) found that with as few as 300-400 SNPs, genetic structure associated with the barrier effects of roads could be detected in amphibian populations where 12 microsatellite loci had previously indicated no structure. SNP data sets of this size are now readily available through methods such as restriction site-associated DNA sequencing (RADseq), allowing for the generation of thousands of loci from non-model organisms with a range of ecological characteristics that may make them prone to the genetic effects of recent habitat fragmentation (Epps and Keyghobadi 2015).

While traditional methods of testing for spatial genetic patterns, such as model-based clustering (e.g., STRUCTURE, Pritchard et al. 2000) or non-parametric exploratory analyses (e.g., DAPC, Jombart et al. 2010) have been used to characterize genetic diversity across a given area (François and Waits 2015), other methods which are able to separate spatial and non-spatial genetic variation may be better equipped to detect patterns of genetic differentiation in recently fragmented systems or those with high rates of gene flow (Jombart et al. 2008, Galpern et al. 2014). These methods use spatial autocorrelation to tease apart patterns of inter- versus intra-population genetic variation,

improving the identification of population structure at fine geographic scales (Galpern et al. 2012). When coupled with genomic data, spatially informed analyses may also allow for the detection of weak spatial structure related to recent habitat fragmentation or incomplete barriers to migration (Richardson et al. 2016, Richardson et al. 2017, Combs et al. 2018, Combs et al. 2018a). However, alongside these methodological improvements, work remains to understand the amount of individual-level genomic data necessary to assess spatial genetic patterns (e.g., McCartney-Melstad et al. 2018), and the effects of genomic data quality on the resolution of recently evolved population structure. Identifying spatial genetic patterns associated with landscape features is especially pertinent in regions experiencing rapid and recent landscape change. Few regions have experienced this change as rapidly as central Appalachia in the eastern United States, chiefly as a result of the large-scale surface coal mining practices often referred to as 'mountaintop removal' (Wickham et al. 2007, Drummond and Loveland 2010, Pericak et al. 2018, Maigret et al. 2019). Alongside mining, the wholesale construction of several high-traffic road systems in the 1970s and 1980s, in part to facilitate the transportation needs of the mining sector, have further subdivided what was formerly a relatively continuous forest landscape with scant high-traffic roads (KTC 2018). Despite the scale of these changes, the effects on native biodiversity are not well understood (Wickham et al. 2013). Given the historically rugged terrain of Appalachia, topographic homogenization produced by surface mining may facilitate dispersal of terrestrial fauna not encumbered by the radically altered soils, flora, and thermal regimes of reclaimed minelands (Wickham et al. 2013), and highways may also facilitate movement in some species (Trombulak and Fissell 2000). Alternatively, less vagile taxa that rely on sparsely

distributed microhabitats may be more sensitive to the effects of forest fragmentation, especially if they are susceptible to road mortality.

We sought to understand the impact of recent and major landscape changes on the population structure of the copperhead (*Agkistrodon contortrix*), an abundant snake in eastern Kentucky (Barbour 1962) generally not capable of long-distance (> 1 km) individual movements (Sutton et al. 2017). Copperheads rely on rocky overwintering hibernacula located high on steep-sided and often south-facing slopes (Maigret and Cox 2018), sites disproportionately destroyed by surface mining (Maigret et al. 2019). Copperheads are also generally intolerant of dense, invasive vegetation common to many reclaimed surface mines (Carter et al. 2015, Carter et al. 2017). Additionally, herpetofauna generally, and pit vipers in particular, have been shown to be especially vulnerable to vehicular traffic (Andrews and Gibbons 2005, Shepard et al. 2008), and elevated genetic differentiation associated with highways has been detected using microsatellite markers (Clark et al. 2010, DiLeo et al. 2013). Pertinent to this point, our study area contains several major highways [> 3,000 Annual Average Daily Traffic (AADT)] constructed between 1970 and 1985 which could be barriers to movement for *A. contortrix*. Nearly all these highways were constructed along new paths and do not follow major hydrological or topographic features for the majority of their route through the study area, thus facilitating a more straightforward analysis of the effects of these highways on gene flow. From at least 1900 until 1970, however, the only highway across the study area was KY State Route 476 (formerly old KY State Route 15; hereafter referred to as KY-476). Prior to 1970, KY-476 was a major thoroughfare through the region, following the sinuous course of Troublesome Creek, a tributary of the North Fork

of the Kentucky River. In the early 1970s, the new KY-15 was opened, leading to markedly decreased traffic volumes on KY-476 (~500 vehicles/day) and pushing most traffic, including many coal-industry commercial vehicles, to the new KY-15 (~ 5,000 vehicles/day).

Using RADseq data and nonspatial and spatially informed analyses, we investigated the potential for recently formed population structure across *A. contortrix* in eastern Kentucky as a result of this landscape change, with a particular focus on the effects of habitat fragmentation via surface coal mining and through the network of historic (c. 1920) and more recently-constructed (c. 1975) high-traffic roads. Specifically, we aimed to: (1) understand the extent and scale of spatial genomic structuring in copperheads across what was until recently a heavily forested landscape; (2) test for associations between current landcover classes and patterns of spatial genomic diversity; (3) test for associations between current or historic highways and contemporary patterns of gene flow, and (4) understand how the number of loci and quality of a data set can affect our ability to detect spatial genomic patterns. More broadly, for any barriers we could detect, we aimed to shed light on the temporal scale at which potential barriers to gene flow are detectable using SNP data sets, to investigate the role of spatially informed methods for identifying recent or weak genetic boundaries, and to provide a starting point for future research into the spatial genetic implications of increasingly popular methods of surface mining.

3.3 Methods

3.3.1 *Sampling Methods*

We sampled *A. contortrix* individuals from an approximately 1,000 km^2 area of Breathitt, Knott, and Perry counties in eastern Kentucky, USA (Figure 1, Figure S1, Table S1). We used a hierarchical sampling strategy to acquire tissue samples. Our strategy was based on individual sampling sites, which consisted of a location where a combination of artificial cover and visual encounter surveys were used to capture snakes. Overall, these were roughly grouped into five sampling clusters, each composed of at least four individual sampling sites, separated by 2-3 km, and arranged roughly in a cross or an 'x' as permitted by the landscape and property access (Figure S1). In turn, each sampling cluster was separated by roughly 10-20 km, providing comparisons at multiple spatial scales both within and between each cluster (Balkenhol and Fortin 2016). We sampled tissues at our individual sites between May 2014 and September 2016.

During the same time period, we augmented this design by including individuals captured opportunistically apart from designated individual capture sites; typically, these snakes were found alive or dead on roadways within the study area or were killed and/or donated by area residents who were able to provide precise locality information for each tissue sample. We found no major differences in the spatial configuration of samples acquired from live individuals versus tissue acquired from dead snakes; both sources of tissue were distributed fairly evenly across the study area. A total of 106 individual snakes were eventually included in our sequencing. Live-captured snakes were restrained and two ventral scales were removed, placed in 95% ethanol, and subsequently frozen at -80°C (Maigret 2019). Muscular tissue from the tails of dead snakes was treated similarly.

3.3.2 *DNA Sequencing and SNP calling*

We extracted genomic DNA using a Qiagen DNeasy Blood and Tissue Extraction Kit and prepared double digest RADseq (ddRADseq) libraries based on Peterson et al. (2012). DNA was quantified using a Qubit 2.0 flourometer (Thermo-Fisher). DNA extractions ≤ 2.0 ng/uL were amplified using a Qiagen REPLI-g high-fidelity whole genome amplification kit. We prepared ddRADseq libraries using ~1000 ng of DNA per individual. DNA was digested using EcoRI and SphI and subsequently cleaned with Agencourt Ampure XP beads (Beckman Coulter). Adaptor ligation was performed using one of 48 unique 5 bp barcodes in combination with a universal 6 bp single-index PCR adaptor. Samples were then pooled in groups of eight, bead cleaned, and size selected (526 bp ± 10%) with a Pippin Prep (Sage Science). Each 8-sample pool was then Qbit quantified and amplified using Phusion high-fidelity PCR (New England Biolabs) with a PCR primer with one of several unique barcodes, permitting each individual to be identified uniquely using a combination of the unique PCR barcode and a unique adaptor index. After cleaning and quantifying PCR product, we used an Agilent 2100 Bioanalyzer to confirm target fragment size distributions before 150 bp paired-end sequencing on two lanes of an Illumina Hi-Seq 2500. Individuals were randomly assigned to a lane with respect to geographic location to reduce downstream genetic artefacts (Meirmans 2015).

We used Stacks v1.37 (Catchen et al. 2013) to identify orthologous loci across individuals. No overlap was expected between sequencing reads; therefore, we used a custom script to stitch together forward and reverse reads. We used process_radtags to demultiplex individuals and discard low-quality reads containing uncalled bases or a

mean quality score < 10 in a sliding window comprising 15% of the read. After quality filtering, reads were assembled using denovo_map, with a minimum stack depth of five (m = 5), three mismatches allowed between stacks within individuals (M = 3), and two mismatches allowed between stacks among individuals (n = 2). To increase confidence in our SNP calls, we used rxstacks to remove SNPs with a low log likelihood (Stacks v1.37 option: --ln_lim = -25) and/or a high proportion of confounded loci (conf_lim = 0.25). After running rxstacks, cstacks and sstacks were re-run with the filtered loci. We sampled a single SNP per locus (--write-single-snp), using only SNPs with < 50% missing data, a minor allele frequency < 0.015, and no evidence of excess heterozygosity. Finally, we removed individuals with > 50% missing data.

3.3.3 *Summary statistics and distance-based analyses*

We generated a genetic dissimilarity matrix using the program bed2diffs v1 in the EEMS package (Petkova et al. 2016). This produced a matrix of average individual pairwise genetic dissimilarity (hereafter referred to as the "GDM") based on allelic frequencies, similar to the proportion of shared alleles (Bowcock et al. 1994). We estimated effective population size using the molecular co-ancestry method of Nomura (2008), as implemented in the linkage disequilibrium method in NeEstimator (Do et al. 2014). We estimated heterozygosity and nucleotide diversity using plink and vcftools, respectively (Purcell et al. 2007, Danecek et al. 2011). We calculated the relationship between geography and the GDM using the ecodist package in R (Goslee and Urban 2007). Mantel correlograms were generated for multiple geographic distances, including Euclidean distance, the natural log of distance, stream (hydrological) distance, and the natural log of stream distance. The distance class size we used was based on estimates of

annual movement distances of adult copperheads, about 1 km in Euclidean distance (Sutton et al. 2017). We also created correlograms defined by one-tenth quantiles of the total distribution of all pairwise distances (about 2.5 km in Euclidean distance). We used 1,000 permutations to determine significance. To quantify stream distances, we used the Origin-Destination Cost Matrix (ODCM) tool in ArcMap v10.1 (ESRI, Redlands, CA) and a shapefile of USGS stream paths obtained from the KY Division of Geographic Information. We chose to use stream paths as a proxy for potential elevation effects because streams represent the least-cost path between sites given the rugged terrain of the study area. Sites not adjacent to streams were connected using a minimum-distance connection in ArcMap's ODCM tool.

3.3.4 *Nonspatial analyses of population structure*

To identify and characterize genetic clusters across our study area, we used both discriminant analysis of principal components (DAPC) in the adegenet R package (Jombart et al. 2010) and Bayesian clustering via STRUCTURE (Pritchard et al. 2000). For our DAPC analyses, we first used the find.clusters function, retaining all principal components (PCs) and selecting the *K* value with the lowest Bayesian information criterion (BIC). Individuals were then ordinated in PC space using the dapc function. To reduce the potential for over-fitting, we selected the number of retained PCs in light of diminishing returns from retaining excess PCs (Jombart et al. 2010).

For our STRUCTURE analyses, we estimated population assignment of individuals using an admixture model with cluster numbers ranging from $K = 1$ to 10, without the LocPrior option. Five replicates were run for each *K*, each for 1,000,000 generations after

a burn-in of 100,000 generations. To investigate potential effects of including sampling locations on STRUCTURE output, we also performed analyses using an admixture model and the LocPrior option, with cluster numbers of K=1 and K=2 with five replicates and the same generation and burn-in parameters used without the LocPrior option. We used Structure Harvester v0.6.9.4 (Earl and von Holt 2012) to generate mean log likelihood values for each K and identify the optimal number of clusters for our data using ΔK (Evanno et al. 2005). We used the program CLUMPAK to compute cluster membership coefficients across replicates (Kopelman et al. 2015). Despite the potential for inaccurate results when genetic diversity is distributed continuously or populations are inbred, we chose to use STRUCTURE due to its continuing popularity, broad array of applications, and the lack of any hard thresholds associated with these potential drawbacks (Pritchard et al. 2007).

3.3.5 *Spatially informed analyses of population structure*

To further test for genetic structure across our study system, we used three recently developed approaches that integrate spatial information into analyses based on genetic dissimilarity. First, we used MEMGENE (Galpern et al. 2014), a regression-based analysis based on the spatial autocorrelation among a given set of georeferenced individuals and a corresponding GDM. Individual samples are mapped based on geographic location, and predicted eigenvector scores from this regression are overlaid to provide a visualization of the uniquely spatial component of genetic dissimilarity among individuals.

Second, we used the program sPCA (Jombart et al. 2008) implemented in the R package adegenet. sPCA is broadly similar to MEMGENE (but see Galpern et al.

2014:Appendix S4), but relies on an ordination approach based on Moran's *I* index to identify eigenvectors that maximize variation in allele frequencies and spatial autocorrelation, and then maps these eigenvectors onto geographic coordinates. We used the function chooseCN to identify a connection network construction scheme; our analyses used a nearest-neighbor connection network with k = 40 neighbors to maximize connectivity across our large number of spatially distinct samples, accounting for potential long-distance dispersal events among aggregations of sampling sites. We relied on the eigenvalue variance and spatial components plots to select the optimal number of positive ("global") and negative ("local") axes to retain, we replaced any NAs in our data with mean allele frequencies, and we used the recommended multivariate significance test to identify significant global and local genomic structure. In this context, we use the term "global structuring" to refer to positive autocorrelation between nearby individuals, and "local structuring" to refer to negative autocorrelation between nearby individuals (*sensu* Jombart et al. 2010).

Third, to take into consideration the impact of landscape features on gene flow, we estimated a resistance model using the R package ResistanceGA (Peterman 2018). ResistanceGA uses a genetic algorithm approach to parameterize the individual resistance values associated with a given resistance surface based on genetic dissimilarity data. By doing so, the optimization of surfaces undertaken by ResistanceGA bypasses the subjective assignment of resistance surface component values based on expert opinion or on modeling of individual movement patterns (Spear et al. 2016, Peterman 2018). Model fit of the optimized surfaces are quantified using AIC values from linear mixed-effects models, both for each surface individually and for all combinations of individual

surfaces. Our ResistanceGA input landscape surfaces consisted of land cover classification data obtained from 2011 National Land Cover Data. We reclassified raw NLCD raster values into three different resistance surfaces of two categories each, including: (1) a mining surface with two categories, mined and unmined land, (2) a surface representing the route of current highways, with two categories, highway and non-highway, and (3) a surface representing the route of KY-476, also with two categories, highway and non-highway (Table S2). We tested both for effects of each of these three surfaces independently and each possible combination of the three. We reclassified NLCD raster classes using the Reclassify tool in the Spatial Analyst extension of ArcMap 10.3.3, producing our three putative resistance surfaces. We relied on historic road maps publicly available from the KY Transportation Cabinet to identify current and historic highway patterns in the study area from 1936 to the present, and historic topographic maps from the US Geological Survey's Historical Topographic Map Explorer for information on routes before 1936. Our response data set was our individual pairwise GDM, and our predictor variable was a least cost paths matrix based on our land cover raster surfaces which were obtained using the 'costDistance' function in the R package gdistance (van Etten 2017). While lacking the comprehensive approach available with random walk commute times, least cost paths represent a much more computationally tractable approach for our spatial and genetic data set (Peterman 2018).

3.3.6 *Subsampling of our SNP data set*

We aimed to assess the relative ability of two of the spatially informed methods, sPCA and MEMGENE, to produce results similar to the full data set based on: (1) the

number of loci, and (2) the amount of missing data. To examine the effect of the number of loci, we randomly subsampled our full 2,140 SNP data set, producing subsets of 25, 50, 100, 250, 500, and 1,000 loci. For each subset, ten replicates were generated using plink and analyzed in sPCA and MEMGENE as described above for the full data set. To examine the effects of missing data, we used our m=5 read depth SNP data (Table S3), without any filtering for missing data (n= 24,385 loci), and we set new missing data thresholds of 0.05 (i.e., retaining only loci present in ≥ 95% of individuals), 0.10, 0.25, 0.40, 0.5, 0.75, 0.90, and 0.95. While these represented our thresholds, our realized data sets typically had smaller amounts of missing data, in aggregate, than each threshold. Only a single data set could be produced for each missing data threshold.

Differences in how sPCA and MEMGENE are designed influenced how we quantified our subsampling and missing data threshold results. For sPCA, we first detected significant patterns of structuring, then tabulated the proportion of replicates with unrelated, similar, or identical spatial genomic patterns as detected in analysis of the full data set. Model outputs for sPCA include global (positive axes) and local (negative axes) permutation tests of structuring, the p-values of which were obtained for each level of subsampling and missing data thresholds; we then averaged these p-values across 10 replicates for the former. MEMGENE, on the other hand, only analyzes significant spatial patterns, and nonsignificant patterns are not retained for downstream analyses. Thus, for MEMGENE, we obtained R^2 values only for levels of subsampling and missing data thresholds where significant spatial patterns were observed, and we quantified spatial patterns which were unrelated, similar, or identical, in a similar fashion to our sPCA results. We defined "identical" patterns as being identical to those produced with the full

2,140 SNP data set in terms of which group each sample was categorized in (represented by the color of each sample) and the approximate strength of each categorical assignment (represented by the size of each symbol). "Similar" patterns, meanwhile, were those that displayed identical sample assignment of the majority of individuals within each sampling cluster (Figure S1), but different assignments of some individuals within clusters. "Unrelated" results denote visualizations where the majority of sites in one or more sampling clusters are assigned differently than when analyzed with the full data set. We summarized these collective results by charting p-values from local (negative autocorrelation) and global (positive autocorrelation) tests from sPCA alongside R^2 values from MEMGENE for each missing data threshold, and by charting both these statistical values and the proportion of identical, similar, and unrelated patterns for each subsampling level. While categorizing spatial patterns in terms of their similarity to those generated using our full data set required some qualitative assessment of the results, we deferred from using more substantial quantitative metrics for comparison given the limited number of sampling sites.

3.4 Results

3.4.1 *Sequencing Results*

We generated ~239 million 150 bp paired-end reads, with a mean of 1,869,394 reads per individual. Increasing or decreasing the minimum read depth between four and seven did not affect any summary statistics, and only marginally affected the number of loci in our data (Table S3). After quality filtering, we recovered genotypes for 77 individuals from 34 different locations (Figure 1). This included a total of 2,140 loci,

with an average missing data rate of 23.5% of loci per individual (min. = 4.4%; max.= 48.9%) and a mean minor allele frequency of 0.166 (Table S5). A total of 29 individual samples were not included in our final data set due to excessive missing data or poor read quality.

3.4.2 *Summary of Genetic Diversity*

Across our study area, we estimated $H_O = 0.193$, $H_E = 0.24$, $\pi = 0.242$, and $F_{IS} = 0.195$. We estimated an N_e of 635.8 (95% CI: 595.6, 681.6). Mantel tests identified weak, but sometimes significant correlations between genetic and different measures of geographic distances, including Euclidean ($p = 0.79$, $R^2 = -0.0003$), natural log of Euclidean ($p < 0.001$, $R^2 = 0.0037$), hydrological distance ($p < 0.001$, $R^2 = 0.0054$), and natural log of hydrological distance ($p = 0.003$, $R^2 = 0.0029$). Mantel correlograms of correlation by distance class similarly showed minimal evidence of isolation-by-distance (Figure S2).

3.4.3 *Non-spatial Population Structure*

Neither DAPC nor STRUCTURE analyses supported the presence of multiple geographically distinct genetic clusters. BIC scores in DAPC were lowest for K = 1 (Figure 2a), and an exploration of cluster assignments using the first PC axis and a K = 2 did not produce individual assignments corresponding to sampling localities or geography (Figure S1). STRUCTURE analyses identified K = 3 as the best-fit clustering model for our data based on the ΔK statistic (Figure 2b). Evidence of convergence was seen in both the α parameter and FST estimates; however, at this level of clustering all

individuals were nearly equally assigned to all three clusters, indicating a lack of population structure. These results were similar at a K = 2. Using prior sampling location information (LocPrior) did not change these results (Figure S3).

3.4.4 *Spatially Informed Population Structure*

sPCA analyses identified significant global structure across the study area ($p = 0.002$). The first global (positive) sPCA axis identified a population genetic break that closely followed the historic highway path of KY-476 (Figure 3a). Based on a scree plot and a plot of eigenvalues, this first global axis contained the most information relative to other axes, and support for any of the local (negative) axes was not of congruent strength (Figure S4a-b). Neither increasing or reducing the number of neighbors used in the analysis by ≤50% nor using other connection network schemes (e.g., distance-based delimitation) changed the identified pattern.

The first variable identified as significant in the MEMGENE analysis explained a high proportion of the total variance across three retained axes (0.81). The proportion of overall genetic variance explained by spatial patterns associated with this first variable may appear to be modest (adj. $R^2 = 0.061$), but this was similar to the proportion explained by other studies at similar spatial scales (e.g., Galpern et al. 2014, Combs et al. 2018a). Visualization of the first and most explanatory MEM variable similarly identified a genetic break that partitioned populations on either side of KY-476 (Figure 3b). No genetic breaks identified an influence of landcover or current highway paths.

Landscape resistance analyses in ResistanceGA supported a null model of no geographic structure, followed by a model of isolation by distance (Table S4). Models

that included the three individual resistance surfaces (landcover, current highways, or historic highways), or any combination of resistance surfaces, were not strongly supported.

3.4.5 *Subsampling of SNP Data Set*

sPCA analysis of subsampled SNP data sets produced significant detection of global structure (positive autocorrelation) with as few as 25 loci (average global p-value of ten replicates = 0.067, Fig. 4a), although data sizes ≥ 250 loci were needed to produce identical patterns to those generated with the full data set (mean global p = 0.0033). At ≥ 500 loci identical patterns were produced in all replicates. Significant local structure (negative autocorrelation) was not supported for any level of subsampling (mean local p-value = 0.34). MEMGENE analysis of subsampled SNP data sets produced identical patterns in a majority of replicates when sampling ≥ 100 loci (Fig. 4b). However, identical results were still detected in 50% of replicates when sampling 50 loci and produced in all replicates when sampling 1000 loci.

The performance of sPCA and MEMGENE was not adversely affected by the inclusion of higher levels of missing data, which naturally also increased the number of SNPs (Fig. 4(c)). Global p-values from sPCA analysis were significant at ≥ 25% missing data and remained so, even when the data set allowed for as much as 95% missing data per individual. Missing data levels ≤ 10% resulted in a loss of significant global spatial structure, and we note the peculiarity that data sets of smaller locus number resulted in significant detection of global structure in our subsampled data replicates, suggesting the potential for Type I error with small data sets. MEMGENE produced R^2 estimates with

data sets permitting ≥ 40% missing and increased with higher levels of missing data, up to 75%. With stricter limits on missing data, no axes were retained.

3.5 Discussion

3.5.1 *Non-spatial vs. spatially informed analyses of population structure*

Here, we present empirical evidence for the ability of some spatially informed methods to detect weak population structure in study systems where more traditional and non-spatially informed methods indicate a lack of structure. Patterns in both DAPC and Structure results were consistent with a $K = 1$ model, with no evidence for geographically distinct genetic clusters across the study area. In contrast, the spatially informed methods sPCA and MEMGENE returned similar results supporting geographic genetic structure with a break coinciding with the path of KY-476, a historically-important highway that served as a major traffic artery in the region between c. 1920-1975. The inference of weak population structure and genetic fragmentation on the landscape of our study system is bolstered by multiple lines of evidence. First, both sPCA and MEMGENE identified the same geographic genetic break. While these methods both use spatial autocorrelation in the analysis of genetic data, they operate in very different ways: sPCA relies on the integration of Moran's I matrix via a connection network, while MEMGENE uses a forward selection method to identify significant MEM eigenvectors, and then uses a regression approach to generate predictions from the regressions that describe spatial patterns (Galpern et al. 2014). The congruence of these results indicates that our result is probably not a spurious pattern driven by an artefact of one particular analysis. Second, while the magnitude of population structure detected in our work was generally weak— MEMGENE-

based regression analyses attributed ~6% of total genetic variation to spatial effects—this amount of spatially explained genetic variation is in the range of that detected with MEMGENE under simulated models of population fragmentation and higher than that detected for panmictic populations (Galpern et al. 2014). This level of spatially driven genetic variation is also similar to that detected in other studies of recently fragmented landscapes (Combs et al. 2018, Combs et al. 2018a). Our overall interpretation of these results is that the use of methods that specifically use spatial patterns of variation, such as sPCA and MEMGENE, seem to be able to identify patterns of weak population structure at temporal and spatial scales where more widely used non-spatial methods (even when using basic locality sampling priors) would fail to discern geographic population structure (Galpern et al. 2014).

In contrast, our estimates of population structure using optimized landscape resistance generated using ResistanceGA did not support a link between genetic differentiation and landscape features. This lack of spatially informed population structure may be related to methodological aspects of this program, as it does not use the autocorrelation approach that is built in to sPCA and MEMGENE. Given the relatively weak nature of the spatial genomic signal associated with the route of KY-476, our ability to detect resistance to gene flow based on landcover classes may have been comparatively limited. Properly testing the hypothesized effects of our putative resistance surfaces on gene flow may require a much larger number of spatially distinct sampling locations, perhaps distributed in a more stratified and evenly-spread manner.

3.5.2 *Data size and quality in the detection of weak population structure*

While our genomic data set may have also increased our ability to detect subtle spatial patterns, random subsampling of our data indicated that thousands of SNPs may not be necessary to detect weak population structure similar to that found with our full data set. In fact, we found that several hundred SNPs may be sufficient to consistently identify weak spatial structure. This result is similar to that of a recent study (McCartney-Melstad et al. 2018), which showed that the use of a more limited set of independent SNPs (~300-400) was sufficient to recover fine-scale population structure using the non-spatial method Admixture (Alexander et al. 2009) with results similar to those obtained with a larger, more-complete data set (3095 SNPs). Our subsampling work extends this finding, indicating that spatially informed methods of population structure may be equally efficient with relatively modest sized data sets of adequately informative loci (~250-500 loci). We do note that minimum locus thresholds will vary based on the intensity of the spatial genetic signal, the number of individuals sampled, and a variety of other factors. However, these developing empirical findings provide an optimistic outlook on the minimum data size required for the detection of weak landscape-level fragmentation.

Our exploration of the inclusion of missing data yielded similarly optimistic results, where, under a wide range of thresholds, missing genotypes did not substantially alter our spatial landscape genomic findings. Using stringent missing genotype thresholds, which also lowered the number of SNPs in the data, actually decreased the spatial signal. Conversely, allowing for more missing data increased the signal of population structure in our data, with a plateau in the level of significance (sPCA) and

amount of spatial variation explained (MEMGENE). The effect of missing data in population and evolutionary studies has seen mixed results. Simulation-based results have indicated that missing genotypes in RADseq data can result in substantial biases in a range of population genetic summary statistics, including F_{ST} (Arnold et al. 2013). In contrast, the use of more liberal missing data thresholds in RADseq-based phylogenetic studies has provided opportunities to recover phylogenetic patterns not detected using more stringent thresholds (Wagner et al. 2013, Leaché et al. 2015, Eaton et al. 2017). This may be due to a bias whereby loci with higher mutation rates, but likely to contain population or phylogenetic information, are eliminated by stringent missing thresholds (Huang and Knowles 2014); however, this may also fail to remove loci with high error rates. The effect of missing data in landscape genomic studies has yet to be thoroughly explored, and we suggest based on our results that some spatially informed analyses may be robust to the recovery of patterns of weak population structure despite the inclusion of a high level of missing genotypes, but that parameter estimation at this geographic scale (e.g., migration rates) may be more strongly influenced. Therefore, when possible, we second the recommendation of others (Wagner et al. 2013, O'Leary et al. 2018) for researchers to explore the sensitivity of their results across a range of different missing data thresholds.

3.5.3 *Copperhead landscape genomics and temporal considerations*

Our results further emphasize an association between high-traffic roads and genetic differentiation in pit vipers (Clark et al. 2010, DiLeo et al. 2010, DiLeo et al. 2013, Bushar et al. 2015, Herrmann et al. 2017; but see Weyer et al. 2014). These

findings are in addition to field studies that have suggested the outsized role played by road mortality in snakes, and herpetofauna more generally (Andrews and Gibbons 2005, Row et al. 2007, Shepard et al. 2008). Furthermore, our results suggest that the effects of high-traffic roads and associated intense human activity might persist for decades after traffic volumes decline, in line with predictions from simulations (Landguth et al. 2010).

We did not find evidence for a strong influence of surface coal mining on genetic connectivity, which was surprising given the widespread nature of surface mining in the study area, and the wholesale shifts in vegetation, soils, topography, and fauna that characterize the mining and mine reclamation process. However, surface mines are not persistent and seamless barriers as highways often are, and effects of mining may be more difficult to detect due to the lack of a finely resolved footprint. Furthermore, surface mining of coal in Appalachia has a high degree of spatial and temporal variance. Portions of mines can exist in various states of reclamation from barren rock to early successional forest, and mining activity can cease for months to years as a result of fluctuating coal prices or labor disputes, thus providing opportunities for animals to maintain genetic connectivity in these novel landscapes. Additionally, the quality of habitat present on partially reclaimed, uncompacted, and/or revegetated mines has not been thoroughly studied. Regardless, we recommend further research into this generally understudied area, as the large scale and radical impacts of this mining practice may well result in detectable impacts in populations of other taxa (Wickham et al. 2013). This may be especially true for species with shorter generation times, smaller population sizes, and more exclusive associations with ridgetop forests (Epps and Keyghobadi 2015, Maigret et al. 2019).

We note that the connection between the identified genetic fragmentation and the historic highway KY-476 is a largely qualitative assessment, and several specific caveats deserve mention. The route of KY-476 corresponds not only to a highway path, but also to a swath of comparatively higher historic human population density and also to the route of Troublesome Creek, either of which could be factors more important than the highway itself. While modeling relative contributions of population density and road mortality is beyond the scope of our study, in terms of parallel geomorphology and hydrology, the historic highway path does not correspond to any major feature which might be expected to seriously reduce movement of copperheads (Figure S5). Other waterways dividing our sampling locations, including Lost Creek and Buckhorn Creek, are of similar size to Troublesome Creek. Moreover, copperheads and other pit vipers regularly cross bodies of water (T. Maigret, unpublished data; Clark et al. 2010), and studies have found that even hydropower reservoirs are ineffective barriers to gene flow in copperheads and similar species (Oyler-McCance and Parker 2010, Levine et al. 2016). More generally, a second caveat is that while we intended our sampling to be hierarchical in design, the broad scales at which genomic patterns exist in our study area means that we are examining a single functional landscape. When possible, landscape-scale replication would provide a more robust assessment of the effects of current and historic landscape features on gene flow in *A. contortrix* and similar taxa (Short Bull et al. 2011), though replication at this scale is usually cost-prohibitive. Moreover, assuming we have detected a spatial genomic pattern stemming from historic highway traffic, we have not determined the traffic threshold which would produce a noticeable spatial genetic pattern, the possibility of any interactions with snake behavior (e.g., scent

trailing), or the precise time lag which must pass before these patterns become detectable. Other research has suggested that even low amounts of traffic can produce genetic differentiation (Clark et al. 2010), and depending on a variety of demographic and behavioral characteristics, numerous generations may need to pass before genetic differentiation becomes apparent (Landguth et al. 2010, Epps and Keyghobadi 2015). Thus, while we may have detected the effect of a historic roadway, we have not conclusively ruled out impacts of current roadways, or even low-traffic and unpaved county roads not included in our analysis. In a similar manner, our findings regarding the spatial genetic implications of surface mines should also be understood tentatively.

Our study adds to a growing list highlighting the potential for genomic data sets to detect weak, recent, or otherwise subtle spatial genetic patterns (Gonzàlez-Serna et al. 2018, McCartney-Melstad et al. 2018, Murphy et al. 2018, Tan et al. 2018). Considering the problems time lags present for conservation planning, the use of SNP data sets and spatially informed analyses of genetic diversity will likely become increasingly important for placing patterns of population structuring in their proper genomic, temporal, and geographic contexts.

3.6 Acknowledgements

Our work was conducted under University of Kentucky Institutional Animal Care and Use Committee (IACUC) Protocol 2012-0954. Funding was provided by a Theodore Roosevelt Memorial Grant (American Museum of Natural History), McIntire Stennis Project KY009031 (US Department of Agriculture, National Institute of Food and Agriculture), a Karri Casner Environmental Sciences Fellowship (Tracy Farmer Institute

for Sustainability and the Environment), and an Ellers-Billing Award (University of Kentucky Appalachian Center). We are grateful for field assistance provided by David Collett, Erwin Williams, Chris Osborne, Ted Sizemore, Neva Williams, Zach Hackworth, Grover Napier, RB Combs, Anthony Campbell, Scotty Brewer, Mark Chaffins, Doran Howard, Taylor Hughes, Rudy Noble, Verle Fugate, the late Geraldine McIntosh, and other residents of Breathitt, Perry, and Knott counties. We thank the University of Kentucky's Center for Computational Sciences and Information Technology Services Research Computing for use of the Lipscomb Computing Cluster resources. We are grateful for the laboratory assistance of Nicolette Lawrence, Kara Jones, Mary Foley, and Ricky Grewelle.

Table 3.1. List of individual tissue samples used in our analysis, with location information, sampling cluster membership, and inclusion status for the final 2,140 SNP data set.

Individual Number	Site Number	Sampling Cluster	Site Name	Lat	Long	Inclusion
2	24	b	Mule Hol	37.46895	-83.1485	1
3	24	b	Mule Hol	37.46895	-83.1485	1
5	25	b	Cotton Hol	37.481	-83.1357	1
9	26	b	John Carpenter Fk	37.4831	-83.1324	1
10	26	b	John Carpenter Fk	37.4831	-83.1324	1
11	27	b	White Oak Fk	37.3998	-83.1238	1
12	27	b	White Oak Fk	37.3998	-83.1238	1
13	27	b	White Oak Fk	37.3998	-83.1238	1
14	27	b	White Oak Fk	37.3998	-83.1238	1
15	27	b	White Oak Fk	37.3998	-83.1238	1
16	27	b	Snag Ridge Fk	37.46438	-83.1191	1
17	27	b	Snag Ridge Fk	37.46438	-83.1191	1
20	25	b	Cotton Hol	37.481	-83.1357	0
24	24	b	Mule Hol	37.46895	-83.1485	0
29	25	b	Cotton Hol	37.481	-83.1357	1
34	27	b	Old Cove Hol	37.46636	-83.1275	1
35	27	b	White Oak Fk	37.3998	-83.1238	0
67	23	b	Mart Br	37.45353	-83.1608	1
74	24	b	Mule Hol	37.46895	-83.1485	0
75	24	b	Mule Hol	37.46895	-83.1485	0
110	28	d	Williams Br	37.3998	-83.1539	1
111	20	b	Bear Br	37.46429	-83.1922	1
112	20	b	Bear Br	37.46429	-83.1922	1
114	21	b	Little Buckhorn	37.44639	-83.1898	1
116	22	b	Engineering Bottom	37.4538	-83.1613	1
117	34	e	Stewart Farm	37.39025	-82.9692	1
118	9	c	Clear Fk	37.34391	-83.2884	1
121	28	d	Williams Br	37.3998	-83.1539	1
122	34	e	Stewart Farm	37.39025	-82.9692	0
124	15	a	Hardshell	37.45625	-83.264	1
125	34	e	Stewart Farm	37.39025	-82.9692	0

Table 3.1 (continued). List of individual tissue samples used in our analysis, with location information, sampling cluster membership, and inclusion status for the final 2,140 SNP data set.

126	4	a	Leatherwood Cr	37.41266	-83.3075	1
127	20	b	Bear Br	37.46429	-83.1922	1
128	14	a	Barge Cr	37.45656	-83.2826	0
132	2	a	Leatherwood Cr	37.43264	-83.3166	0
136	19	d	Rowdy	37.40221	-83.2074	1
137	12	c	Shinglepin Br	37.29126	-83.2792	0
138	10	c	Napier Br	37.31974	-83.3094	1
139	34	e	Stewart Farm	37.39025	-82.9692	1
140	14	a	Barge Cr	37.45656	-83.2826	1
141	1	a	Mill Br	37.44973	-83.3262	1
142	16	a	Ganderbill Br	37.43878	-83.2963	1
143	16	a	Ganderbill Br	37.43878	-83.2963	1
144	14	a	Barge Cr	37.45656	-83.2826	0
146	14	a	Barge Cr	37.45656	-83.2826	1
147	7	c	Trace Fk	37.36081	-83.2936	1
150	12	c	Shinglepin Br	37.29126	-83.2792	1
151	34	e	Stewart Farm	37.39025	-82.9692	1
152	34	e	Stewart Farm	37.39025	-82.9692	1
153	35	e	Terry Br	37.38292	-82.9626	1
155	12	c	Shinglepin Br	37.29126	-83.2792	0
156	22	b	Engineering Bottom	37.4538	-83.2963	1
157	12	c	Shinglepin Br	37.29126	-83.2792	0
158	12	c	Shinglepin Br	37.29126	-83.2792	0
159	12	c	Shinglepin Br	37.29126	-83.2792	1
160	10	c	Napier Br	37.31974	-83.3094	0
161	10	c	Napier Br	37.31974	-83.3094	1
162	10	c	Napier Br	37.31974	-83.3094	1
163	34	e	Stewart Farm	37.39025	-82.9692	1
164	34	e	Stewart Farm	37.39025	-82.9692	1
165	35	e	Terry Br	37.38292	-82.9626	1
166	10	c	Napier Br	37.31974	-83.3094	1
167	14	a	Barge Cr	37.45656	-83.2826	0
168	31	d	Toms Br	37.37692	-83.1869	1
169	1	a	Mill Br	37.44973	-83.3262	0

Table 3.1 (continued). List of individual tissue samples used in our analysis, with location information, sampling cluster membership, and inclusion status for the final 2,140 SNP data set.

170	5	a	River Caney	37.40012	-83.3316	1
171	20	b	Bear Br	37.46429	-83.1922	1
172	11	c	Rocklick Br	37.30327	-83.293	1
174	28	d	Williams Br	37.3998	-83.1539	1
175	not listed	(c)	Spencer Fk	37.3438	-83.3266	0
176	1	a	Mill Br	37.44973	-83.3262	0
180	7	c	Trace Fk	37.36081	-83.2936	1
181	31	d	Toms Br	37.37692	-83.1869	1
182	16	a	Ganderbill Br	37.43878	-83.2963	0
183	31	d	Toms Br	37.37692	-83.1869	0
184	2	a	Leatherwood Cr	37.43155	-83.3167	1
186	12	c	Shinglepin Br	37.29126	-83.2792	1
187	35	e	Terry Br	37.38292	-82.9626	1
188	33	e	Hard Fk	37.39902	-83.0227	1
189	8	c	Chavies	37.35668	-83.329	1
190	7	c	Trace Fk	37.36081	-83.2936	0
191	7	c	Trace Fk	37.36081	-83.2936	1
193	16	a	Ganderbill Br	37.43878	-83.2963	1
194	31	d	Toms Br	37.37692	-83.1869	0
195	31	d	Toms Br	37.37692	-83.1869	0
197	not listed	(d)	476	37.42618	-83.2116	0
199	31	d	Toms Br	37.37692	-83.1869	0
201	22	b	Engineering Bottom	37.4538	-83.2963	0
202	9	c	Clear Fk	37.34391	-83.2884	0
203	3	a	Leatherwood Cr	37.42997	-83.3152	1
204	1	a	Mill Br	37.44973	-83.3262	0
205	9	c	Clear Fk	37.34391	-83.2884	1
206	6	a	Oatspatch Hol	37.39487	-83.3561	1
207	30	d	Rowdy	37.37378	-83.2096	1
208	32	d	Hunter Ch	37.35696	-83.1979	1
210	15	a	Hardshell	37.45625	-83.264	0
212	15	a	Hardshell	37.45625	-83.264	1
213	17	d	Rowdy	37.4056	-83.2139	1
214	18	d	Rowdy	37.40381	-83.2096	1

Table 3.1 (continued). List of individual tissue samples used in our analysis, with location information, sampling cluster membership, and inclusion status for the final 2,140 SNP data set.

215	15	a	Hardshell	37.45625	-83.264	1
216	35	e	Terry Br	37.38292	-82.9626	1
217	32	d	Hunter Ch	37.35696	-83.1979	1
226	13	c	Busy	37.27562	-83.2891	1
227	36	e	Soft Shell	37.40261	-83.941	1
228	33	e	Hard Fk	37.39902	-83.0227	1
229	33	e	Hard Fk	37.39902	-83.0227	1
230	33	e	Hard Fk	37.39902	-83.0227	1

Table 3.2. Landcover reclassification scheme for our ResistanceGA resistance surface.

NLCD 2011 Class	Percent of Study Area	Reclassified Class
41 Deciduous Forest	60.6%	1 Unmined land
42 Mixed Forest	0.5%	
43 Evergreen Forest	4.4%	
90 Woody Wetlands	0.004%	
95 Emergent Herbaceous Wetlands	0.005%	
31 Barren Land (Rock, Sand, Clay)	8.4%	2 Minelands
52 Shrub/Scrub	0.1%	
71 Grassland/Herbaceous	17.5%	
21 Developed, Open	4.3%	1 Unmined land[1]
22 Developed, Low Intensity	2.0%	
23 Developed, Medium Intensity	0.9%	
24 Developed, High Intensity	0.2%	
81 Pasture/Hay	1.0%	
82 Cultivated Crops	0.3%	
Route of KY State Highways 15, 28, 80, and 550	0.5%	Current Highways (dichotomous raster, highway/non-highway)
Route of current KY 476, northernmost portion of KY 15	0.3%	Historic Highways (dichotomous raster, highway/non-highway)

[1]Where portions of these categories overlap with Reclassified Classes 6 and 7 they are replaced by the reclassified class designation associated with the highway(s).

Table 3.3. Summary statistics for read depths from m = 4, m = 5, and m = 7, each using the same locus and individual filtering protocols as described in the text.

Read Depth (m)	**Number of Loci After Filtering**	**Number of Individuals after Filtering**	**H_O**	**H_E**	**π**	**F_{IS}**	**N_e (95% CI)**
4	2174	77	0.199	0.244	0.245	0.184	640.9 (600.7, 686.8)
5	2140	77	0.193	0.240	0.242	0.195	635.8 (595.6, 681.6)
7	2039	77	0.204	0.245	0.247	0.168	629.5 (588.0, 577.1)

Table 3.4. Model output from our ResistanceGA least-cost path analyses. A null model of no geographic structure and a model of isolation-by-distance outperformed all combinations of resistance surfaces based on historic roads, current roads, and surface mining.

Surface	k	AIC	AICc	R^2m	R^2c	LL	ΔAICc	Weight
null	1	-10766.7	-10770.6	0	0.7057	5386.35	0	0.563
distance	2	-10764.8	-10768.6	1.30e-05	0.7057	5386.39	2.034	0.204
new_rds	3	-10764.9	-10766.5	4.17e-05	0.7059	5386.44	4.110	0.072
mines	3	-10764.8	-10766.5	2.23e-05	0.7057	5386.42	4.146	0.071
old_rds	3	-10764.8	-10766.4	1.30e-05	0.7057	5386.39	4.210	0.069
mines. + new_rds	5	-10764.8	-10761.9	1.30e-05	0.7057	5386.39	8.758	0.007
mines. + old_rds	5	-10764.8	-10761.9	1.30e-05	0.7057	5386.39	8.758	0.007
new_rds. + old_rds	5	-10764.8	-10761.9	1.30e-05	0.7057	5386.39	8.758	0.007
mines. + new_rds. + old_rds	7	-10764.8	-10757	1.30e-05	0.7057	5386.39	13.585	0.001

Table 3.5. Minor allele frequencies for each level of subsampling and missing data.

Number of loci subsets (ten replicates each)	**Mean minor allele frequency**	**Minor allele frequency range among ten replicates**
n = 25	0.181	(0.140, 0.251)
n=50	0.163	(0.127, 0.193)
n=100	0.165	(0.144, 0.187)
n=250	0.165	(0.150, 0.176)
n=500	0.169	(0.165, 0.182)
n=1000	0.166	(0.163, 0.169)
Missing data thresholds (a single data set per threshold)	**Minor allele frequency**	
5%	0.059	
10%	0.08	
25%	0.112	
40%	0.124	
50%	0.129	
75%	0.145	
90%	0.161	
95%	0.175	

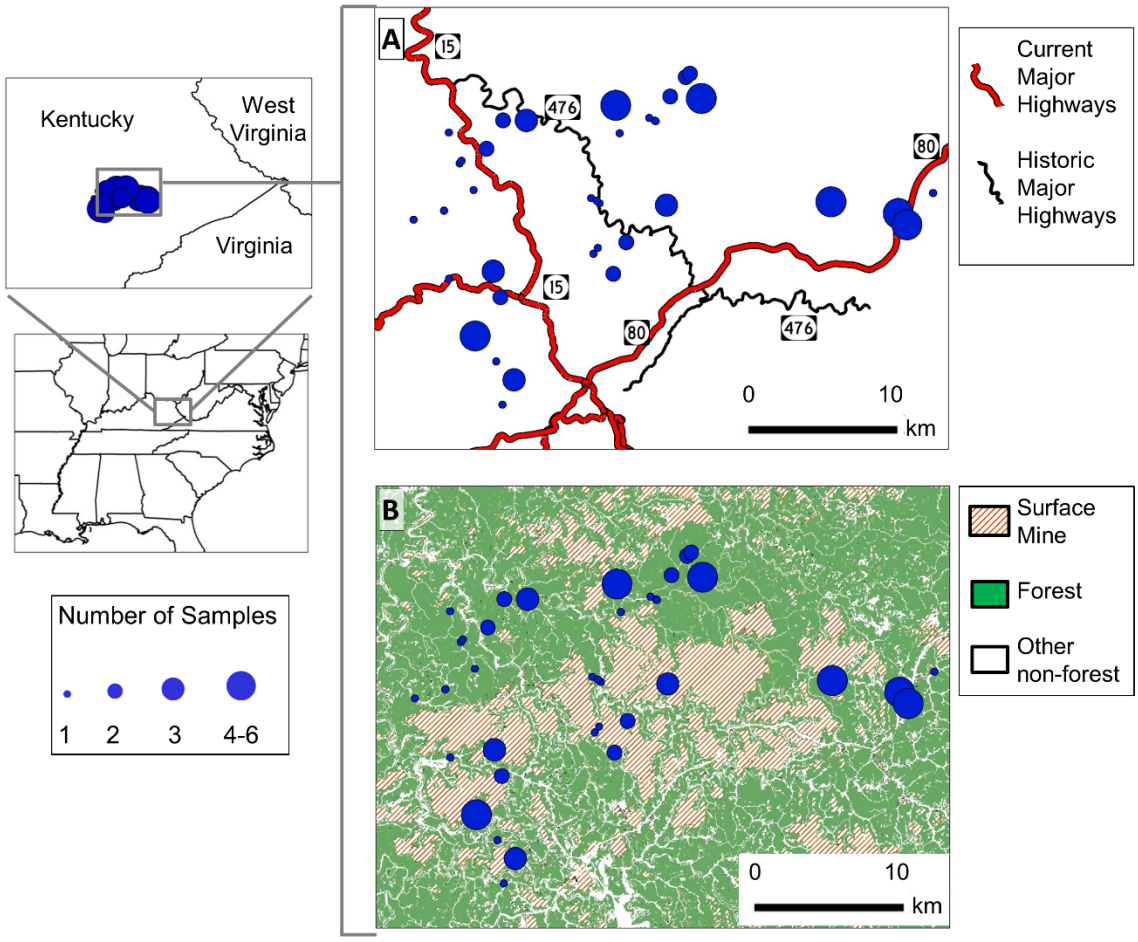

Figure 3.1. Map of our study area and sampling localities superimposed over (A) the current and historic highway network, and (B) landcover, including surface coal mines, forest, and other non-forest habitat. The number of samples from each site is indicated by the size of each circle overlaying each sampling location and refers to samples included in our final analysis. For further information regarding sampling site locations and sampling cluster arrangement, see Figure S1.

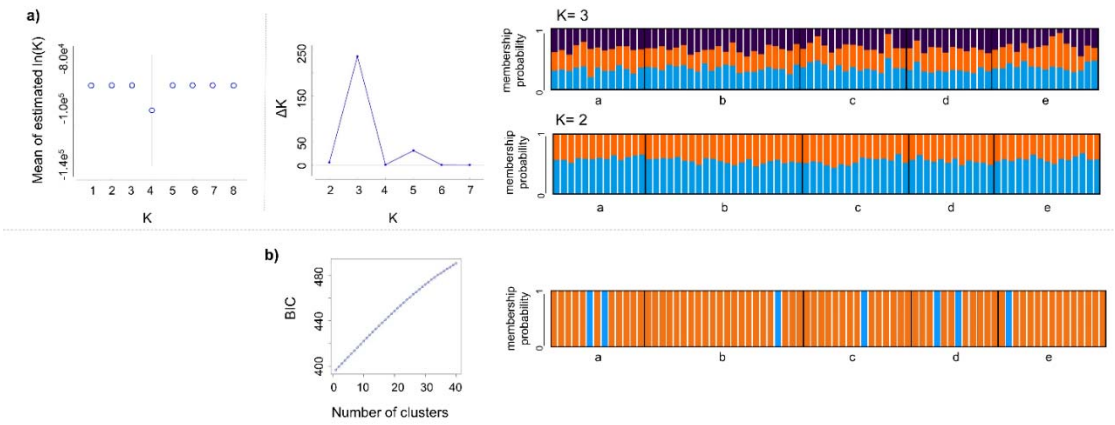

Figure 3.2. Results of nonspatial population structure analyses, including (a) ln(*K*), Δ*K*, and individual assignment plots from Structure for *K* = 3 and *K* = 2, and (b) BIC and individual assignment plots from DAPC. Letters beneath each individual assignment plot correspond to the geographically distinct sampling clusters depicted in Figure S1.

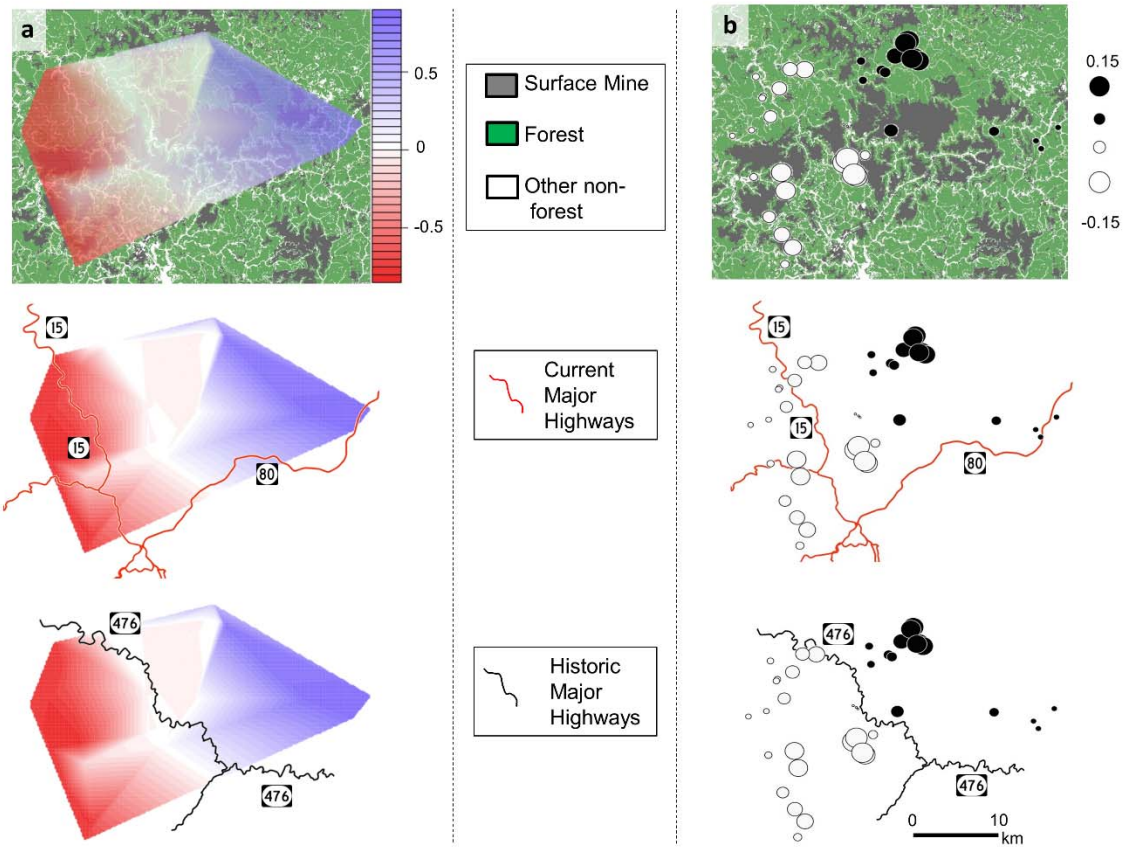

Figure 3.3. Results of our spatially informed population structure analyses. (a) Results of sPCA analyses visualized using interpolated vector scores, showing divergence coinciding with the historic highway path (designated in this study as KY-476), but not with landcover or current highway infrastructure. (b) Results of MEMGENE analysis, which suggests similar patterns of population structure associated with KY-476. Circle color and size represent the association and genetic similarity, respectively, along the first MEM variable axis.

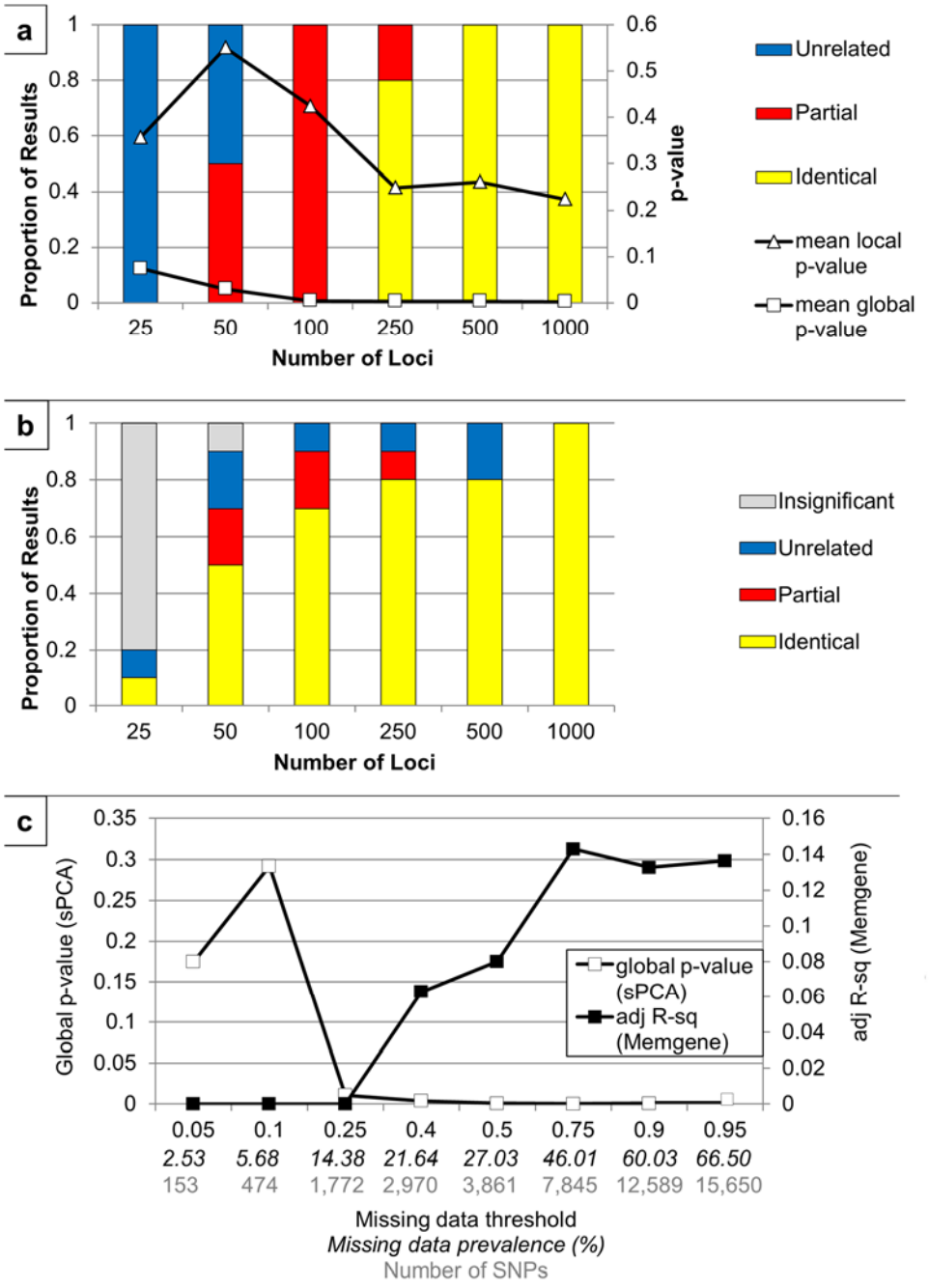

Figure 3.4. Effects of the number of loci and missing data on (a) sPCA and (b) MEMGENE results, and the effects of missing data levels on both sets of results (c). For (a) and (b), the left y-axis represents the proportion of results which were identical, similar, or unrelated to the results obtained from the full data set depicted in Figure 3. Visualization

results from each replicate are available in Figure S6. The right y-axis for (a) represents p-values from global (positive autocorrelation) and local (negative autocorrelation) tests for structuring. The x-axis of (c) displays the missing data threshold for inclusion, the actual missing data prevalence, and the number of loci for each level of analysis.

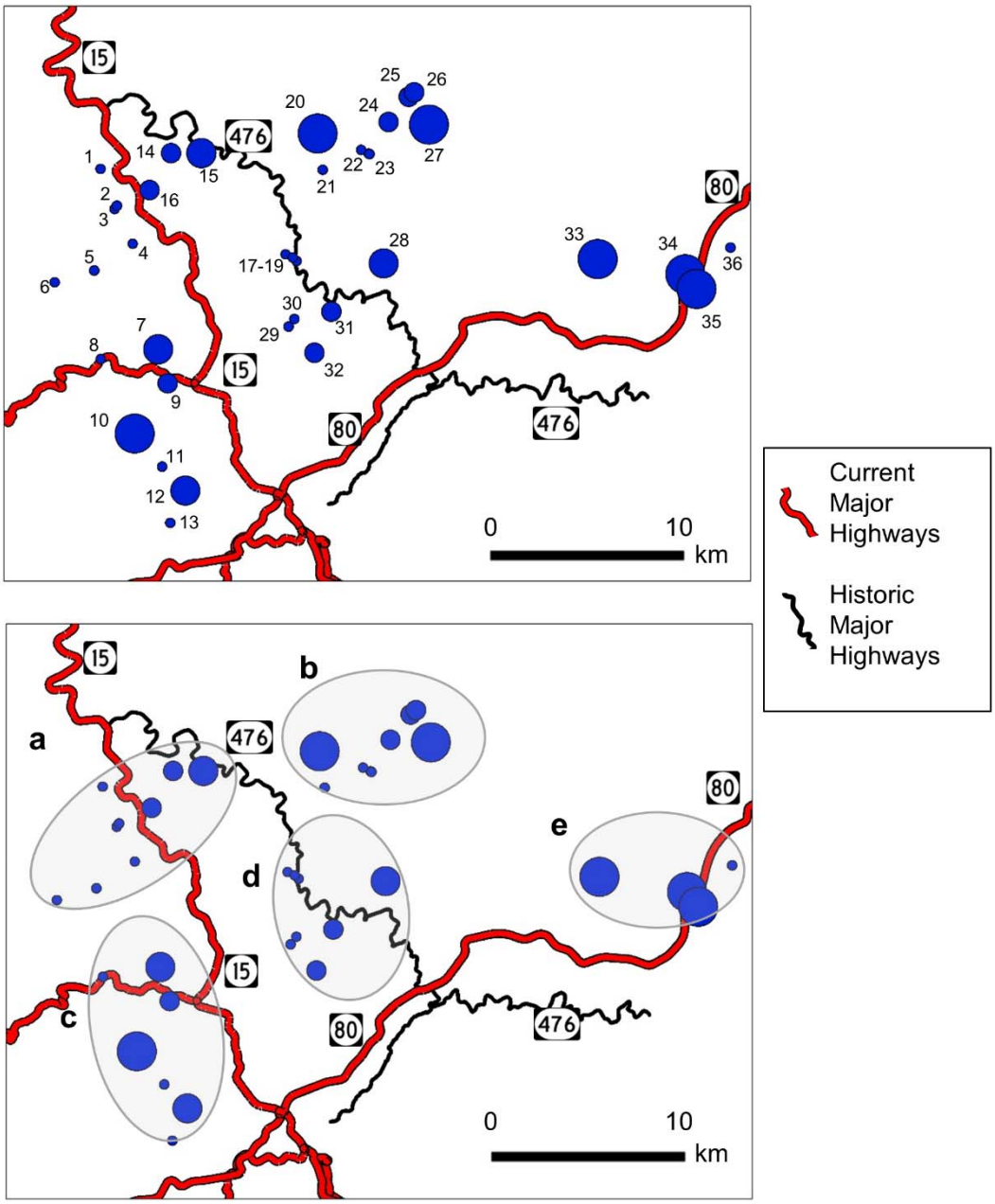

Figure 3.5. Map of study area with sampling locations marked individually (1-36) and by sampling cluster membership (a-e). Cluster numbers correspond to Figure 2 assignment plots, while sampling location numbers correspond to locations listed in Table S1.

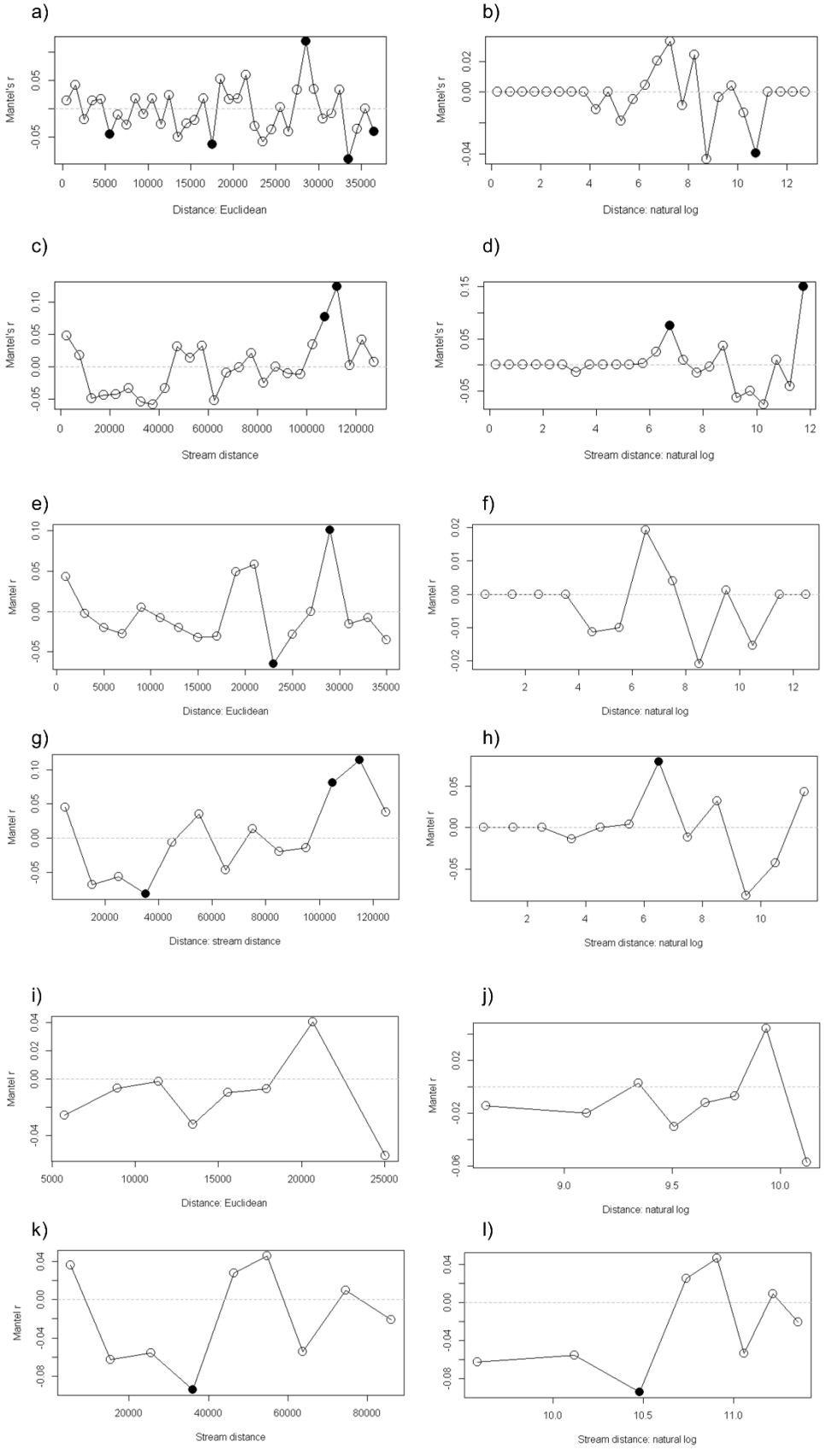
a)
Mantel's r
Distance: Euclidean
b)
Mantel's r
Distance: natural log
c)
Mantel's r
Stream distance
d)
Mantel's r
Stream distance: natural log
e)
Mantel r
Distance: Euclidean
f)
Mantel r
Distance: natural log
g)
Mantel r
Distance: stream distance
h)
Mantel r
Stream distance: natural log
i)
Mantel r
Distance: Euclidean
j)
Mantel r
Distance: natural log
k)
Mantel r
Stream distance
l)
Stream distance: natural log

Figure 3.6 (previous page). Mantel correlograms for individual genetic differentiation versus (a) Euclidean distance, lag of 1 km (b) natural log of Euclidean distance, lag of 0.5, (c) stream distance, lag of 10 km and (d) natural log of stream distance, lag of 0.5. Filled circles represent significant values at $\alpha = 0.05$. Parts (e) – (h) represent the same categories as (a) –(d), only with double the lag distance. Parts (i) – (l) represent lag distances with equivalent sample sizes in each class: each class is defined by one-tenth quantile boundaries.

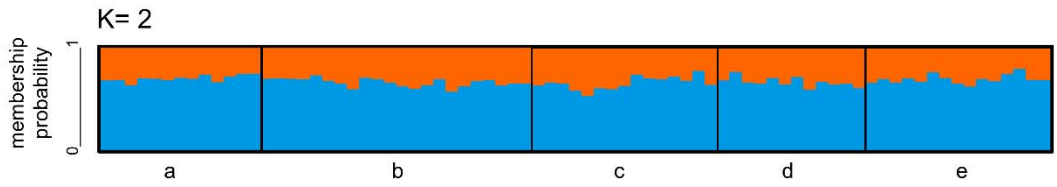

Figure 3.7. Individual assignment plot resulting from our Structure analyses conducted with prior information regarding sampling location (LocPrior).

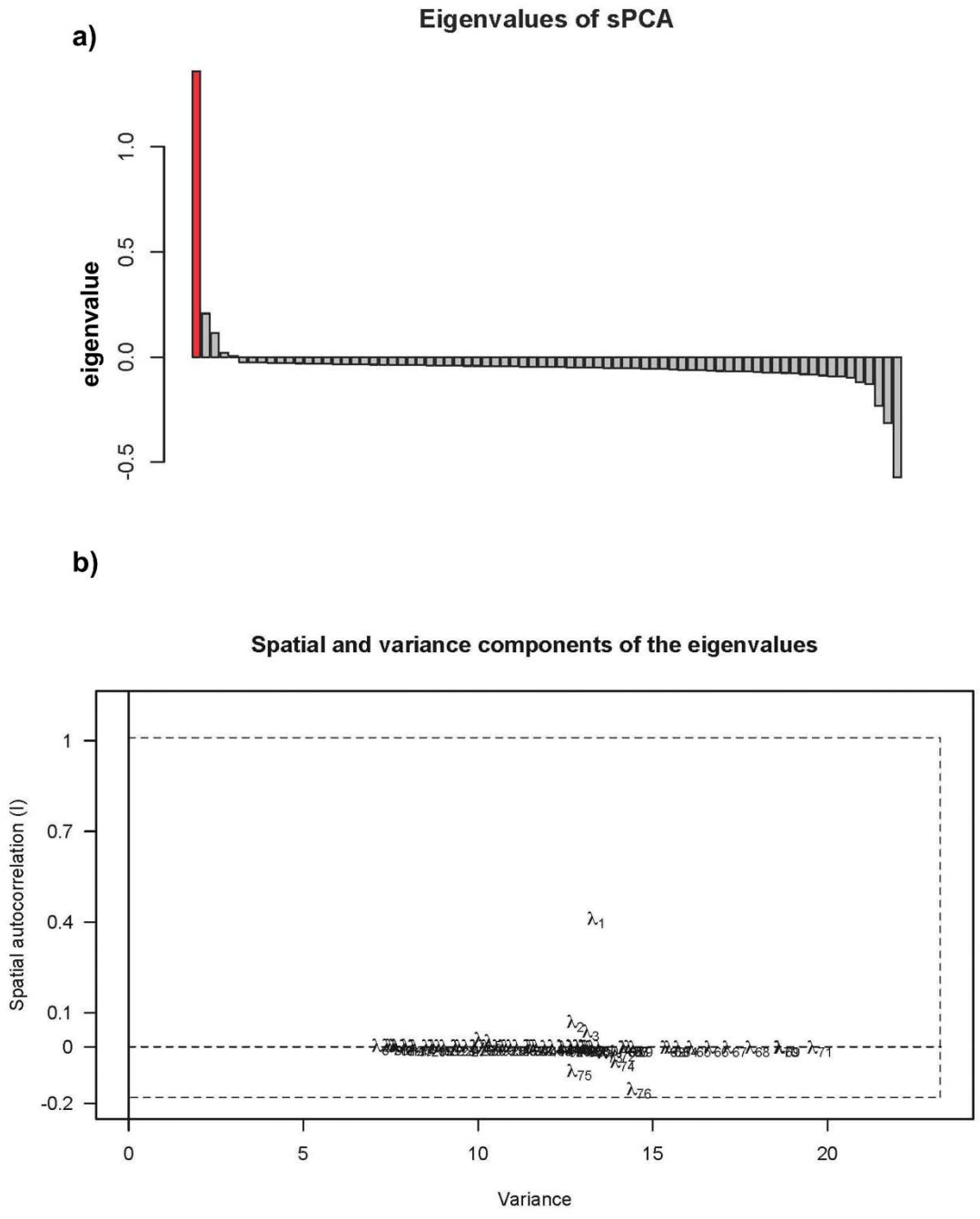

Figure 3.8. Eigenvalue plot (a) and scree plot (b) of local (negative) and global (positive) axes obtained from our sPCA analyses. The first global axis, in red, was the only axis retained, and displays unique separation from other potential axes in the scree plot (labeled as λ_1).

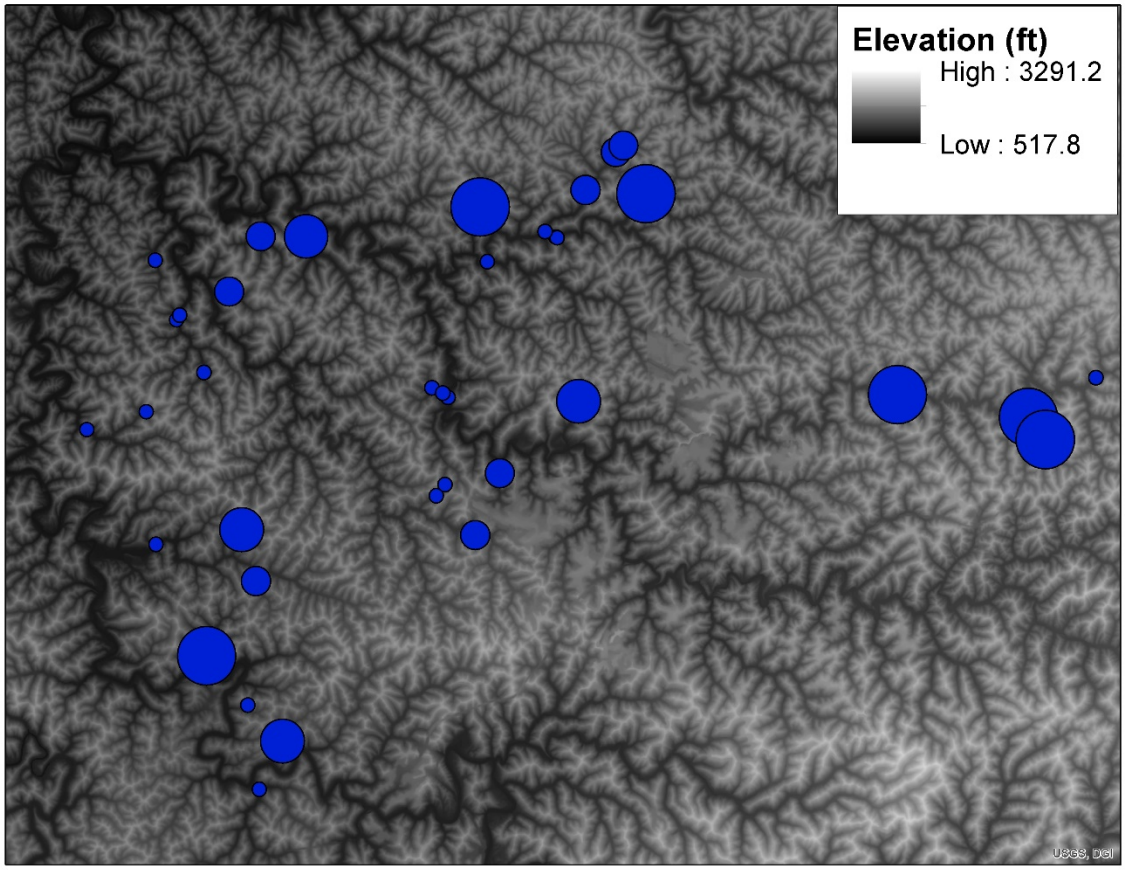

Figure 3.9. Digital elevation model of study area, with sample points corresponding to Figure 1.

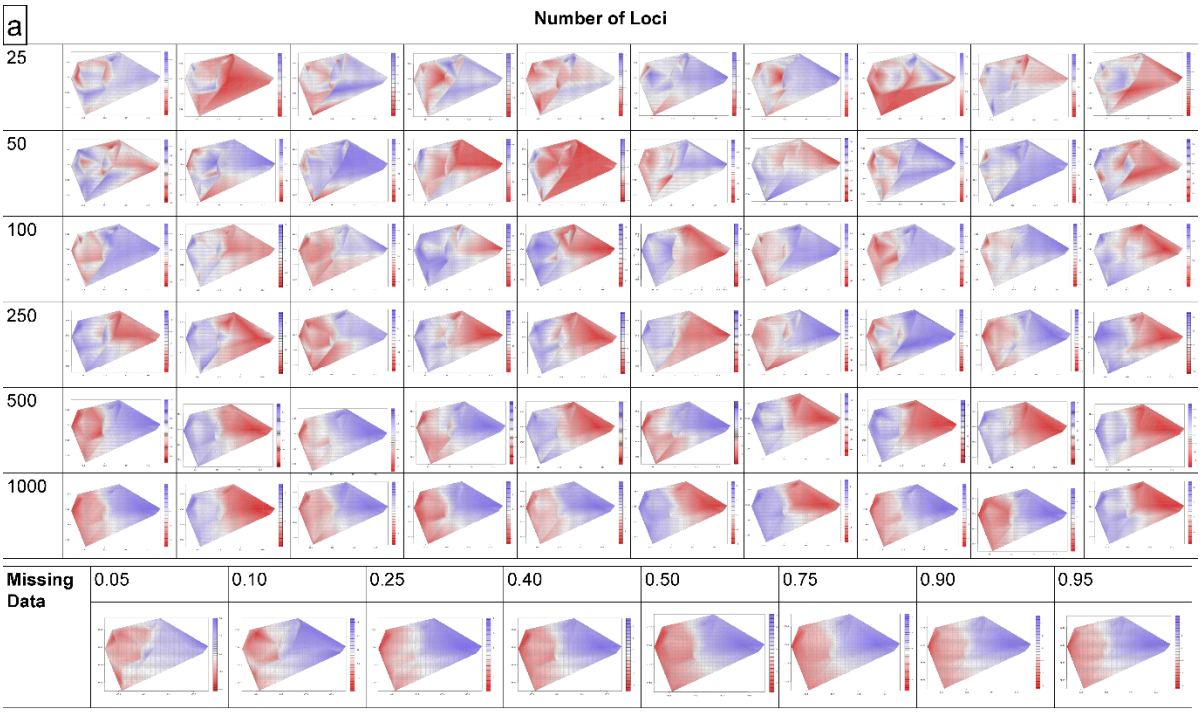

Figure 3.10. Visualizations of results from each of the ten replicates for each random subset of loci, and each level of missing data. Includes (a) interpolated vector scores from sPCA, (b) plotted scores from sPCA, and (c) plotted MEM scores for significant results.

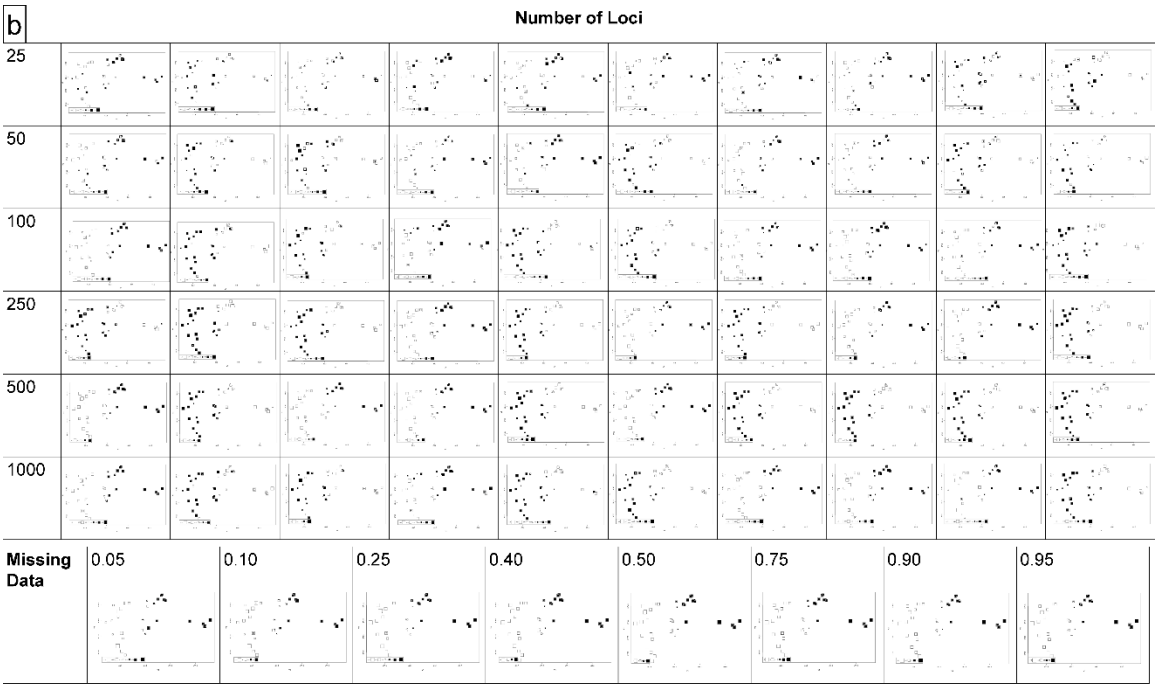

Figure 3.10 (continued). Visualizations of results from each of the ten replicates for each random subset of loci, and each level of missing data. Includes (a) interpolated vector scores from sPCA, (b) plotted scores from sPCA, and (c) plotted MEM scores for significant results.

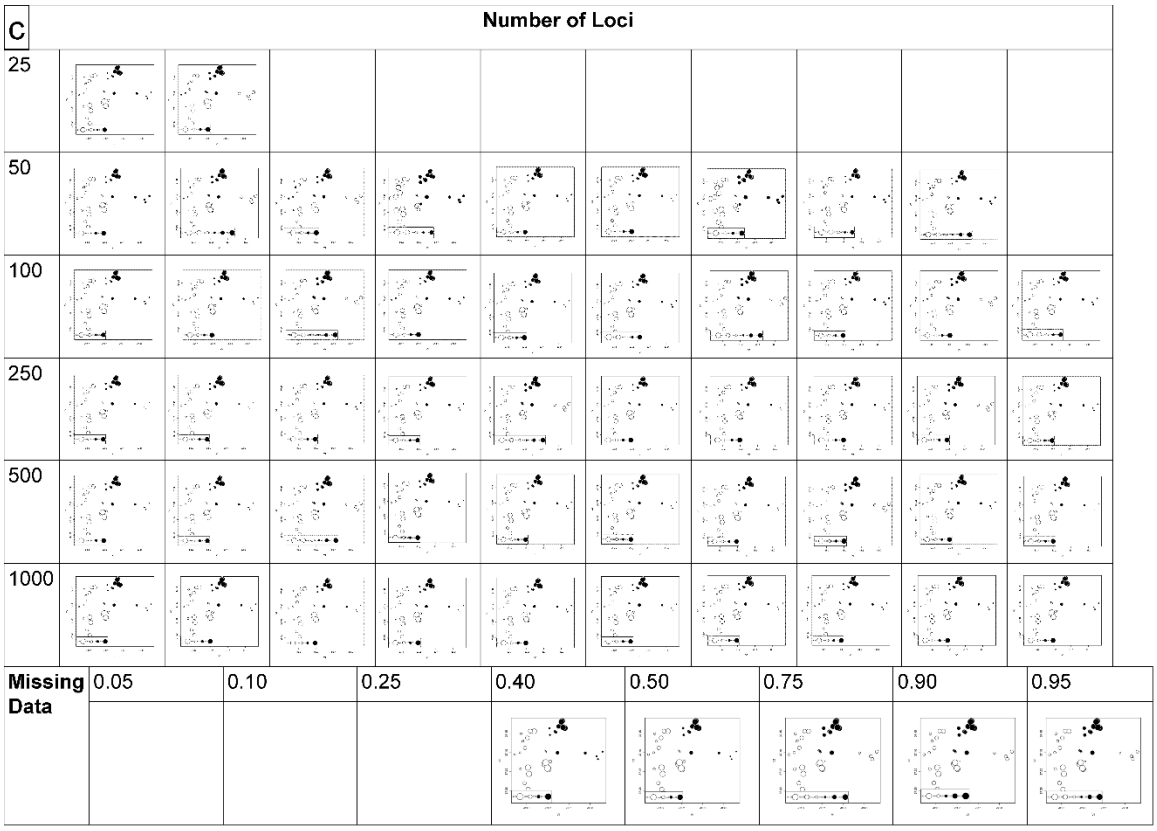

Figure 3.10 (continued). Visualizations of results from each of the ten replicates for each random subset of loci, and each level of missing data. Includes (a) interpolated vector scores from sPCA, (b) plotted scores from sPCA, and (c) plotted MEM scores for significant results.

CHAPTER 4:

SHIFTING ENERGY POLICY PRIORITIES REGULATE IMPACTS OF COAL MINING ON EARTH'S TOPOGRAPHY

4.1 Abstract

Long a primary source of energy, coal will continue to be a major fuel for electricity generation in developing and developed countries alike (IEA 2018, Normile 2018). However, as surface mining methods have increased in popularity, coal extraction has radically altered the topography of many coal-producing regions worldwide, with far-reaching consequences for terrestrial and freshwater ecosystems (Palmer et al. 2010, Wickham et al. 2013, Ross et al. 2016). Advances in geospatial technology now allow researchers to create accurate time-series data sets of land use change, permitting longitudinal analyses of the landscape-level effects of resource extraction (Vierling et al. 2008, Pericak et al. 2018); yet the extent to which regulatory policies can mitigate the environmental consequences of coal extractive activities, including methods known as "mountaintop removal" mining, remains unclear. Here we used historical topographic maps and current three dimensional LiDAR imagery to show evidence for an abrupt shift in the topographic patterns of surface coal mining across a major eastern US coalfield, which followed directly after a 2010 realignment of federal policies imposing stricter regulation of the filling of stream valleys with mining spoil. While mining impacts on stream valleys showed a substantial decline since 2010, our data suggest an unintended consequence of this policy shift may be that mining has become more concentrated in ridgetops. Furthermore, while the new policy has caused stream valleys to be restored to elevations more similar to pre-mining elevations, patterns of elevation loss for ridgetops continue unabated. Our results are evidence for the efficacy of federal policies aimed at

protecting aquatic ecosystems from surface mining, but also their inadequacy towards preserving terrestrial ecosystem biodiversity. We recommend that LiDAR-derived elevation data continue to be gathered to investigate the future impacts of surface mining as energy and environmental policies change with the political winds in the US and elsewhere.

4.2 Main Text

Coal was a crucial source of energy for the industrialization of developed nations throughout the 19th and 20th centuries, and coal is projected to remain a dominant fuel for electricity generation in developing countries in the 21st century (Chabukdhara and Singh 2016, IEA 2018, Zeng et al. 2018, Tongia and Gross 2019). While underground coal mining methods remain in use, surface coal mining has become increasingly adopted, both due to improvements in surface mining technology and because surface mining can extract a higher proportion of coal than underground mining. In regions where mining takes place, the economic benefits of the coal industry for local communities can be transformative, catapulting rural hinterlands into wealth and political influence. For example, surface coal mining has recently helped propel the economy of Ordos City, in Inner Mongolia, China, from among the poorest to among the wealthiest cities in China, with a GDP per capita rivaling that of Hong Kong and Macau (Zeng et al. 2018). However, the drawbacks of surface coal mining operations are also noteworthy, as this practice has been implicated as the cause of numerous environmental problems ranging from water and air pollution to deforestation and landscape homogenization

(Wickham et al. 2007, Palmer et al. 2010, Lindberg et al. 2011, Maigret et al. 2019). This is especially true in mountainous terrain, where mining spoil is most cost-effectively disposed of by the filling of adjacent stream valleys in a practice often described as "mountaintop removal" mining (Palmer et al. 2010). Burying freshwater streams under large amounts of mining spoil not only destroys the streams which are buried, but can increase pollutants downstream of valley fills, and numerous studies have documented significant negative consequences for aquatic life across multiple trophic levels (Pond et al. 2008, Lindberg et al. 2011, Muncy et al. 2014).

To mitigate these negative externalities, many governments have sought to implement statutes regulating surface coal mining operations. In the United States, where for decades most coal has been produced from surface mines, surface mining is generally regulated at the federal level by two mechanisms: the Surface Mining Control and Reclamation Act (SMCRA), enforced by the Office of Surface Mining (OSM), and the Clean Water Act (CWA), enforced by the Army Corps of Engineers (ACE) in tandem with the Environmental Protection Agency (EPA). While SMCRA requires 'approximate original contours' of mined land to be restored, variances from this requirement are frequently granted by OSM because restoration of steep-relief topography with fragmented rock is often impossible, and strict enforcement of this rule would effectively prohibit surface mining in rugged terrain (Copeland 2015). Federal permits granted by ACE are required for the dumping of spoil into stream valleys ("valley fills") and are thus mandated for most large-scale surface mining operations. Although for decades these stream fill permit applications were typically assessed without any additional scrutiny by EPA, in 2009 the Obama administration directed EPA and ACE to more strictly oversee

the granting of permits for stream valley fills associated with surface coal mining in Appalachia, a major coal-producing region of the eastern US, to combat negative consequences of surface mining for aquatic ecosystems (US EPA 2009, 2011). This resulted in more stringent reclamation requirements for valley fills, and in many cases permits which would have passed scrutiny under past administrations were no longer granted or were delayed to the point where the potential mining operations were unprofitable (Copeland 2015).

The primary motivation for this shift in federal policy was the concern regarding the impacts of surface coal mining on freshwater ecosystems (US EPA 2009), but the effects on terrestrial ecosystems are comparably severe despite being generally overlooked by researchers and policymakers (Wickham et al. 2013). Restoration of surface mining sites is challenging, as mining reclamation often produces landscapes where reforestation is impeded due to soil compaction, herbivory, and competition from invasive species (Zipper et al. 2011, Oliphant et al. 2017, Hackworth et al. 2018). The radical landscape-scale homogenization of topography, which characterizes many surface mining operations, is likely to produce less diverse landscapes by eliminating microhabitats associated with topographic diversity (Wickham et al. 2013, Maigret et al. 2019). Thus while the motivations for the circa 2010 policy shift were based on research into the surface mining impacts on freshwater ecosystems, the impacts on terrestrial ecosystems are considerable, but have not been at the forefront of policy formulation.

Recently, three-dimensional LiDAR-based remote sensing technologies have allowed researchers to examine the influence of surface mining on the geomorphologic trajectories of coal-producing landscapes, and new uses of long time series of Landsat

imagery have allowed for accurate estimates of mining activity across time (Vierling et al. 2008, Ross et al. 2016, Pericak et al. 2018, Yu et al. 2018, Maigret et al. 2019). We used geospatial data of active mining extent derived from Landsat imagery to quantify newly mined land in Appalachian Kentucky, a major coal-producing region of the eastern US, on an annual basis for the period of 1986-2018. To explore the topographic trends of surface coal mining across time in light of shifting federal policy priorities, we used historic pre-mining elevation data to categorize the land into five landform categories based on topographic position index (TPI), and tested for change points and outliers in the proportion of newly mined land assigned to different topographic positions during each year (see Methods). We considered the possibility that factors alongside policy can affect topographic trends of surface mining in our study area and used an autoregressive modeling approach to estimate the importance of policy among a set of alternative variables associated with mining activity. By making comparisons to post-mining Lidar-derived elevation data, we found patterns in how mined land transitioned between different landforms across three decades of mining and how raw elevation of landforms were transformed as mining practices adapted to different regulatory conditions.

Our longitudinal analyses revealed a substantial shift in the topographic effects of surface mining coinciding with the circa 2010 shift in federal policy, which made permits for the filling of streams more difficult to acquire. While trends in the topographic effects of surface mining held relatively constant from 1986-2004, a gradual decline beginning in 2005 slowly reduced the proportion of newly mined land that consisted of stream valleys. This gradual trend was hastened in 2010 by a sudden precipitous drop in the proportion of newly mined land consisting of stream valleys (Figure 1). Commensurately,

the proportion of mined land positioned in upper slope areas increased gradually from 2005 until plateauing in 2010, while land with very high topographic positions (i.e., ridgetops) experienced a steep increase in proportional new mining beginning in 2010. Beginning in 2016, this trend sharply reversed. Stream bottom, lower slope, and middle slope land became mined more frequently, and upper slope and ridgetop positions less frequently. However, the total amount of land newly mined annually from 2015-2018 was only about half that during the period from 2010-2015, and about a quarter of a typical year before 2010.

We detected a significant level-shift outlier in 2011, whereby the percentage of total land mined that fell into the lowest TPI category ("stream bottom") significantly declined (Figure 2). This pattern was found across a panel incorporating two distinct TPI classification schemes and three spatial scales of analysis (see Methods; Figure S3). Along similar lines, our calculations of topographic transition show that during and before 2010, land with very low topographic position ("stream bottom") frequently transitioned to land with middle topographic position, consistent with valley-filling practices (Figure 3). This trend, however, shifts abruptly after 2010, contemporaneous with a trend of land with very high ("ridgetops") and very low topographic position remaining in its original classification more frequently. We were unable to assess topographic transitioning after 2015 due to a lack of recent elevation data; the last year of LiDAR-derived data available was 2017.

Contemporaneously, both the amount of coal produced from Appalachian surface mines and the amount of land mined decreased precipitously beginning in the late 2000s (Figure 1); thus the effects of the policy may be diluted among the general decline in

mining due to economic and efficiency factors such as the price of coal, declining cost-effectiveness of mining, and declining reliance on coal for electricity generation in the US. Yet when modeling the annual proportion of newly mined land that fell into the lowest and the highest topographic class, both generalized least-squares (GLS) models and autoregressive models with order 1 (AR-1) designs were the best fit when the variable representing policy was integrated as a predictor (Table S1). For modeling the trend in the proportion of mined land consisting of stream bottom, the best fit GLS and AR-1 models included policy and coal price; the best-fit AR-1 model contained policy alone (GLS AICc = 124.9, AR-1 AICc = 122.5). For ridgetops, the GLS model included policy and coal mining efficiency in the best fit model; the best-fit AR-1 model included policy alone (GLS AICc = 153.7, AR-1 AICc = 148.7).. Out of the top five models in each of the four model categories (GLS and AR-1 for stream bottom and ridgetop), only three of the top twenty models weighted by AICc did not include policy as a predictor, all for ridgetop proportion. Moreover, our 32-year data set includes several boom-bust cycles, where the amount of land mined fluctuated substantially, and no topographic shifts like those seen in 2010-2018 are visible during previous cycles (Figure 1, Figure S2).

Our analysis not only demonstrated the efficacy of the Obama's environmental policy in protecting stream bottoms, but also uncovered a potential unintended consequence of this policy shift. As permits for valley fills became less common, the proportion of mined land which would have been stream bottoms was not redistributed proportionally to other topographic classes; rather, ridgetops and upper slopes become a greater proportion of the total land affected by mining (see example, Figure 4). In

addition, we found that while changes in mine reclamation post-2010 have resulted in stream bottoms possessing post-mining raw elevations more similar to pre-mining elevations, ridgetops experienced elevation losses of a nearly identical nature both before and after 2010 (Figure 3). Between 2011-2015, land that transitioned from stream bottom to middle slope and lower slope positions was about 12.4 m and 5.0 m lower, respectively, than the pre-2010 average. In contrast, ridgetop that transitioned to middle slope and upper slope between 2011 and 2015 was only about 0.7 m higher and 0.4 m lower, respectively, than the pre-2010 average. This suggests that companies operating large mines may be adapting to the new regulatory environment by depositing spoil atop land flattened by mining that occurred years or decades beforehand, allowing for continued mining of ridgetops without the need for valley fills; however, the extent of this practice has not been investigated. The results did show that post-2010, ridgetops are more likely than in previous years to maintain their original topographic position, and since less land is being mined overall, gross impacts were lower from 2011-2015 than in previous years. Yet due to the inertia of this policy shift, if new markets or higher domestic demand for coal causes a return of surface mining at the scale of the 1990s or 2000s, the potential now exists for even greater disproportionate losses of ridgetops than the disparity which preceded the policy shift (Figure 1). The topographic distribution of mining permits for unmined land also suggests a disproportionate emphasis on ridgetops in the years to come (Maigret et al. 2019). Meanwhile, data from 2016-2018 appear to show a much lower proportion of newly mined land consisting of ridgetop. This may be due to new mining along the contours of middle and lower topographic positions, which now constitutes a larger proportion of total mined land than in years past. Contour mining

typically does not result in valley fills (Figure S3), though new elevation data will need to be collected to determine the extent to which elevation change is occurring in mined stream bottoms and lower slopes post-2015.

Our findings highlight both the long-term and annually temporal trend of regulatory mechanisms for mitigating portions of the environmental damage caused by an increasingly popular yet highly controversial method of coal extraction. While future work seeking to predict topographic influences of mining could benefit from big data encompassing multiple geographically distinct regions and the implementation of more sophisticated time-series analyses, our results offer a starting point for understanding the crucial effects policy formulations can have on the topographic trajectory of coalfield regions. Although consequences for ridgetops and other topographic positions remain mostly unaddressed, future regulations formulated by OSM or EPA to prioritize the restoration of original topographic contours could potentially mitigate the unintended consequence of exacerbating the disproportionate mining of ridgetops. Despite our concerns regarding terrestrial ecosystems, protecting aquatic ecosystems at such a large scale in a major American coalfield is a substantial step towards controlling the environmental impacts of surface coal extraction. Given the ability to detect these topographic patterns afforded by new technologies, we recommend the continued gathering of LiDAR imagery from American coalfields to facilitate future research as the policy priorities of the Trump administration continue to play out. In coal-producing regions across the globe where surface mining is growing in popularity, we anticipate that increasingly informative geospatial data sets will continue to inform policymaking and help to optimize tradeoffs between economics, energy, and environmental outcomes.

4.3 Methods

We focused our attention on the Cumberland Plateau (CP) of eastern Kentucky, a 14,020 km^2 physiographic province representing the vast majority of the eastern Kentucky coalfield, which is itself an important component of the more extensive Appalachian coalfield in the eastern United States. The CP is best characterized as a highly-dissected plateau, containing steep-sided low hills, narrow ridgetops, and narrow low-order stream valleys. Elevations rise gradually from 160m in the northwest to a peak of 995m at Pine Mountain, a thrust-fault mountain that marks the southeastern boundary of the region. The CP is known for its mixed-mesophytic deciduous forests, which are among the most diverse temperate forests on Earth (Braun 1950, Ricketts et al. 1999). Topographic gradients due to the tightly-packed physiography promote high beta diversity, and many flora and fauna are associated with specific microhabitats and microclimates (Whittaker 1956).

We utilized three sources of data for our analyses: (1) a filtered subset of the annual GIS shapefiles of mined land throughout Appalachia generated by Pericak et al. (2018), (2) a pre-mining digital elevation (DEM) model of the CP based on circa 1970 USGS topographic maps obtained from the Kentucky Division of Geographic Information, and (3) a post-mining DEM of a portion of the CP based on LiDAR data collected in 2017 by the Kentucky Division of Geographic Information. The Pericak et al. (2018) data set was constructed from annual Landsat imagery, and identified minelands using a formula based on normalized difference vegetation index (NDVI). To reduce potential Type-I errors, we filtered the Pericak et al. (2018) shapefiles of minelands using a shapefile of past and present surface mining permits obtained from the KY Division of

Mine Permits. Since we were interested in newly mined land, and not the mining of land which had already been mined previously or was mined repeatedly across multiple years, we clipped each permit-filtered shapefile for each year by a combined shapefile of all previous years in ArcMap.

Our pre-mining DEM was based on USGS topographic maps constructed from approximately 1950-1980, before most surface mining was conducted. Any portions of the pre-mining DEM that showed signs of surface mining were removed from the analysis by drawing polygons around areas where mining signatures were found; and the land that appeared to have been mined before 1980 totaled 193.6 km^2, about 1.4% of the CP. For our analyses of topographic transition, we relied on a post-mining DEM based on LiDAR data gathered in 2017, which covered 5041.3 km^2, or approximately 36.5% of the study area (Figure S1).

We converted the DEMs to topographic position index (TPI), a standardized measure of elevation based on the difference between a local elevation and a regional average, which provides a more reliable identification of ridgetops and valleys than is possible by using elevation alone (Weiss 2001). Due to potential influences of spatial scale on geomorphological classification, we used three different geographic window sizes to generate TPI: 91.4m, 457.2m, and 914.4m (corresponding to 10, 50, and 100 30-ft raster cells). We next classified TPI from the historical DEM layer as one of five topographic position categories (stream bottom, lower slope, middle slope, upper slope, and ridgetop) using one of two classification schemes. The first scheme classified land into discrete topographic positions based on standard deviations of TPI, while the second scheme classified land based on even one-fifth quantiles of TPI. By clipping our shapefile

of newly mined land by our TPI classification raster in ArcMap, we were able to estimate the proportion of each topographic class which was mined each year from 1986-2015. Using an identical TPI and classification protocol for the post-mining DEM, we were able to identify what topographic class this land transitioned to after mining, and how this transition process has changed across three decades.

To test for differences in the topographic composition of surface mines across time, we used change point detection methods in the R statistical packages *changepoint* (Killick and Eckley 2012) and *tsoutliers* (Lopez-de-Lacalle 2016). These packages allowed us to identify the year at which the proportion of different topographic classes changed within our annual newly mined land data set, and identify the magnitude, nature, and temporal location of any outliers in our data.

Shifting policy was only one factor that could explain long-term topographic trends in surface coal mining throughout our study area. To determine the extent to which policy may have been a contributing factor, we used both a generalized least squares (GLS) approach and an auto-regressive model with order 1 (AR-1) to estimate which factors were most important in determining the proportion of newly mined land in the lowest and highest topographic classes on an annual basis between 1986 and 2015. We selected independent variables thought to be important indicators of pressures affecting the coal industry, these included: (a) policy coded as 0-1 categorical variable, with values of 1 beginning in 2011, (b) annual inflation-adjusted per-ton coal prices for eastern Kentucky surface-mined coal, (c) the annual percent of US electricity generation from coal, and (d) an estimate of the efficiency of coal mining, consisting of a ratio of total annual land disturbed by surface mining (m^2) divided by tons of surface-mined coal

produced from eastern Kentucky surface mines for each year between 1986 and 2015. Our data for coal prices came from the Kentucky Geological Survey (KGS) database of coal production (KGS 2019), and our comparative energy data were derived from data published by the US Energy Information Administration (US EIA 2019). Our estimate of land disturbed per ton of coal produced came from our filtered Pericak et al. (2018) shapefiles, using the annual total amount of land being mined instead of newly mined land used elsewhere in our analyses and using eastern Kentucky surface coal production data from KGS. Model selection for both the GLS and AR frameworks relied on Akaike's information criterion (AIC) to identify the best-fit model among all possible modeling configurations.

Table 4.1. Model results and AICc values for each of the four models used to estimate the effects of four independent variables on topographic trends in surface coal mining in the study area from 1986-2015.

Model 1: Stream-bottom, generalized least-squares, lm										
Global model call: gls(model = str ~ energ + policy + price + effic)										
Model	Intrcpt	effic	energ	policy	price	df	loglik	AICc	delta	weigh
13	21.33			-5.229	-0.115	4	-57.76	124.9	0	0.904
15	18.11		0.0615	-4.241	-0.114	5	-59.13	130.5	5.52	0.057
14	21.33	0.0005		-5.236	-0.115	5	-59.86	131.9	6.99	0.027
16	8.49	0.134	0.2136	-3.878	-0.094	6	-59.51	134.2	9.29	0.009
8	-9.10	0.322	0.443	-4.303		5	-62.89	138	13.06	0.001
5	15.58			-7.319		3	-65.88	138.6	13.65	0.001
11	8.98		0.252		-0.131	4	-65.31	140	15.1	0
12	-3.41	0.187	0.443		-0.100	5	-64.97	142.2	17.21	0
7	11.09		0.087	-5.880		4	-66.90	143.2	18.28	0
6	15.12	0.0748		-8.312		4	-67.04	143.5	18.56	0
4	-23.81	0.397	0.718			4	-67.94	145.3	20.36	0
10	25.36	-0.192			-0.180	4	-70.52	150.5	25.53	0
3	-3.86		0.374			3	-73.55	153.9	28.97	0
9	25.17				-0.209	3	-75.94	158.7	33.75	0
2	16.44	-0.282				3	-83.77	174.4	49.41	0
1	13.80					2	-88.80	182	57.05	0
Model 2: Stream-bottom, AR(1)										
Global model call: gls(model = str ~ energ + policy + price + effic, correlation = corAR1(form = ~year))										
Model	Intrcpt	effic	energ	policy	price	df	loglik	AICc	delta	weigh
13	21.33			-5.086	-0.115	5	-55.15	122.5	0	0.695
5	15.30			-6.192			-57.82	125.1	2.56	0.193

Table 4.1 (continued). Model results and AICc values for each of the four models used to estimate the effects of four independent variables on topographic trends in surface coal mining in the study area from 1986-2015.

15	18.71		0.0483	-4.422	-0.111		-56.59	128.4	5.89	0.037
14	21.14	0.015		-5.264	-0.113		-57.05	129.3	6.82	0.023
7	10.11		0.105	-5.061			-58.66	129.5	7.03	0.021
6	14.57	0.0758		-6.385			-59.06	130.3	7.82	0.014
8	-0.97	0.205	0.296	-4.667			-57.76	130.7	8.23	0.011
16	10.76	0.112	0.170	-4.238	-0.092		-57.32	133.1	10.61	0.003
9	22.02				-0.151		-63.54	136.5	13.99	0.001
11	10.01		0.230		-0.129		-62.15	136.5	14.01	0.001
1	13.08						-65.01	136.8	14.33	0.001
3	-0.077		0.294				-64.17	137.8	15.24	0
4	-12.13	0.232	0.502				-63.06	138.3	15.83	0
2	9.66	0.157					-65.29	140	17.5	0
12	0.54	0.138	0.373		-0.104		-62.65	140.5	18.02	0
10	23.77	-0.072			-0.169		-64.98	142.2	19.66	0
Model 3: Ridgetop, generalized least-squares										
Global model call: gls(model = rid ~ energ + policy + price + effic)										
Model	Intrcpt	effic	energ	policy	price	df	loglik	AICc	delta	weigh
6	30.55	-0.217		4.069		4	-72.14	153.7	0	0.415
5	29.22			1.182		3	-74.12	155.1	1.35	0.211
1	29.51					2	-75.74	155.9	2.17	0.14
8	41.96	-0.334	-0.209	2.181		5	-72.26	156.7	3.02	0.092
7	21.02		0.160	3.816		4	-74.43	158.3	4.57	0.042
4	49.42	-0.372	-0.348			4	-74.46	158.3	4.63	0.041
14	32.55	-0.241		5.058	-0.0371	5	-74.02	160.3	6.54	0.016

Table 4.1 (continued). Model results and AICc values for each of the four models used to estimate the effects of four independent variables on topographic trends in surface coal mining in the study area from 1986-2015.

16	56.43	-0.489	-0.397	2.531	-0.0771	6	-72.69	160.6	6.89	0.013
2	29.91	-0.0427				3	-77.41	161.6	7.93	0.008
3	30.73		-0.0257			3	-77.62	162.1	8.36	0.006
13	29.56			1.304	-0.0067	4	-76.45	162.3	8.62	0.006
12	64.19	-0.524	-0.547		-0.0727	5	-75.10	162.4	8.71	0.005
9	28.60				0.0167	3	-78.14	163.1	9.4	0.004
15	21.21		0.159	3.862	-0.0032	5	-76.78	165.8	12.07	0.001
10	28.66	-0.0553			0.0252	4	-79.61	168.7	14.94	0
11	29.53		-0.0144		0.0122	4	-79.93	169.3	15.57	0
Model 4: Ridgetop, AR(1)										
Global model call: gls(model = rid ~ energ + policy + price + effic, correlation = corAR1(form = ~year))										
Model	Intrcpt	effic	energ	policy	price	df	loglik	AICc	delta	weigh
5	28.90			1.373		4	-69.61	148.7	0	0.48
1	29.29					3	-71.35	149.5	0.87	0.311
6	30.03	-0.146		2.913		5	-70.15	152.5	3.87	0.069
7	23.73		0.103	2.72		5	-70.40	153	4.36	0.054
2	29.70	-0.0444				4	-72.77	155	6.31	0.02
3	29.95		-0.0152			4	-72.82	155.1	6.41	0.02
13	29.15			1.50	-0.0057	5	-71.54	155.3	6.65	0.017
9	28.50				0.0137	4	-73.40	156.2	7.56	0.011
8	33.56	-0.186	-0.0642	2.434		6	-70.86	156.9	8.28	0.008
4	40.63	-0.210	-0.197			5	-73.16	158.5	9.89	0.003
14	31.33	-0.152		3.355	-0.0251	6	-72.09	159.4	10.76	0.002

Table 4.1 (continued). Model results and AICc values for each of the four models used to estimate the effects of four independent variables on topographic trends in surface coal mining in the study area from 1986-2015.

15	23.74		0.0991	2.628	0.0029	6	-72.31	159.9	11.2	0.002
11	28.67		-0.0047		0.0136	5	-74.69	161.6	12.94	0.001
10	28.82	-0.0453			0.0157	5	-74.77	161.8	13.1	0.001
16	46.19	-0.337	-0.2349	2.706	-0.0577	7	-72.43	163.3	14.67	0
12	51.84	-0.338	-0.3524		-0.0478	6	-74.87	165	16.31	0

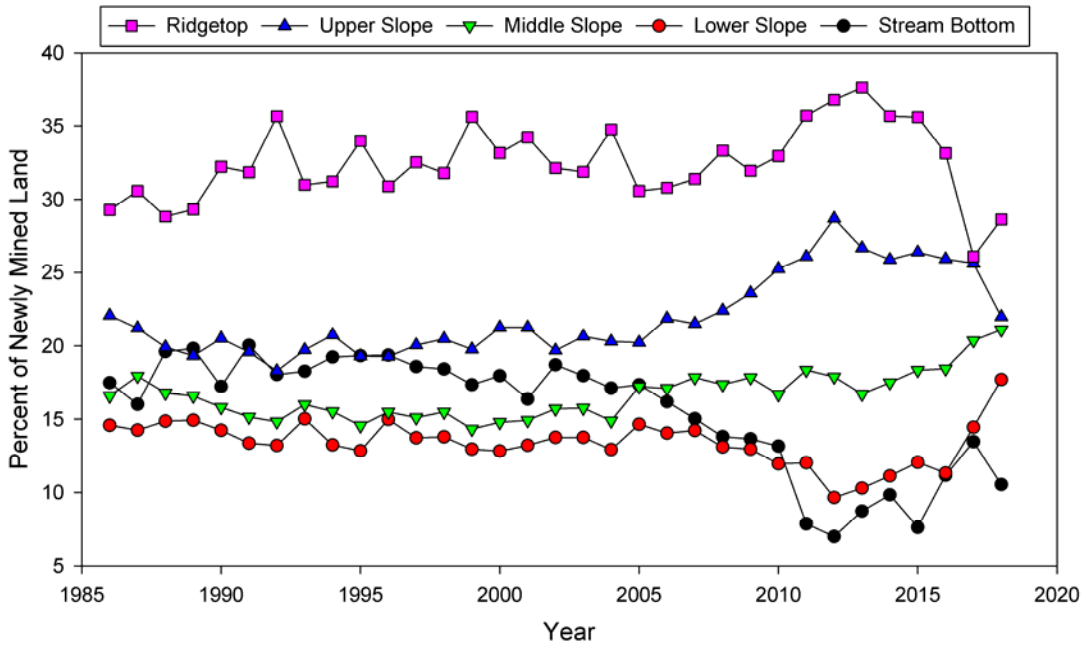

Figure 4.1. Topographic position of newly surface mined land in the Cumberland Plateau of Kentucky, 1986-2015, based on TPI classifications conducted using the five landform class protocol with a 457.2 m window.

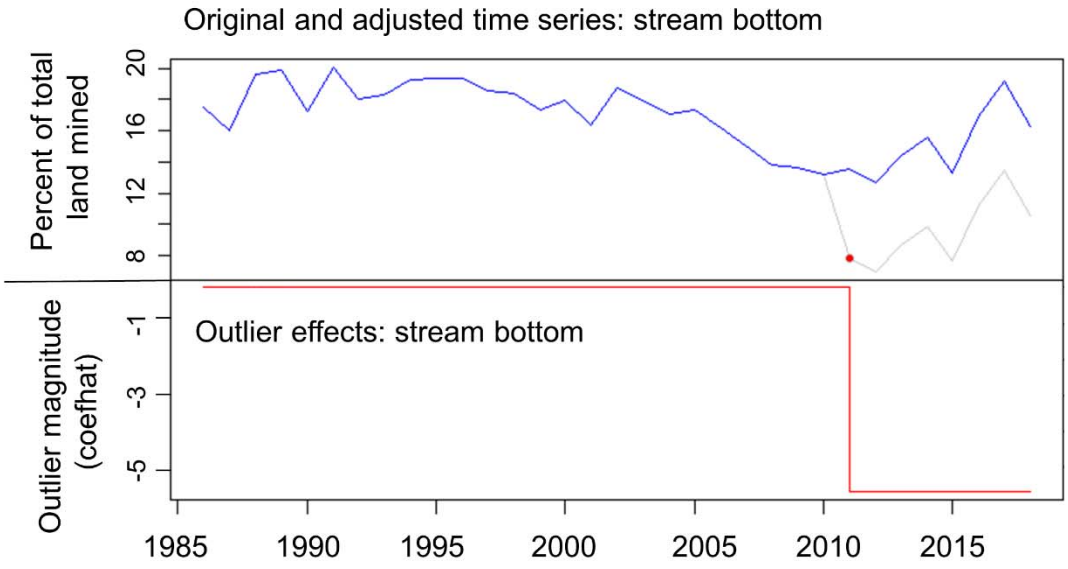

Figure 4.2. Outlier detection results for the 457.2 m five class TPI classification scheme for the topographically lowest TPI class ("stream bottom"). Above, red dot indicates outlier, gray line indicates actual percent of stream bottom mind while blue line indicates hypothesized trend if the outlier was not present; below, magnitude of 2011 outlier.

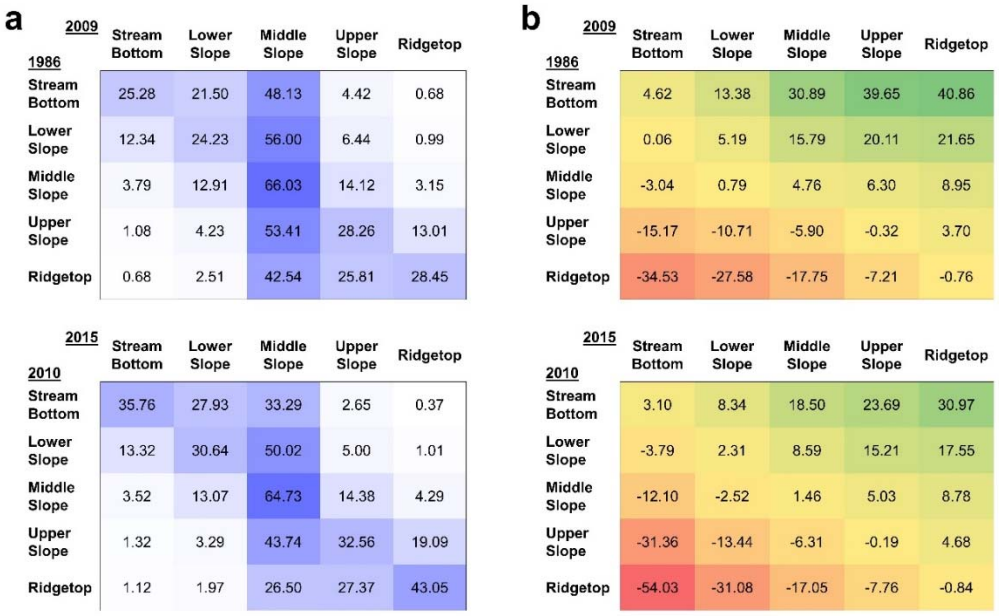

Figure 4.3. (a) Heatmap of topographic transitioning, 1986-2009 and 2010-2015, for 94.1 m five-class SPL TPI classification scheme. Numbers refer to the percent of land from each class in the right column that transitioned to each class in the top row; for example, an average of 48.13% of stream bottom land mined between 1986 and 2009 transitioned to a middle slope topographic position after mining, while from 2010 to 2015 this number declines to 33.29% (b) Heatmap of raw elevation changes (m above sea level) from 1986-2009 and 2010-2015, for each topographic class transition as defined in (a).

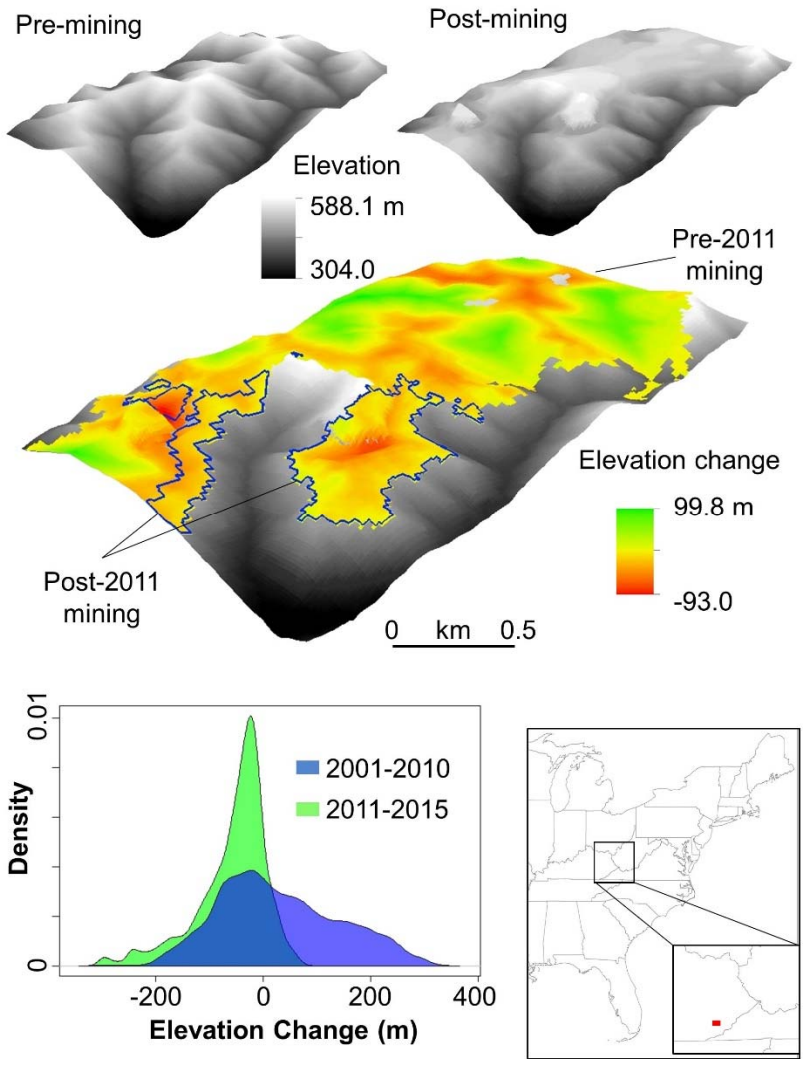

Figure 4.4. Patterns of surface mining at a mine near Lower Bad Creek in Leslie County, Kentucky, 2001-2015, demonstrating pre-2011 valley fills and post-2010 avoidance of valley filling despite continued ridgetop mining. At center, a digital elevation model (DEM) of the site with elevation changes after mining before and after 2010 (areas mined after 2010 are marked by a blue boundary.); above, the pre-mining and post-mining DEMs. Below, a density plot of the elevation changes shows the lack of positive elevation values (i.e., "valley fills") after strict federal regulations were put in place in 2010.

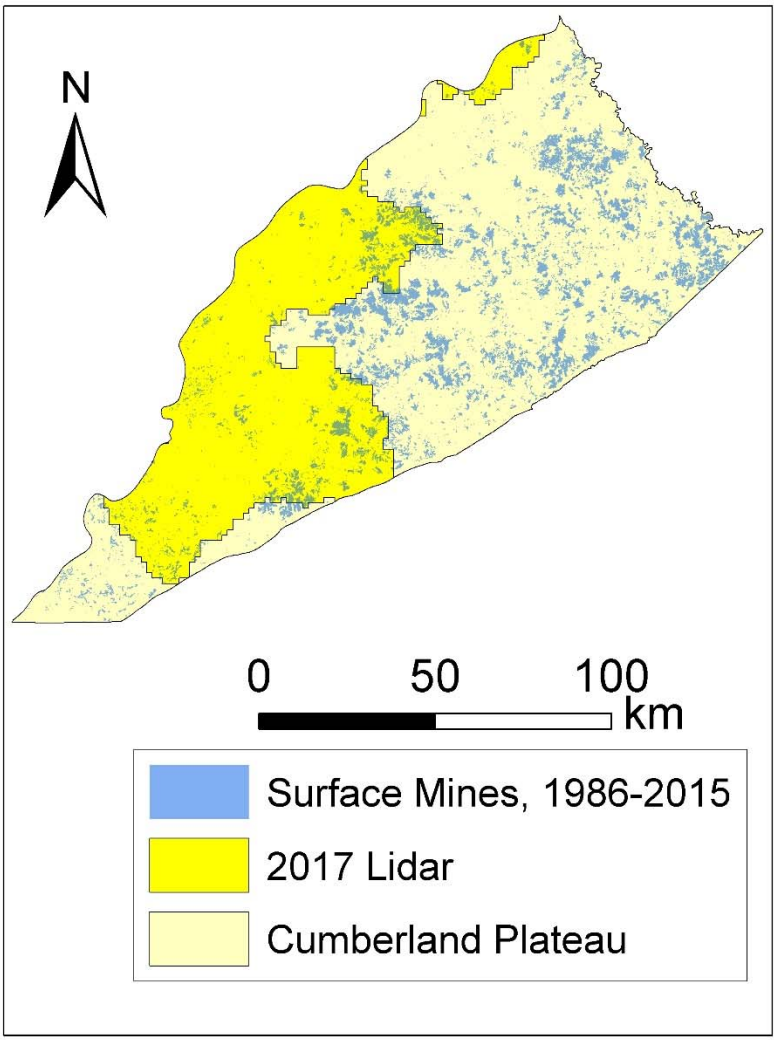

Figure 4.5. Portion of the Cumberland Plateau covered by LiDAR data gathered by the Kentucky Division of Geographic Information in 2017; surface mines included in our topographic transition analyses are also shown.

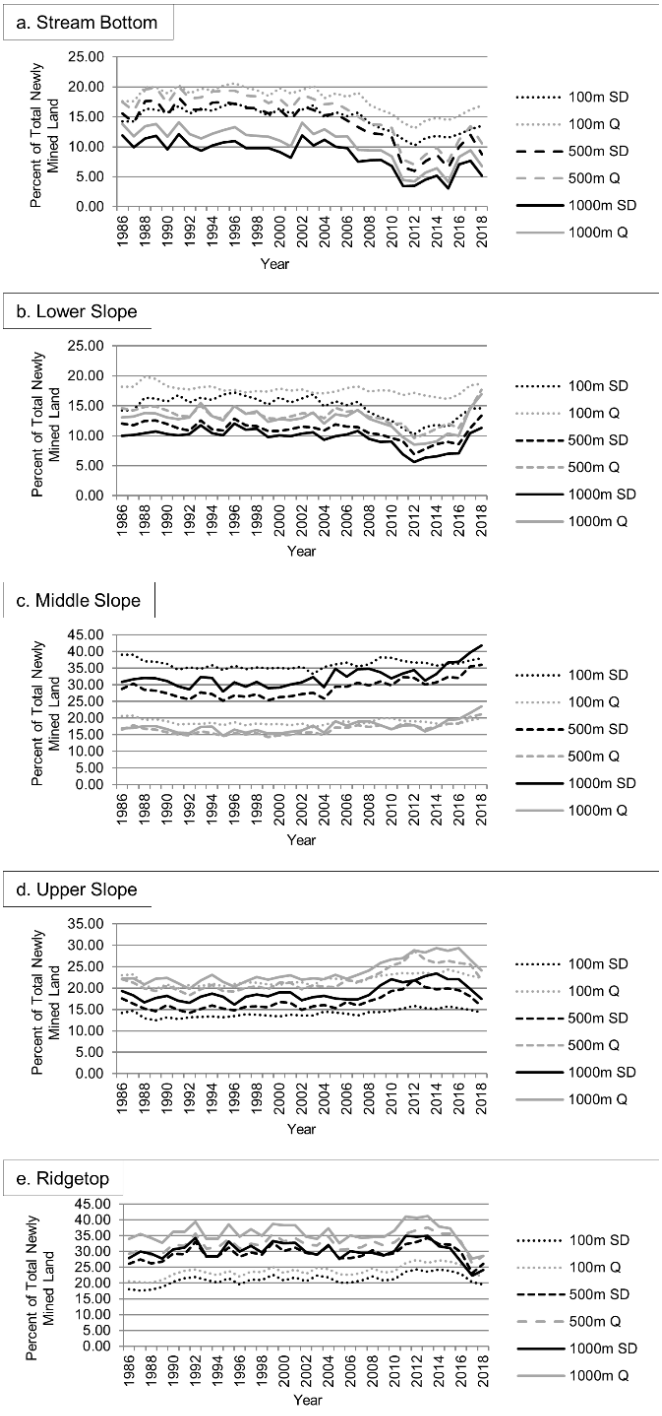

Figure 4.6. Topographic position of newly surface mined land in the Cumberland Plateau of Kentucky, 1986-2015, for both TPI classification schemes and all three spatial scales.

CHAPTER 5:

IMPROVING MODELS OF THERMOREGULATORY BEHAVIOR IN TIMBER RATTLESNAKES (CROTALUS HORRIDUS) USING AIRBORNE LIDAR IMAGERY

5.1 Abstract

The ability of organisms to thermoregulate efficiently is key to surviving in a changing environment. Especially for ectotherms, the use of microhabitats to maintain homeostasis is dynamic and occurs in three dimensions and at a variety of spatial and temporal scales. Newly developed remote-sensing imagery may improve our ability to understand the drivers of thermoregulatory behavior in ectotherms, especially in complex environments such as mature deciduous forests. We used a combination of high-resolution (0.61 m) Lidar imagery and temperature-sensitive radiotelemetry data to model thermoregulatory movements in the timber rattlesnake, *Crotalus horridus*, in a mature mixed-mesophytic forest of southeastern Kentucky, USA. We collected 516 location-specific temperatures from 13 individuals across four years, and using a centrally-located weather station, we calculated the time-specific difference between air and internal body temperatures. Using this difference as a response variable, we identified key predictors of thermoregulation using linear mixed models. Temporal factors such as time of day and day of year strongly influenced thermoregulation, as did air temperatures. However, vegetation height was strongly negatively associated with the difference between body and air temperatures, and canopy closure was weakly associated. Topographic factors were less important, though aspect was slightly influential. Both anthropogenic and natural features were used for basking, including features associated with recent timber harvesting. Vegetation height was most predictive when averaged over a 25m wide

circular buffer centered on the snake's location, suggesting that incorporating hill slope and sun angle effects might improve our model. Overall, we found that local features and microhabitats play an important role in thermoregulation in *C. horridus*, and our results underscore other research highlighting the important thermal buffering capacity present in forest ecosystems in light of potential consequences of climate change.

5.2 Introduction

Understanding the relationship between organisms and their thermal environment is becoming increasingly important as global climate change continues to threaten ecosystems. While much attention has been paid to global and regional predictive modeling and data analysis, downscaling predicted climate conditions to scales relevant to the experience of individual organisms has been comparatively overlooked (Dobrowski 2011, Suggitt et al. 2011, Potter et al. 2013). Shifts in temperature regimes resulting from anthropogenic climate change will ultimately be filtered by local thresholds related to topography, surface and subsurface geology, and vegetation, among other fine-scale variables (Daly 2006, Suggitt et al. 2011). However, while downscaling these effects can help translate global climate changes into local consequences, predicting the impacts of shifting thermal regimes on surface-dwelling organisms is challenging, especially across heterogeneous landscapes and habitats such as high-relief terrain or dense forest (Sunday et al. 2014, Oyler et al. 2015).

Fine-scale thermal habitat characteristics can be especially consequential for ectothermic organisms, which must rely on individual-level optimization of the costs and benefits of thermally heterogeneous environments for effective thermoregulation (Huey

and Slatkin 1976, Stevenson et al. 1985, Rice et al. 2006). As global temperature averages rise, many ectothermic taxa may see local temperature regimes approach critical thresholds, and opportunities for mating and foraging may be lost by avoiding extreme heat (Sinervo et al. 2010). Even moreso than changes in temperature averages, the effect of temperature fluctuations and especially the range of temperatures experienced by ectotherms on a daily basis can have important consequences for rate processes such as development, growth, and reproduction (Clusella-Trullas et al. 2011, Paaijmans et al. 2013). However, the use of microhabitats, especially in three-dimensionally complex ecosystems such as forests, provides a broad spectrum of thermal environments which might accommodate a diversity of species with a plethora of optimal temperature ranges, providing a buffer against both fluctuations and higher average temperatures in particular (Scheffers et al. 2014, Agha et al. 2018). Predicting the effects of altered temperature patterns originating from global climate change for a scenario involving a specific ectotherm therefore depends both on temporally informative temperature data and accurate, high-density three-dimensional data sets.

Technological advances now permit researchers to more closely examine the influence of fine-scale habitat variables on thermoregulatory behavior of animals, including ectotherms such as reptiles and amphibians. On top of the greater availability, resolution, and geographic coverage of geospatial data sets in general, three-dimensional LiDAR data sets have allowed for more accurate models of thermal behavior for a wide variety of species in situ (Vierling et al. 2008). Additionally, the development of miniaturized temperature-sensitive radiotransmitters capable of being attached to or implanted inside herpetofauna has permitted the widespread collecting of body

temperature data associated with a specific time and geographic location. These advances hold promise for augmenting our understanding of the relationship between ectothermic organisms and their environments, including forest-dwelling fauna which rely on microclimates for thermoregulation (Davies and Asner 2014, Algar et al. 2018).

We explored the relationship between habitat structure and thermoregulation in adult timber rattlesnakes (*Crotalus horridus*) by modeling the relationship between the difference in internal body temperatures (IBT) of adult snakes radiotracked across four years and temporally corresponding air temperatures using an array of raw and transformed environmental variables gathered from high-resolution LiDAR imagery. Our goals were (i) to quantify temporal factors affecting thermoregulatory behavior in radiotracked *C. horridus*, (ii) to test for associations between three-dimensional habitat variables and thermoregulation in radiotracked *C. horridus*, and (iii) to construct a parsimonious model which explains differences between *C. horridus* IBT and air temperature as a function of local and landscape-level variables. More broadly, our study aims to explore potential uses of high-resolution imagery for quantifying the drivers of individual movement and thermoregulatory behavior in ectotherms, and also to investigate how fine-scale forest microhabitats are used by organisms to maintain homeostasis in thermally unstable environments, especially in light of potential future shifts in temperature patterns.

5.3 Methods

5.3.1 Study Site and Focal Species

We conducted our study in the University of Kentucky's Robinson Forest (RF), a 5267 ha research forest located in Breathitt, Knott, and Perry counties, in eastern Kentucky, USA. Elevations in RF vary from 243-500 m, and the topography is typical of the broader Cumberland Plateau physiographic region in which RF is located; namely, the terrain consists mostly of very steep-sided hills and narrow rocky ridgetops heavily dissected by tightly-packed, narrow, low-order stream valleys. Vegetative cover consists principally of mature second-growth hardwood forests, best characterized as mixed-mesophytic, with up to 30 co-dominant canopy tree species (Braun 1950, Overstreet 1984). Stream valleys are characterized by deeper alluvial soil and hemlock, beech, and maple forests, while ridgetops generally contain oak, hickory, and pine assemblages with thinner soil and frequent exposed sandstone outcrops. Canopy cover across RF averages approximately 93%; open areas are generally small and scattered throughout the landscape. However, portions which were harvested between 2008 and 2010 averaged approximately 63% canopy cover when our geospatial data sets were collected (Staats 2015; for details of harvests see Witt 2012). Additionally, small portions of RF and larger portions of the surrounding land is composed of active and abandoned surface coal mines, which display a homogenized and flattened topography, little to no canopy cover, and are typically dominated by alien herbaceous vegetation, unpaved roads, and abandoned mining infrastructure (Maigret et al. 2019).

Our study species, the timber rattlesnake (*Crotalus horridus*), is a large-bodied pit viper native to eastern North America. Like most pit vipers, timber rattlesnakes depend

on the surrounding environment to maintain homeostasis, and thus are typically reliant on insolation and often engage in basking behavior to accomplish this (Brown et al. 1982, Brown 1993). After emerging from hibernacula, adult timber rattlesnakes move in a roughly circular pattern during the late spring, summer, and early fall before ingress and overwintering; typically, they return to the same hibernacula each year (Brown 1993). While movements may be motivated by foraging (Reinert et al. 2011), mate-seeking (Anderson 2015), or perhaps predator avoidance, thermoregulation is thought to be a primary factor in habitat selection (Brown et al. 1982, Brown 1993). Preferences for forest clearings and field edges are likely based on access both to prey and thermally suitable environments (Brown 1993, Wittenberg 2012). This is especially true in gravid females, which often have very reduced home ranges consisting almost entirely of basking sites (Gardner-Santana and Beaupre 2009). Yet despite these preferences for small clearings exposed to sun, previous research has found that large-scale timber harvests did not produce detectable changes in broad behavioral patterns or habitat preferences (Reinert et al. 2011a).

5.3.2 Radiotelemetry and Internal Body Temperature Data Collection

Between 2014 and 2015, we captured 13 adult *C. horridus* at RF. Snakes were located by carefully examining basking areas, in addition to opportunistic captures by RF personnel. All snakes were transported to a local veterinary facility for implantation surgery, which generally followed the methods of Reinert and Cundall (1982). We used

Advanced Telemetry Systems (ATS, Isanti, MN, USA) models R1535, R1540, and R1680 VHF transmitters, with a thermosensitive component which varies the pulse rate based on the device's temperature, allowing for remote measurement of the temperature each time the animal is located. Animals were held briefly after surgery to ensure wound closure prior to being released at the precise point of capture, upon which tracking began immediately. Snakes were tracked continuously until they entered their hibernacula in the fall, after which they were immobile until emerging in spring. Snake handling and processing were approved under University of Kentucky IACUC Protocol 2012-0954.

Between 1 April and 1 November each year, we recorded air temperatures for each individual snake at each relocation if the individual was at least partly visible. Local air temperatures were gathered from a Campbell Scientific CR10X (Campbell Scientific, Logan, Utah, USA) data logger associated with a permanent weather station centrally located in RF (Figure 1); temperatures were recorded every 15 minutes. Thus, temperature data were accessible within 7.5 minutes for each snake location, with the exception of a small number of missing air temperatures due to weather station technological malfunctions from April 19th 2017 to May 10th 2017; these points were not included in our analyses.

5.3.3 Geospatial and Airborne Lidar Data Collection

We utilized a high density (~25 points/m2) airborne lidar dataset collected across RF during leaf-on season between May 28-30th, 2013. Data were gathered using a Leica ALS60 system, at an average height of 1305 m above ground and an average flight speed

of 105 knots. The swath width was 183.0 m with 50% swath overlap, resulting in approximately 95% of each swath consisting of a usable central portion (Staats 2015, Hamraz et al. 2016). Nominal pulse spacing was <0.2m on average, with a 0.1 m average footprint dimeter. Raw lidar returns were processed by the vendor using TerraScan to discriminate ground from non-ground points.

To construct a GIS layer representing estimates of vegetation height, we first constructed a digital elevation model (DEM) based on a layer of lidar ground returns identified by the vendor. We used the LAS to Raster tool in ArcMap 10.6.1 to create a 0.61 m resolution DEM raster based on these points, assigning cells based on averages and filling voids using natural neighbors. We then calculated vegetation height by subtracting the DEM from a layer of the highest lidar points, representing the canopy and emergent layer of the forest. To create a layer depicting canopy cover, we discriminated ground and above-ground points from our entire lidar data set and created 0.61 m resolution rasters of the total number of above-ground points and total points in each cell using the LAS Point Statistics as Raster tool in ArcMap 10.6.1. We then divided the count of above-ground points by the total number of points in each 0.61 m cell, resulting in a layer which estimates the proportion of lidar returns which did not reach the ground in each cell.

Geomorphological variables used in our analyses included aspect and topographic position index (TPI). Aspect was estimated using our 0.61m DEM and the Aspect tool in ArcMap 10.6.1. TPI is a relative estimate of elevation based on the distance (in meters) between each cell and a local elevation mean of all cells within a given radius. Using TPI instead of raw elevation allows for consistent comparisons of landforms, whereby valley

floors and ridgetops exhibit strongly negative and positive values, respectively. We estimated TPI using a 100m window in the Land Facet Analysis extension (Jenness Enterprises, Flagstaff, AZ).

5.3.4 Thermoregulation Modeling

We used the difference in contemporaneous air temperature and internal body temperature (hereafter ΔT) as our response variable. To evaluate potential predictors for the variation we observed in ΔT, we used a mixed effects linear regression model. We included year and individual nested within year as random effects, and air temperature, time of day, day of year, TPI, aspect, vegetation height (ft), and canopy closure (percent) as fixed effects. Variables with nonlinear patterns including aspect, time of day, and day of year were included as second-degree polynomials. To screen out potential multicollinearity, we removed variables with excessive variance inflation factors (>5). which were calculated in JMP 14.0.0 (SAS Institute Inc., Cary, North Carolina). The scale at which average vegetation height and canopy closure estimates were analyzed was determined by sequential multivariate tests of vegetation height and canopy closure averaged at different scales. Values were averaged across all cells within circular buffers of variable radii, including 0.25m (the individual raster cell at which the snake's location was recorded), 1m, 2m, 5m, 10m, 25m, 37.5m, and 50m. Candidate models composed of each predictor variable, including optimally scaled vegetation height and canopy closure, were compared using Akaike's Information Criterion (AIC) in JMP 14.0.0.

5.4 Results

We tracked eight male and five female timber rattlesnakes in RF between 2014 and 2017. Snakes were tracked across a minimum of two years; eight snakes were tracked across two years, four snakes were tracked across three years, and one snake was tracked for four years (Table S1). Of the five females tracked, two were gravid for at least one season. We included 516 temperature-location combinations after filtering for missing data or locations where the individual snake was not visible. Our ΔT values were normally distributed with a mean of -0.211 and standard deviation of 3.85 (Figure 2).

No variance inflation factor exceeded our limit for inclusion into our candidate models. The best-supported scale for our vegetation predictor variables was a 25m average for vegetation height and a 5m average for canopy closure (Table S2). Our best-fit linear model (Table 1) included the predictor variables time of day and aspect as second-degree polynomials, in addition to day of year, air temperature, and the variables vegetation height (25m average) and canopy cover (5m average). Random effects were found to be significant at the level of the individual nested within year ($p=0.0012$).

Among the variables included in the best-supported model, effects were generally stronger for air temperature, time, and day of year than for remotely-sensed vegetation variables. Nonetheless, a highly significant effect of vegetation height was found ($p = 0.0001$), and while canopy cover was not significant ($p = 0.098$), the best fit model included canopy cover effects. Topographic predictors explained less variance; aspect (treated as a second degree polynomial) was identified as a significant predictor of ΔT

($p = 0.01$), but topographic position index was unrelated and not included in the best-fit model.

5.5 Discussion

Integrating lidar-derived vegetation height and canopy closure significantly improved models predicting the difference between air temperatures and contemporaneous IBTs of timber rattlesnakes. While in the past high-density lidar data sets have been used to predict suitable habitat (Graf et al. 2009), species richness and diversity (Simonson et al. 2014), and resource selection functions (George et al. 2017), our results are the first we know of using Lidar-derived vegetation data to quantify direct impacts on in-situ individual body temperatures. Our empirical results underscore broader, model-based analyses which have suggested the important role three-dimensional data sets will play in improving both our understanding of the landscape pattern-ecological process relationship in forest dwelling fauna and the potential for proactive management of wildlife populations (Algar et al. 2018). This is notwithstanding, however, the significant influence of seasonal and diurnal associations on ΔT, as we also found thermoregulation to be more pronounced in spring and fall and during morning and evening (Figure 3).

Increasingly, the thermal buffering capacities of forests are hypothesized to be important bulwarks against elevated risk of hyperthermia resulting from rising global temperatures (De Frenne et al. 2019). Our results add to other research highlighting the importance of forest microhabitats for thermoregulation in herpetofauna (Scheffer et al. 2014, Sillero and Goncalves-Seco 2014) including previous behavioral research

conducted on *C. horridus* (Gardner-Santana and Beaupre 2009). Measurements of ΔT indicate that differences of up to 5 degrees C are well within the normal range of thermoregulation for timber rattlesnakes within our study area (Figure 2). Our modeling results further indicate that thermoregulation is occurring at very fine spatial scales in timber rattlesnakes due in large part to vegetation height (25 m) and canopy closure (5 m). The utility of vegetation data for modeling thermoregulation in ectotherms in apparent both when examining usage of anthropogenic basking areas (e.g., forest roads) and also naturally occurring features (e.g., storm damage) (Figure 4). This effect appears to occur regardless of topographic position though is somewhat related to the cardinal direction of exposure.

Aside from climate-related concerns, our findings add to the broader complexity in relationship between timber extraction and herpetofauna populations. While some species reliant on streams or humid microhabitats have seen marked declines (Peterman and Semlitsch 2009, Maigret et al. 2012), other species seem to prefer the disturbance regimes produced by some forms of timber harvest (Sutton et al. 2013), even harvests resulting in relatively small (< 1.0 ha) canopy gaps (Agha et al. 2018). We found numerous instances of small gaps in vegetation being used by snakes for thermoregulation, including gaps created by timber harvest (Figure 4). Overall, our findings appear to be most in line with studies indicating that some fauna, including *C. horridus*, have been comparatively unaffected by timber harvests, and may even take advantage of increased basking opportunities (Reinert et al. 2011a). These potential advantages will nevertheless need to be balanced against direct killing of snakes during harvesting, and we second the recommendation of Reinert et al. (2011a) for increased

communication between wildlife agencies and logging workers which stresses the importance of preventing the killing of rattlesnakes by individuals.

As our model outputs and summary statistics allude, more comprehensive data sets and analyses are needed to capture a greater share of the variation in predictor variables driving thermoregulation in *C. horridus*. We found significant variation in thermoregulation at the level of individuals, likely resulting from our inclusion of both adult males, nongravid females, and gravid females, the last of which typically displays higher body temperatures during gestation (Gardner-Santana and Beaupre 2009). Future analyses may profit from including a great number of animals or a single category of adult snakes (e.g., gravid females or adult males). Other studies have also indicated that depending on the season, thermoregulation may be less important than foraging in terms of resource selection (George et al. 2017). Furthermore, our model did not account for potentially influential meteorological variables cloud cover, rainfall, or wind speed.

More specifically, however, we suspect that the vertical gap between the hillside and canopy creates inaccuracies when attempting to map canopy gaps in two dimensions. A more comprehensive model which uses trigonometry to integrate sun angle, insolation intensity, canopy gaps, canopy height, and hill slope could potentially predict sun penetration into the forest floor much more effectively. Such a model may be cumbersome, but could likely be constructed with sufficiently high-density lidar return data similar to those used in this study. In addition, an accurate three-dimensional model of solar heating and canopy density could be used to determine thresholds of canopy size and vegetation height which could be useful in assessing impacts of forest management techniques such as canopy harvests (Agha et al. 2018). We suspect that the lack of

accuracy in our forecasting of canopy gaps may partially explain why vegetation height was found to be more much more powerful in explaining body temperature than canopy closure, and why vegetation height had more explanatory power at a relatively coarse scale (25 m) than at fine scales.

Based on three-dimensional remote sensing imagery, we found significant effects of vegetation cover on the thermoregulatory behavior of timber rattlesnakes inhabiting a mature mixed-mesophytic deciduous forest. Our fine-scale results confirm broader-scale, model-based findings which have indicated the importance of integrating three-dimensional vegetation data into predictions of thermoregulation in ectotherms, especially in forests (Algar et al. 2018). We expect that as more high resolution and three-dimensional data sets become accessible, our ability to understand the drivers of thermoregulation in ectotherms will continue to improve, allowing for both better forest management and a more comprehensive understanding of the local and individual-level effects of a warming climate.

Table 5.1. Model fit results, quantified by AIC and log likelihood, for the fixed effects of each candidate model describing ΔT in *C. horridus*. Each model also includes a random effect of individual nested within year.

Model	AIC	ΔAIC	LL
ΔT = date + air + asp + asp^2 + time + time^2 + vh25 + cc5	2584.48	-	-2559.86
ΔT = date + air + asp + asp^2 + time + time^2 + vh25	2585.16	0.68	-2562.63
ΔT = date + date^2 + air + asp + asp^2 + time + time^2 + vh25 + cc5	2585.72	1.24	-2559.00
ΔT = date + date^2 + air + asp + asp^2 + time + time^2 + vh25	2586.75	2.27	-2562.13
ΔT = date + date^2 + air + asp + asp^2 + time + time^2 + tpi + vh25 + cc5	2586.79	2.31	-2557.95
ΔT = date + air + asp + asp^2 + time + time^2 + cc5	2596.62	12.14	-2574.10
ΔT = date + air + asp + asp^2 + time + time^2	2606.71	22.23	-2586.28

Table 5.2. Components and parameter estimates for the best-fit model describing ΔT in *C. horridus*.

Random effects				
Variance component	Estimate	Standard Error	95% Confidence Interval	p-value
year(individual)	4.20	1.30	(1.65, 6.75)	0.0012
Fixed effects				
Term	Estimate	Standard Error	95% Confidence Interval	p-value
intercept	8.18	1.34	(5.55, 10.80)	<.0001
date	-0.014	0.0031	(-0.020, -0.0079)	<.0001
air temperature (C)	-2.57 e-01	3.23 e-02	(-0.32, -0.19)	<.0001
aspect (deg)	-0.0030	0.0018	(-0.0065, 0.00061)	0.1041
(aspect-196.628) * (aspect-196.628)	-5.3 e-05	2.05 e-05	(-9.34 e-05, -1.27 e-05)	0.0101
time	7.09	1.28	(4.58, 9.59)	<.0001
(time-0.53347) * (time-0.53347)	48.47	9.65	(29.50, 67.44)	<.0001
vh25	-3.24 e-02	8.44 e-03	(-0.049, -0.016)	0.0001
cc5	-1.65	0.10	(-3.61, 0.31)	0.098

Table 5.3. Years tracked, sex, number of temperatures, and average body temperatures (with standard deviation) for each individual *C. horridus* included in our analysis.

Individual	Year(s) tracked	Sex	Number of temperatures included	Mean IBT (sd)
S16	2014-2017	m	72	24.04 (4.84)
S17	2014-2015	m	47	22.32 (4.37)
S18	2014-2015	m	29	19.68 (4.69)
S19	2015-2017	m	72	22.61 (5.37)
S20	2015-2017	m	66	23.34 (4.59)
S21	2015-2016	f-gravid	24	25.90 (5.10)
S22	2015-2016	m	25	21.15 (5.14)
S23	2015-2016	f-gravid	27	21.86 (5.76)
S24	2015-2016	m	28	21.56 (5.24)
S25	2015-2016	f	24	22.61 (4.20)
S26	2015-2017	f	57	21.10 (4.79)
S27	2015-2016	f	15	20.13 (6.77)
S28	2015-2017	m	54	21.28 (6.24)

Table 5.4. Model performance (AIC) for varying scales of predictor variables vegetation height and canopy closure. Predictors are either the individual raster cell in which each snake relocation was placed, or average values among all cells in a circular buffer of varying radius (1m-50m). Asterisks denote optimal scales used in the main analysis.

Scale	Model AIC values	
	vegetation height (m)	canopy closure (%)
cell	2599.1333	2611.4572
1m	2598.5364	2612.7681
2m	2598.3421	2609.9444
5m	2597.0954	2602.1346*
10m	2592.681	2602.321
25m	2590.5011*	2609.3692
37.5m	2593.1213	2611.8728
50m	2598.1265	2613.2514

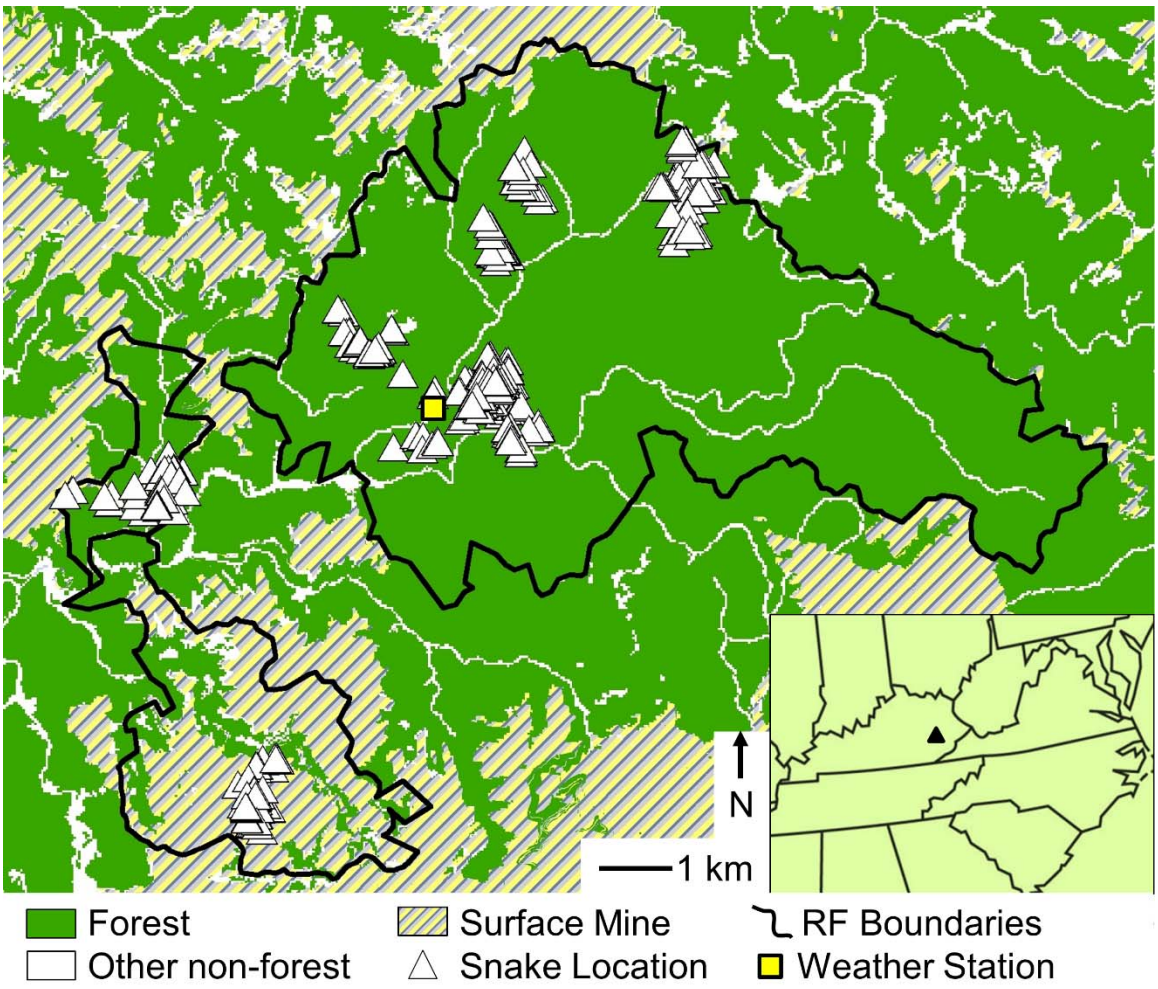

Figure 5.1. Study area, weather station, and temperature locations included in our analyses.

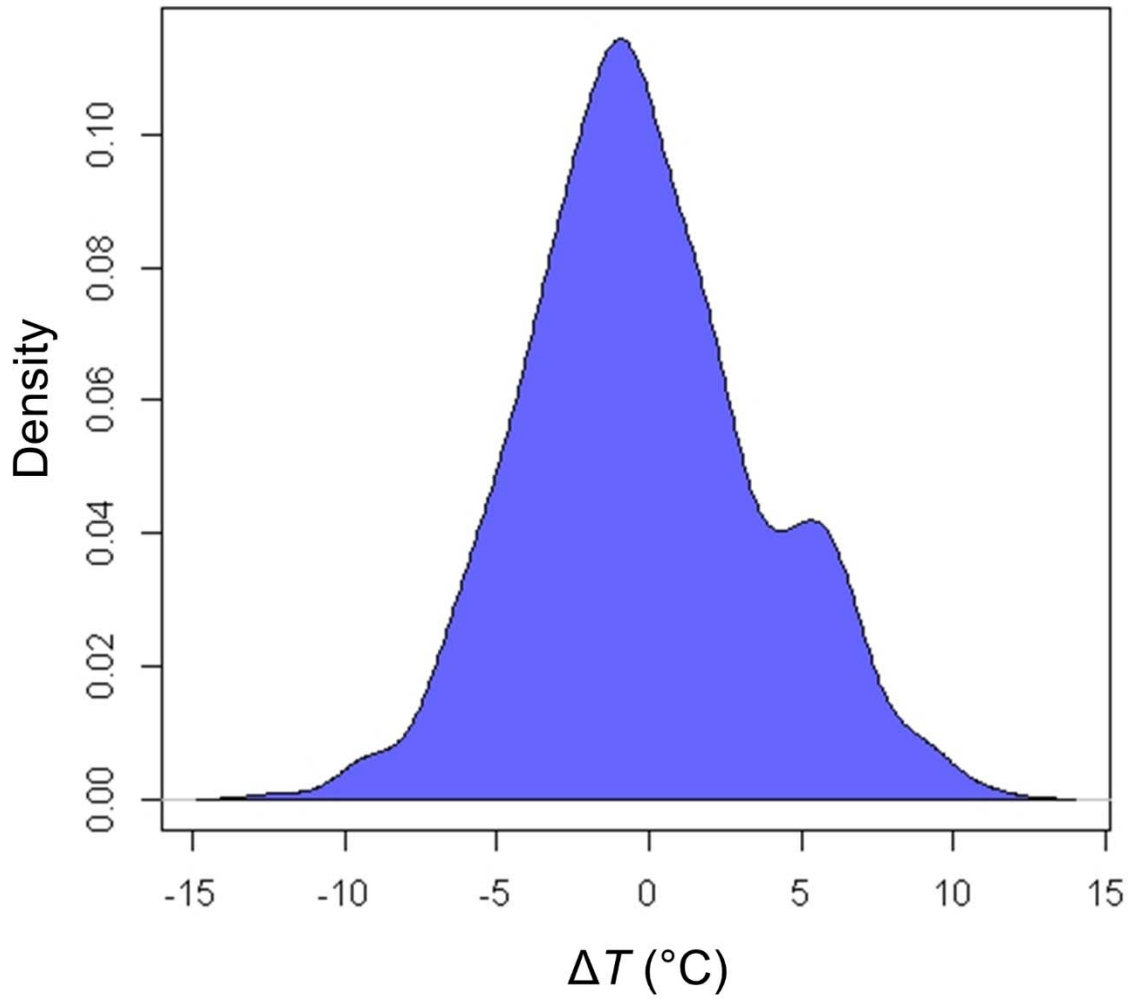

Figure 5.2. Distribution of the differences between internal body temperatures of *C. horridus* and air temperatures (ΔT) for telemetry locations used in our analysis.

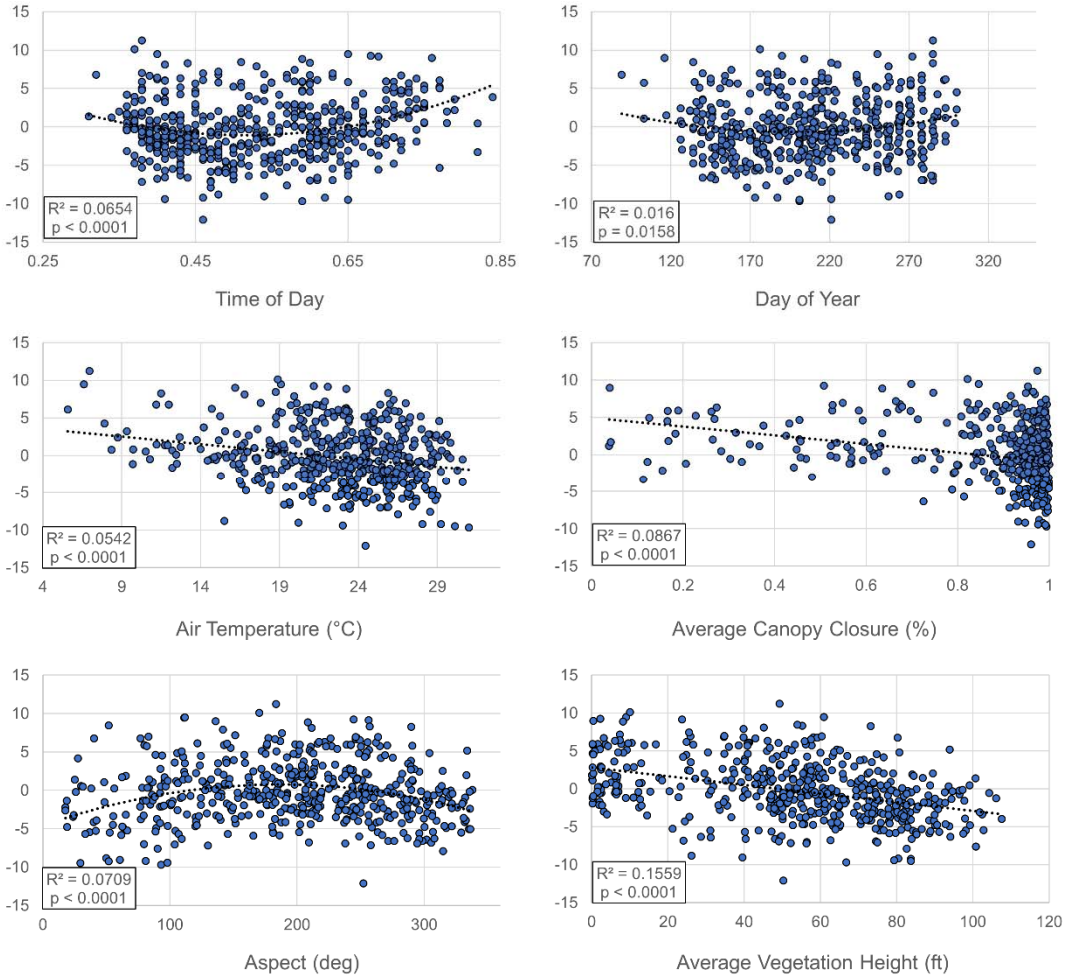

Figure 5.3. Univariate regressions for each predictor variable included in the best-fit model against ΔT.

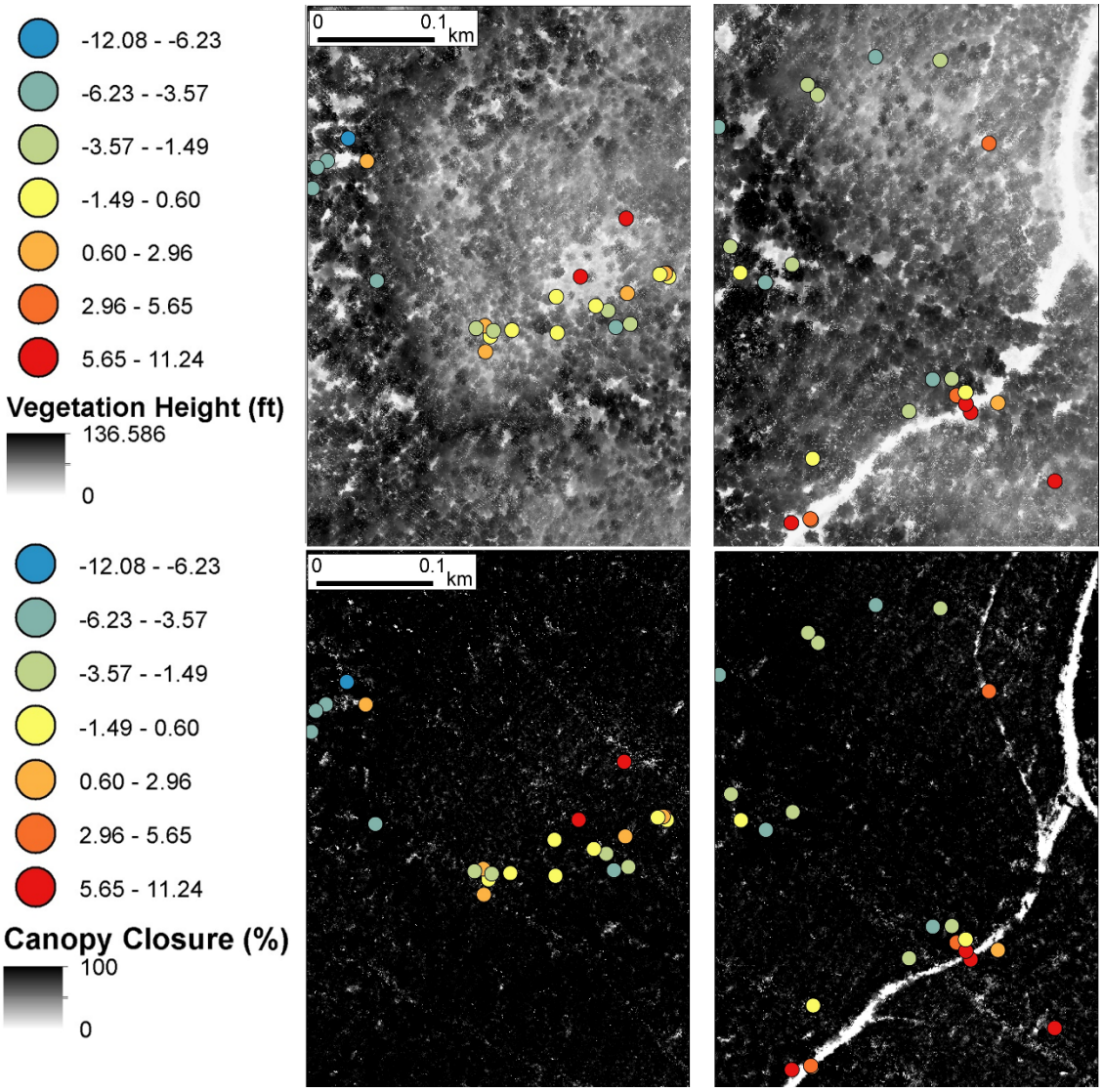

Figure 5.4. Locations of timber rattlesnakes and associated ΔT values (colored circles) superimposed over vegetation height (above) and canopy cover (below). Left, despite relatively high canopy closure, areas of low vegetation height resulting from natural processes (i.e., storms) are associated with elevated ΔT; right, anthropogenic features such as forest access and logging roads are used for basking and associated with elevated ΔT.

REFERENCES

Agha, M., Todd, B.D., Augustine, B., Lhotka, J.M., Fleckenstein, L.J., Lewis, M., Patterson, C., Stringer, J.W. and Price, S.J. 2018. Effects of gap-based silviculture on thermal biology of a terrestrial reptile. Wildlife Research 45: 72-81.

Aguilar, A., Roemer, G., Debenham, S., Binns, M., Garcelon, D., and Wayne, R. K. 2004. High MHC diversity maintained by balancing selection in an otherwise genetically monomorphic mammal. Proceedings of the National Academy of Sciences 101: 3490-3494.

Algar, A. C., Morley, K., and Boyd, D. S. 2018. Remote sensing restores predictability of ectotherm body temperature in the world's forests. Global Ecology and Biogeography 27: 1412-1425.

Alexander, D. H., Novembre, J., and Lange, K. 2009. Fast model-based estimation of ancestry in unrelated individuals. Genome Research 19: 1655–1664.

Anderson, C.D., Epperson, B.K., Fortin, M.J., Holderegger, R., James, P.M., Rosenberg, M.S., Scribner, K.T. and Spear, S. 2010. Considering spatial and temporal scale in landscape-genetic studies of gene flow. Molecular Ecology 19: 3565-3575

Anderson, C. D. 2015. Variation in male movement paths during the mating season exhibited by the Timber Rattlesnake (*Crotalus horridus*) in St. Louis County, Missouri. Herpetology Notes 8: 267-274.

Andrews, K. M., and Gibbons, J. W. 2005. How do highways influence snake movement? Behavioral responses to roads and vehicles. Copeia 2005: 772-782.

Arnold, B., Corbett-Detig, R. B., Hartl, D., and Bomblies, K. 2013. RADseq underestimates diversity and introduces genealogical biases due to nonrandom

haplotype sampling. Molecular Ecology 22:3179–3190.

Balkenhol, N., and Fortin, M. J. 2016. Basics of study design: Sampling landscape heterogeneity and genetic variation for landscape genetic studies. In: Landscape Genetics: Concepts, Methods, Applications, First Edition. John Wiley and Sons Ltd., p. 58-76.

Balkenhol, N., Cushman, S. A., Waits, L. P., and Storfer, A. 2016. Current status, future opportunities, and remaining challenges in landscape genetics. In: Landscape Genetics: Concepts, Methods, Applications, First Edition. John Wiley and Sons Ltd., p. 247-255.

Barbour, R.W. 1962. An aggregation of copperheads, Agkistrodon contortrix. Copeia 1962: 640.

Baudry J., Merriam H.G. 1988. Connectivity and connectedness: functional versus structural patterns in landscapes. In: Proceedings of the 2nd international seminar of the international association for landscape ecology: Connectivity in landscape ecology. Münster, Germany, p. 43–51.

Bernhardt, E.S., Palmer, M.A. 2011. The environmental costs of mountaintop mining valley fill operations for aquatic ecosystems of the Central Appalachians. Annals of the New York Academy of Sciences 1223: 39-57.

Bowcock, A. M., Ruiz-Linares, A., Tomfohrde, J., Minch, E., Kidd, J. R., and Cavalli-Sforza, L. L. 1994. High resolution of human evolutionary trees with polymorphic microsatellites. Nature 368: 455-457.

Braun, E.L. 1950. Deciduous forests of eastern North America. Hafner, New York, New York, USA.

Brown, W. S., Pyle, D. W., Greene, K. R., and Friedlaender, J. B. 1982. Movements and temperature relationships of timber rattlesnakes (*Crotalus horridus*) in northeastern NewYork. Journal of Herpetology 151-161.

Brown, W.S. 1993. Biology, status, and management of the timber rattlesnake (*Crotalus horridus*): a guide for conservation. SSAR Publication No. 22.

Browning, D,M,, Beaupre, S,J,, and Duncan, L. 2005. Using partitioned Mahalanobis D2 (k) to formulate a GIS-based model of timber rattlesnake hibernacula. Journal of Wildlife Management 69: 33-44.

Buehler, D.A., Welton, M.J., Beachy, T.A. 2006 Predicting cerulean warbler habitat use in the Cumberland Mountains of Tennessee. Journal of Wildlife Management 70: 1763-1769.

Bushar, L. M., Bhatt, N., Dunlop, M. C., Schocklin, C., Malloy, M. A., and Reinert, H. K. 2015. Population isolation and genetic subdivision of timber rattlesnakes (*Crotalus horridus*) in the New Jersey Pine Barrens. Herpetologica 71: 203-211.

Canty, A. 2005. Bootstrap R (S-plus) functions. Report by B. Ripley R Package, version 1.2–24.

Carter, E. T., Eads, B. C., Ravesi, M. J., and Kingsbury, B. A. 2015. Exotic invasive plants alter thermal regimes: implications for management using a case study of a native ectotherm. Functional Ecology 29: 683-693.

Carter, E. T., Ravesi, M. J., Eads, B. C., and Kingsbury, B. A. 2017. Invasive plant management creates ecological traps for snakes. Biological Invasions 19: 443-453.

Catchen, J., Hohenlohe, P. A., Bassham, S., Amores, A., and Cresko, W. A. 2013. Stacks:

an analysis tool set for population genomics. Molecular Ecology 22: 3124-3140.

Chabukdhara, M., and Singh, O. P. 2016. Coal mining in northeast India: an overview of environmental issues and treatment approaches. International Journal of Coal Science & Technology 3: 87-96.

Chamblin, H.D., Wood, P.B., Edwards, J.W. 2004. Allegheny woodrat (*Neotoma magister*) use of rock drainage channels on reclaimed mines in southern West Virginia. American Midland Naturalist. 151: 346-354.

Clark J.D., Dunn, J.E., Smith, K.G. 1993. A multivariate model of female black bear habitat use for a geographic information system. The Journal of Wildlife Management 519-526.

Clark, R.W. 2002. Diet of the timber rattlesnake, *Crotalus horridus*. Journal of Herpetology: 36: 494-499.

Clark, R. W., Brown, W. S., Stechert, R., and Zamudio, K. R. 2008. Integrating individual behaviour and landscape genetics: the population structure of timber rattlesnake hibernacula. Molecular Ecology 17: 719-730.

Clark, R. W., Brown, W. S., Stechert, R., and Zamudio, K. R. 2010. Roads, interrupted dispersal, and genetic diversity in timber rattlesnakes. Conservation Biology 24:1059-1069.

Clusella-Trullas, S., Blackburn, T. M., and Chown, S. L. 2011. Climatic predictors of temperature performance curve parameters in ectotherms imply complex responses toclimate change. The American Naturalist 177: 738-751.

Combs, M., Puckett, E.E., Richardson, J., Mims, D. and Munshi-South, J., 2018. Spatial

population genomics of the brown rat (*Rattus norvegicus*) in New York City. Molecular Ecology 27: 83-98.

Combs, M., Byers, K.A., Ghersi, B.M., Blum, M.J., Caccone, A., Costa, F., Himsworth, C.G., Richardson, J.L. and Munshi-South, J., 2018a. Urban rat races: spatial population genomics of brown rats (*Rattus norvegicus*) compared across multiple cities. Proceedings of the Royal Society B: Biological Sciences 285: 20180245.

Copeland, C. 2015. Mountaintop mining: background and current controversies. US Congressional Research Service, No. RS-21421.

Daly, C. 2006. Guidelines for assessing the suitability of spatial climate data sets. International Journal of Climatology 26: 707-721.

Danecek, P., Auton, A., Abecasis, G., Albers, C.A., Banks, E., DePristo, M.A., Handsaker, R.E., Lunter, G., Marth, G.T., Sherry, S.T. and McVean, G. 2011. The variant call format and VCFtools. Bioinformatics 27: 2156-2158.

Davies, A. B., and Asner, G. P. 2014. Advances in animal ecology from 3D-LiDAR ecosystem mapping. Trends in Ecology & Evolution 29: 681-691.

Davies, K. F., Margules, C. R., and J.F. Lawrence. 2000. Which traits of species predict population declines in experimental forest fragments? Ecology 81: 1450-1461.

De Frenne, P., Zellweger, F., Rodriguez-Sanchez, F., Scheffers, B.R., Hylander, K., Luoto, M., Vellend, M., Verheyen, K. and Lenoir, J. 2019. Global buffering of temperatures under forest canopies. Nature Ecology & Evolution, 3:744-749.

DiLeo, M. F., Row, J. R., and Lougheed, S. C. 2010. Discordant patterns of population structure for two co-distributed snake species across a fragmented Ontario landscape. Diversity and Distributions 16: 571-581.

DiLeo, M. F., Rouse, J. D., Dávila, J. A., and Lougheed, S. C. 2013. The influence of landscape on gene flow in the eastern massasauga rattlesnake (*Sistrurus c. catenatus*): insight from computer simulations. Molecular Ecology 22: 4483-4498.

Do, C., Waples, R.S., Peel, D., Macbeth, G.M., Tillett, B.J. and Ovenden, J.R. 2014. NeEstimator v2: re-implementation of software for the estimation of contemporary effective population size (Ne) from genetic data. Molecular Ecology Resources 14: 209-214.

Dobrowski, S.Z. 2011. A climatic basis for microrefugia: the influence of terrain on climate. Global Change Biology 17: 1022–35.

Drummond, M. A., and Loveland, T. R. 2010. Land-use pressure and a transition to forest-cover loss in the eastern United States. BioScience 60: 286-298.

Earl, D. A., and von Holdt, B. M. 2012. STRUCTURE HARVESTER: a website and program for visualizing STRUCTURE output and implementing the Evanno method. Conservation Genetics Resources 4: 359-361.

Eaton, D. A. R., Spriggs, E. L., Park, B., and Donoghue, M. J. 2017. Misconceptions on missing data in rad-seq phylogenetics with a deep-scale example from flowering plants. Systematic Biology 66: 399–412.

Epps, C.W. and Keyghobadi, N. 2015. Landscape genetics in a changing world: disentangling historical and contemporary influences and inferring change. Molecular Ecology 24: 6021-6040.

Ernst, C. H., and Ernst, E. M. 2003. Snakes of the United States and Canada. Smithsonian Books.

Evanno, G., Regnaut, S. and Goudet, J. 2005. Detecting the number of clusters of individuals using the software STRUCTURE: a simulation study. Molecular Ecology 14:2611-2620.

Ewers, R. M., and R.K. Didham. 2006. Confounding factors in the detection of species responses to habitat fragmentation. Biological Reviews 81: 117-142.

Fahrig, L., and Merriam, G. 1994. Conservation of fragmented populations. Conservation Biology 8: 50-59.

Fahrig, L. 2003. Effects of habitat fragmentation on biodiversity. Annual Review of Ecology, Evolution, and Systematics 34: 487-515.

François, O., and Waits, L. P. 2015. Clustering and assignment methods in landscape genetics. In: Landscape Genetics: Concepts, Methods, Applications, First Edition. John Wiley and Sons Ltd., p.114-128.

Frankham, R. 2005. Genetics and extinction. Biological Conservation 126: 131-140.

Frankham, R., Ballou, J. D., Eldridge, M. D., Lacy, R. C., Ralls, K., Dudash, M. R., and Fenster, C. B. 2011. Predicting the probability of outbreeding depression. Conservation Biology 25: 465-475.

Frankham, R., Ballou, J.D., Ralls, K., Eldridge, M., Dudash, M.R., Fenster, C.B., Lacy, R.C. and Sunnucks, P. 2017. Genetic management of fragmented animal and plant populations. Oxford University Press.

Fraser, D. J., Debes, P. V., Bernatchez, L., and Hutchings, J. A. 2014. Population size, habitat fragmentation, and the nature of adaptive variation in a stream fish. Proceedings of the Royal Society of London B: Biological Sciences 281: 20140370.

Ford, W.M., Chapman, B.R., Menzel, M.A., Odom, R.H. 2002 Stand age and habitat influences on salamanders in Appalachian cove hardwood forests. Forest Ecology and Management 155: 131-141.

Galpern, P., Manseau, M. and Wilson, P. 2012. Grains of connectivity: analysis at multiple spatial scales in landscape genetics. Molecular Ecology 21: 3996-4009.

Galpern, P., Peres-Neto, P. R., Polfus, J., and Manseau, M. 2014. MEMGENE: Spatial pattern detection in genetic distance data. Methods in Ecology and Evolution 5: 1116-1120.

Gardner-Santana, L. C., and Beaupre, S. J. 2009. Timber rattlesnakes (*Crotalus horridus*) exhibit elevated and less variable body temperatures during pregnancy. Copeia 2009: 363-368.

George, A. D., Connette, G. M., Thompson III, F. R., and Faaborg, J. 2017. Resource selection by an ectothermic predator in a dynamic thermal landscape. Ecology and Evolution 7: 9557-9566.

Gess S.W., Ellington, E.H., Dzialak, M.R., Duchampt, J.E., Lovallo, M., Larkin, J.L. 2013. Rest site selection by fishers (*Martes pennanti*) in the eastern deciduous forest. Wildlife Society Bulletin. 37: 805-814.

Gibbs, H. L., and P.J. Weatherhead. 2001. Insights into population ecology and sexual selection in snakes through the application of DNA-based genetic markers. Journal of Heredity 92:173-179.

Gilpin, M.E. and Soule´, M.E. 1986. Minimum viable populations: processes of extinction. In: Conservation Biology: The Science of Scarcity and Diversity. Sinauer Associates, p. 19–34.

González-Serna, M. J., Cordero, P. J., and Ortego, J. 2018. Using high-throughput sequencing to investigate the factors structuring genomic variation of a Mediterranean grasshopper of great conservation concern. Scientific Reports 8: 13436.

Goslee, S. C., and Urban, D. L. 2007. The ecodist package for dissimilarity-based analysis of ecological data. Journal of Statistical Software 22: 1-19.

Graf, R. F., Mathys, L., and Bollmann, K. 2009. Habitat assessment for forest dwelling species using LiDAR remote sensing: Capercaillie in the Alps. Forest Ecology and Management 257: 160-167.

Hackworth, Z., Lhotka, J., Cox, J., Barton, C., and Springer, M. 2018. First-year vitality of reforestation plantings in response to herbivore exclusion on reclaimed Appalachian surface-mined land. Forests 9: 222.

Haddad, N.M., Brudvig, L.A., Clobert, J., Davies, K.F., Gonzalez, A., Holt, R.D., Lovejoy, T.E., Sexton, J.O., Austin, M.P., Collins, C.D., and Cook, W.M. 2015. Habitat fragmentation and its lasting impact on Earth's ecosystems. Science Advances 1: e1500052.

Haering K.C., Daniels, W.L., Galbraith, J.M. 2004. Appalachian mine soil morphology and properties. Soil Science Society of America Journal 68: 1315-1325.

Hammerson G.A. 2007. *Crotalus horridus*. The IUCN Red List of Threatened Species 2007:e.T64318A12765920.ttp://dx.doi.org/10.2305/IUCN.UK.2007.RLTS.T64318A12765920.en. Downloaded on 31 January 2017.

Hamraz, H., Contreras, M. A., and Zhang, J. 2016. A robust approach for tree

segmentation in deciduous forests using small-footprint airborne LiDAR data. International Journal of Applied Earth Observation and Geoinformation. 52: 532-541.

Herrmann, H. W., Pozarowski, K. M., Ochoa, A., and Schuett, G. W. 2017. An interstate highway affects gene flow in a top reptilian predator (Crotalus atrox) of the Sonoran Desert. Conservation Genetics 18: 911-924.

Hilty, J. A., Lidicker Jr, W. Z., and Merenlender, A. 2012. Corridor ecology: the science and practice of linking landscapes for biodiversity conservation. Island Press, Washington, D.C., USA.

Hinkle, C.R., McComb, W.C., Safely, J.M. Jr, Schmalzer, P.A. 1993. Mixed mesophytic forests. Biodiversity of the Southeastern United States: Upland Terrestrial Communities. John Wiley and Sons, New York, 203-253.

Holderegger, R., and H.H. Wagner. 2008. Landscape genetics. Bioscience 58: 199-207.

Holt, R. D., Lawton, J. H., Polis, G. A., and N.D. Martinez. 1999. Trophic rank and the species-area relationship. Ecology 80: 1495-1504.

Homer C., Dewitz, J., Yang, L., Jin, S., Danielson, P., Xian, G., Coulston, J., Herold, N., Wickham, J., and K. Megown. 2015. Completion of the 2011 National Land Cover Database for the conterminous United States–representing a decade of land cover change information. Photogrammetric Engineering and Remote Sensing 81: 345-354.

Huang, H., and Knowles, L. L. 2014. Unforeseen consequences of excluding missing data from next-generation sequences: simulation study of RAD sequences. Systematic Biology 65: 357-365.

Huey, R. B., and Slatkin, M. 1976. Cost and benefits of lizard thermoregulation. The Quarterly Review of Biology 51: 363-384.

International Energy Agency (IEA). 2018. Coal 2018: Analysis and forecasts to 2023. <https://www.iea.org/coal2018/> Accessed 17 May 2019.

Jantz, S.M., Barker, B., Brooks, T.M., Chini, L.P., Huang, Q., Moore, R.M., Noel, J. and Hurtt, G.C. 2015. Future habitat loss and extinctions driven by land-use change in biodiversity hotspots under four scenarios of climate-change mitigation. Conservation Biology 29: 1122-1131.

Jenness, J. 2006. Topographic Position Index (tpi_jen.avx) extension for ArcView 3.x, v. 1.2. Jenness Enterprises. Available at: http://www.jennessent.com/arcview/tpi.htm.

Jombart, T., Devillard, S., Dufour, A. B., and Pontier, D. 2008. Revealing cryptic spatial patterns in genetic variability by a new multivariate method. Heredity 101: 92-103.

Jombart, T., Devillard, S., and Balloux, F. 2010. Discriminant analysis of principal components: a new method for the analysis of genetically structured populations. BMC Genetics 11: 94.

Jones, R. 2005. Plant life of Kentucky. The University Press of Kentucky, Lexington, KY, USA.

Kabay, E. 2013. Timber rattlesnakes may reduce incidence of Lyme disease in the northeastern United States. 98th Annual Meeting of the Ecological Society of America, 2013 Aug 4-9, Minneapolis, MN. Washington, DC: Ecological Society of America.

Keinath, D.A., Doak, D.F., Hodges, K.E., Prugh, L.R., Fagan, W., Sekercioglu, C.H., Buchart, S.H. and Kauffman, M. 2017. A global analysis of traits predicting species sensitivity to habitat fragmentation. Global Ecology and Biogeography 26: 115-127.

Keller, D., Holderegger, R., van Strien, M. J., and Bolliger, J. 2015. How to make landscape genetics beneficial for conservation management? Conservation Genetics 16: 503-512.

Kentucky Transportation Cabinet [KTC]. 2018. Historical Maps: download archived county road aid maps. <https://transportation.ky.gov/Planning/Pages/Historical-Maps.aspx> Accessed 1 January 2019.

Kentucky Transportation Cabinet [KTC]. 2019. Interactive statewide traffic counts map. <https://transportation.ky.gov/Planning/Pages/Traffic-Counts.aspx> Accessed 30 January 2019.

Keller, D., Holderegger, R., van Strien, M. J., and Bolliger, J. 2015. How to make landscape genetics beneficial for conservation management? Conservation Genetics 16: 503-512.

Kentucky Geological Survey (KGS). 2019. Kentucky coal production database. Lexington, Kentucky, USA. <https://www.uky.edu/KGS/coal/coal-ky-info-coal-production.php> Accessed 17 June 2019.

Kentucky Transportation Cabinet [KTC]. 2018. Historical Maps: download archived county road aid maps. <https://transportation.ky.gov/Planning/Pages/Historical-Maps.aspx> Accessed 1 January 2019.

Kentucky Transportation Cabinet [KTC]. 2019. Interactive statewide traffic counts map.

<https://transportation.ky.gov/Planning/Pages/Traffic-Counts.aspx> Accessed 30 January 2019.

Keyghobadi, N. 2007. The genetic implications of habitat fragmentation for animals. Canadian Journal of Zoology 85: 1049-1064.

Killick, R. and Eckley, I. 2014. changepoint: An R package for changepoint analysis. Journal of Statistical Software 58: 1-19.

Kiser J., Meade, L. 1993. A survey of small mammals in the Morehead Ranger District, Daniel Boone National Forest, Kentucky. Transactions of the Kentucky Academy of Science 54: 87-92.

Koenig, W. D., Van Vuren, D., and Hooge, P. N. 1996. Detectability, philopatry, and the distribution of dispersal distances in vertebrates. Trends in Ecology and Evolution 11: 514-517.

Kopelman, N.M., Mayzel, J., Jakobsson, M., Rosenberg, N.A. and Mayrose, I. 2015. Clumpak: a program for identifying clustering modes and packaging population structure inferences across K. Molecular Ecology Resources 15: 1179-1191.

Koskinen, M. T., Haugen, T. O., and Primmer, C. R. 2002. Contemporary fisherian life-history evolution in small salmonid populations. Nature 419: 826-830.

Krupa, J.J., Lacki, M.J. 2002. Mammals of Robinson Forest: species composition of an isolated, mixed-mesophytic forest on the Cumberland Plateau in southeastern Kentucky. Museum of Texas Tech University Bulletin No. 45.

Lande, R. 1988. Genetics and demography in biological conservation. Science 241: 1455-1460.

Landguth, E.L., Cushman, S.A., Schwartz, M.K., McKelvey, K.S., Murphy, M. and

Luikart, G. 2010. Quantifying the lag time to detect barriers in landscape genetics. Molecular Ecology 19: 4179-4191.

Landguth, E.L., Fedy, B.C., Oyler-McCance, S.J., Garey, A.L., Emel, S.L., Mumma, M., Wagner, H.H., Fortin, M.J. and Cushman, S.A. 2012. Effects of sample size, number of markers, and allelic richness on the detection of spatial genetic pattern. Molecular Ecology Resources 12: 276-284.

Larkin, J.L., Maehr, D.S., Krupa, J.J., Cox, J.J., Alexy, K., Unger, D.E., Barton, C, 2008. Small mammal response to vegetation and spoil conditions on a reclaimed surface mine in eastern Kentucky. Southeastern Naturalist. 7: 401-412.

Leaché, A.D., Banbury, B. L., Felsenstein, J., De Oca, A. N.-M., and Stamatakis, A. 2015. Short tree, long tree, right tree, wrong tree: new acquisition bias corrections for inferring snp phylogenies. Systematic Biology 64: 1032–1047.

Levine, B. A., Smith, C. F., Douglas, M. R., Davis, M. A., Schuett, G. W., Beaupre, S. J., and Douglas, M. E. 2016. Population genetics of the copperhead at its most northeastern distribution. Copeia 104: 448-457.

Lindberg, T.T., Bernhardt, E.S., Bier, R., Helton, A.M., Merola, R.B., Vengosh, A. and Di Giulio, R.T., 2011. Cumulative impacts of mountaintop mining on an Appalachian watershed. Proceedings of the National Academy of Sciences 10:.20929-20934.

Lopez-de-Lacalle, J. 2016. tsoutliers R Package for Detection of Outliers in Time Series. (https://jalobe.com/doc/tsoutliers.pdf).

Maigret, T. A., Cox, J. J., Schneider, D. R., Barton, C. D., Price, S. J., and Larkin, J. L.

2014. Effects of timber harvest within streamside management zones on salamander populations in ephemeral streams of southeastern Kentucky. Forest Ecology and Management 324: 46-51.

Maigret, T.A., and J.J. Cox. 2018. Agkistrodon contortrix: Hibernacula. Herpetological Review 49:123.

Maigret, T.A. 2019. Snake scale clips as a source of high-quality DNA suitable for RAD sequencing. Conservation Genetics Resources: in press.

Maigret, T.A., Cox, J.J., and J. Yang. 2019. Persistent geophysical effects of mining threaten ridgetop biota of Appalachian forests. Frontiers in Ecology and the Environment 17: 85-91.

Manel, S., Schwartz, M. K., Luikart, G., and Taberlet, P. 2003. Landscape genetics: combining landscape ecology and population genetics. Trends in Ecology and Evolution, 18: 189-197.

Manel, S., and Holderegger, R. 2013. Ten years of landscape genetics. Trends in Ecology and Evolution 28: 614-621.

McCartney-Melstad, E., Vu, J. K., and Shaffer, H. B. 2018. Genomic data recover previously undetectable fragmentation effects in an endangered amphibian. Molecular Ecology 27: 4430-4443.

McEwan, R.W., Muller, R.N. 2011. Dynamics, diversity, and resource gradient relationships in the herbaceous layer of an old-growth Appalachian forest. Plant Ecology 212: 1179–1191.

Meirmans, P. G. 2015. Seven common mistakes in population genetics and how to avoid them. Molecular Ecology 24: 3223-3231.

Milanesi, P., Holderegger, R., Bollmann, K., Gugerli, F., and Zellweger, F. 2017. Three-dimensional habitat structure and landscape genetics: a step forward in estimating functional connectivity. Ecology 98: 393-402.

Muller, R.N. 2003. Landscape patterns of change in coarse woody debris accumulation in an old- growth deciduous forest on the Cumberland Plateau, southeastern Kentucky. Canadian Journal of Forest Research 33: 763–769.

Muller, R.N. 1982. Vegetation patterns in the mixed mesophytic forest of eastern Kentucky. Ecology 63: 1901-1917.

Muncy, B.L., Price, S. J., Bonner, S. J., and Barton, C. D. 2014. Mountaintop removal mining reduces stream salamander occupancy and richness in southeastern Kentucky (USA). Biological Conservation, 180, 115-121.

Murphy, M. O., Jones, K. S., Price, S. J., and Weisrock, D. W. 2018. A genomic assessment of population structure and gene flow in an aquatic salamander identifies the roles of spatial scale, barriers, and river architecture. Freshwater Biology 63: 407-419.

Nazareno, A. G., Bemmels, J. B., Dick, C. W., and Lohmann, L. G. 2017. Minimum sample sizes for population genomics: An empirical study from an Amazonian plant species. Molecular Ecology Resources 17: 1136-1147.

Neumann, W., Martinuzzi, S., Estes, A. B., Pidgeon, A. M., Dettki, H., Ericsson, G., and Radeloff, V. C. 2015. Opportunities for the application of advanced remotely-sensed data in ecological studies of terrestrial animal movement. Movement Ecology 3: 8-21.

Newell, F.L., Rodewald, A.D. 2011. Role of topography, canopy structure, and floristics

in nest-site selection and nesting success of canopy songbirds. Forest Ecology and Management 262: 739-749.

Nomura, T. 2008. Estimation of effective number of breeders from molecular coancestry of single cohort sample. Evolutionary Applications 1: 462-474.

Normile, D. 2018. Bucking global trends, Japan again embraces coal power. Science 360: 476-477.

Oliphant, A.J., Wynne, R.H., Zipper, C.E., Ford, W.M., Donovan, P.F., Li, J. 2017. Autumn olive (*Elaeagnus umbellata*) presence and proliferation on former surface coal mines in Eastern USA. Biological Invasions 19: 179-195.

O'Leary, S. J., Puritz, J. B., Willis, S. C., Hollenbeck, C. M., and Portnoy, D. S. 2018. These aren't the loci you're looking for: principles of effective SNP filtering for molecular ecologists. Molecular Ecology 27: 3193-3206.

(OSM) US Office of Surface Mining. 2000. Postmining land use: exceptions to approximate original contour requirements for mountaintop removal operations and steep slope mining operations. https://www.osmre.gov/lrg/docs/mtpmlureport.pdf Viewed 16 March 2018

Overstreet, J.C. 1984. Robinson forest inventory: 1980-1982. University of Kentucky, College of Agriculture, Department of Forestry, Lexington, KY.

Oyler, J. W., Ballantyne, A., Jencso, K., Sweet, M., and Running, S. W. 2015. Creating a topoclimatic daily air temperature dataset for the conterminous United States using homogenized station data and remotely sensed land skin temperature. International Journal of Climatology 35: 2258-2279.

Paaijmans, K. P., Heinig, R. L., Seliga, R. A., Blanford, J. I., Blanford, S., Murdock, C.

C., and Thomas, M. B. 2013. Temperature variation makes ectotherms more sensitive to climate change. Global Change Biology 19: 2373-2380.

Palmer, M.A., Bernhardt, E.S., Schlesinger, W.H., Eshleman, K.N., Foufoula-Georgiou, E., Hendryx, M.S., Lemly, A.D., Likens, G.E., Loucks, O.L., Power, M.E. and White, P.S. 2010. Mountaintop mining consequences. Science, 327(5962), pp.148-149.

Pericak, A.A., Thomas, C.J., Kroodsma, D.A., Wasson, M.F., Ross, M.R., Clinton, N.E., Campagna, D.J., Franklin, Y., Bernhardt, E.S. and Amos, J.F. 2018. Mapping the yearly extent of surface coal mining in Central Appalachia using Landsat and Google Earth Engine. PloS one 13: e0197758.

Peterson, B. K., Weber, J. N., Kay, E. H., Fisher, H. S., and Hoekstra, H. E. 2012. Double digest RADseq: an inexpensive method for de novo SNP discovery and genotyping in model and non-model species. PloS one 7: e37135.

Peterman, W. E., and Semlitsch, R. D. 2009. Efficacy of riparian buffers in mitigating local population declines and the effects of even-aged timber harvest on larval salamanders. Forest Ecology and Management 257: 8-14.

Peterman, W. E. 2018. ResistanceGA: An R package for the optimization of resistance surfaces using genetic algorithms. Methods in Ecology and Evolution 9: 1638-1647.

Petkova, D., Novembre, J., and Stephens, M. 2016. Visualizing spatial population structure with estimated effective migration surfaces. Nature Genetics 48: 94-100.

Pond, G. J., Passmore, M. E., Borsuk, F. A., Reynolds, L., and Rose, C. J. 2008.

Downstream effects of mountaintop coal mining: comparing biological conditions using family-and genus-level macroinvertebrate bioassessment tools. Journal of the North American Benthological Society. 27: 717-737.

Porter J.H., Hanson P.C., and Lin C.C. 2012. Staying afloat in the sensor data deluge. Trends in Ecology and Evolution 27:121–129

Potter, K. A., Arthur Woods, H., and Pincebourde, S. 2013. Microclimatic challenges in global change biology. Global Change Biology 19: 2932-2939.

Pritchard, J. K., Stephens, M., and Donnelly, P. 2000. Inference of population structure using multilocus genotype data. Genetics 155: 945-959.

Pritchard, J.K., Wen, X., and Falush, D. 2007. Documentation for Structure software, Version 2.2. <https://web.stanford.edu/group/pritchardlab/software/structure22/readme.pdf> Accessed 21 November 2019.

Purcell, S., Neale, B., Todd-Brown, K., Thomas, L., Ferreira, M.A., Bender, D., Maller, J., Sklar, P., De Bakker, P.I., Daly, M.J. and Sham, P.C. 2007. PLINK: a tool set for whole-genome association and population-based linkage analyses. The American Journal of Human Genetics 81: 559-575.

Reed, D.H. and Frankham, R., 2001. How closely correlated are molecular and quantitative measures of genetic variation? A meta-analysis. Evolution 55: 1095-1103.

Reinert H.K., Cundall, D. 1982. An improved surgical implantation method for radio-tracking snakes. Copeia, 1982: 702-705.

Reinert, H. K., and Zappalorti, R. T. 1988. Field observation of the association of adult

and neonatal timber rattlesnakes, *Crotalus horridus*, with possible evidence for conspecific trailing. Copeia 1988: 1057-1059.

Reinert, H.K. 1993. Habitat selection in snakes. In R. A. Seigel and J. T. Collins (eds.), Snakes: Ecology and Behavior, pp. 201-240. McGraw-Hill, New York.

Reinert, H. K., MacGregor, G. A., Esch, M., Bushar, L. M., and Zappalorti, R. T. 2011. Foraging ecology of timber rattlesnakes, *Crotalus horridus*. Copeia 2011: 430-442.

Reinert, H. K., Munroe, W. F., Brennan, C. E., Rach, M. N., Pelesky, S., and Bushar, L. M. 2011a. Response of timber rattlesnakes to commercial logging operations. The Journal of Wildlife Management 75: 19-29.

Rice, A. N., Roberts IV, T. L., and Dorcas, M. E. 2006. Heating and cooling rates of eastern diamondback rattlesnakes, *Crotalus adamanteus*. Journal of Thermal Biology 31: 501-505.

Richardson, J. L., Brady, S. P., Wang, I. J., and Spear, S. F. 2016. Navigating the pitfalls and promise of landscape genetics. Molecular Ecology 25: 849-863.

Richardson, J.L., Burak, M.K., Hernandez, C., Shirvell, J.M., Mariani, C., Carvalho-Pereira, T.S., Pertile, A.C., Panti-May, J.A., Pedra, G.G., Serrano, S. and Taylor, J. 2017. Using fine-scale spatial genetics of Norway rats to improve control efforts and reduce leptospirosis risk in urban slum environments. Evolutionary Applications 10: 323-337.

Ricketts, T.H. 1999. Terrestrial ecoregions of North America: a conservation assessment. Island Press.

Ross, M.R., McGlynn, B.L., Bernhardt, E.S. 2016. Deep impact: Effects of mountaintop

mining on surface topography, bedrock structure, and downstream waters. Environmental Science and Technology 50: 2064-2074.

Row, J. R., Blouin-Demers, G., and Weatherhead, P. J. 2007. Demographic effects of road mortality in black ratsnakes (*Elaphe obsoleta*). Biological Conservation 137: 117-124.

Scheffers, B. R., Edwards, D. P., Diesmos, A., Williams, S. E., and Evans, T. A. 2014. Microhabitats reduce animal's exposure to climate extremes. Global Change Biology 20: 495-503.

Schou, M. F., Loeschcke, V., Bechsgaard, J., Schlötterer, C., and Kristensen, T. N. 2017. Unexpected high genetic diversity in small populations suggests maintenance by associative overdominance. Molecular Ecology 26: 6510-6523.

Segelbacher, G., Cushman, S. A., Epperson, B. K., Fortin, M. J., Francois, O., Hardy, O. J., Holderegger, R., Taberlet, P., Waits, L. P. and S. Manel. 2010. Applications of landscape genetics in conservation biology: concepts and challenges. Conservation Genetics 11: 375-385.

Shepard, D. B., Dreslik, M. J., Jellen, B. C., and Phillips, C. A. 2008. Reptile road mortality around an oasis in the Illinois corn desert with emphasis on the endangered eastern massasauga. Copeia 2008: 350-359.

Short Bull, R.A., Cushman, S.A., Mace, R., Chilton, T., Kendall, K.C., Landguth, E.L., Schwartz, M.K., McKelvey, K., Allendorf, F.W. and Luikart, G. 2011. Why replication is important in landscape genetics: American black bear in the Rocky Mountains. Molecular Ecology 20: 1092-1107.

Sillero, N., and Goncalves-Seco, L. 2014. Spatial structure analysis of a reptile

community with airborne LiDAR data. International Journal of Geographical Information Science 28: 1709-1722.

Simberloff, D., Farr, J. A., Cox, J., and Mehlman, D. W. 1992. Movement corridors: conservation bargains or poor investments? Conservation Biology 6: 493-504.

Simmons, J.A., Currie, W.S., Eshleman, K.N., Kuers, K., Monteleone, S., Negley, T.L., Pohlad B.R., and C.L.Thomas 2008. Forest to reclaimed mine land use change leads to altered ecosystem structure and function. Ecological Applications 18: 104-118.

Simonson, W. D., Allen, H. D., and Coomes, D. A. 2014. Applications of airborne lidar for the assessment of animal species diversity. Methods in Ecology and Evolution 5: 719-729.

Sinervo, B., Mendez-De-La-Cruz, F., Miles, D.B., Heulin, B., Bastiaans, E., Villagrán-Santa Cruz, M., Lara-Resendiz, R., Martínez-Méndez, N., Calderón-Espinosa, M.L., Meza-Lázaro, R.N. and Gadsden, H. 2010. Erosion of lizard diversity by climate change and altered thermal niches. Science 328: 894-899.

Soulé, M. E. 1987. Viable populations for conservation. Cambridge University Press.

Spielman, D., Brook, B. W., and R. Frankham. 2004. Most species are not driven to extinction before genetic factors impact them. Proceedings of the National Academy of Sciences of the United States of America 101: 15261-15264.

Staats, W.A. 2015. Use of LiDAR-derived terrain and vegetation information in a deciduous forest in Kentucky. M.S. Thesis, University of Kentucky, Lexington, KY, USA.

Steen, D.A., McClure, C.J., Sutton, W.B., Rudolph, D.C., Pierce, J.B., Lee, J.R., Smith,

L.L., Gregory, B.B., Baxley, D.L., Stevenson, D.J. and Guyer, C. 2014. Copperheads are common when kingsnakes are not: relationships between the abundances of a predator and one of their prey. Herpetologica 70: 69-76.

Stevenson, R. D. 1985. The relative importance of behavioral and physiological adjustments controlling body temperature in terrestrial ectotherms. The American Naturalist 126: 362-386.

Suggitt, A. J., Gillingham, P. K., Hill, J. K., Huntley, B., Kunin, W. E., Roy, D. B., and Thomas, C. D. 2011. Habitat microclimates drive fine-scale variation in extreme temperatures. Oikos 120: 1-8.

Sunday, J. M., Bates, A. E., Kearney, M. R., Colwell, R. K., Dulvy, N. K., Longino, J. T., and Huey, R. B. 2014. Thermal-safety margins and the necessity of thermoregulatory behavior across latitude and elevation. Proceedings of the National Academy of Sciences 111: 5610-5615.

Sutton, W. B., Wang, Y., and Schweitzer, C. J. 2013. Amphibian and reptile responses to thinning and prescribed burning in mixed pine-hardwood forests of northwestern Alabama, USA. Forest Ecology and Management 295: 213-227.

Sutton, W. B., Wang, Y., Schweitzer, C. J., and McClure, C. J. 2017. Spatial ecology and multi-scale habitat selection of the Copperhead (*Agkistrodon contortrix*) in a managed forest landscape. Forest Ecology and Management 391: 469-481.

Tan, D.J., Chattopadhyay, B., Garg, K.M., Cros, E., Ericson, P.G., Irestedt, M. and Rheindt, F.E. 2018. Novel genome and genome-wide SNPs reveal early fragmentation effects in an edge-tolerant songbird population across an urbanized tropical metropolis. Scientific Reports 8: 12804.

Tongia, R., and Gross, S. 2019. Coal in India: Adjusting to transition. Brookings Institution, Washington, D.C., USA.

Trombulak, S. C., and Frissell, C. A. 2000. Review of ecological effects of roads on terrestrial and aquatic communities. Conservation Biology 14: 18-30.

US Energy Information Administration. 2015. Annual coal report: 2015. Washington, D.C., USA.

US Energy Information Administration (US EIA). 2019. Total energy reports . Washington, DC, USA. <https://www.eia.gov/totalenergy/> Accessed 17 June 2019.

US Environmental Protection Agency. 2005. Final Programmatic Environmental Impact Statement (PEIS) on Mountaintop Mining/Valley Fills in Appalachia (EPA 9-03-R-05002). https://www.epa.gov/sc-mining/programmatic-environmental-impact-statement-eis-mountaintop-miningvalley-fill-appalachia. Viewed 3 January 2018.

US Environmental Protection Agency. 2009. Memorandum of Understanding Among the U.S. Department of the Army, U.S. Department of the Interior, and EPA Implementing the Interagency Action Plan on Appalachian Surface Coal Mining. US Environmental Protection Agency, Washington, D.C., USA. (https://www.epa.gov/sc-mining/june-2009-memorandum-understanding-among-army-department-interior-and-epa-implementing)

US Environmental Protection Agency. 2011. Improving EPA Review of Appalachian Surface Coal Mining Operations Under the Clean Water Act, National Environmental Policy Act, and the Environmental Justice Executive Order. US

Environmental Protection Agency, Washington, D.C., USA. (https://www.epa.gov/sc-mining/july-2011-memorandum-improving-epa-review-appalachian-surface-coal-mining-operations-under)

van Etten, J.V. 2017. R package gdistance: distances and routes on geographical grids. Available: https://cgspace.cgiar.org/handle/10568/83180. Accessed 1 September 2018.

Vierling, K.T., Vierling, L.A., Gould, W.A., Martinuzzi, S. and Clawges, R.M. 2008. Lidar: shedding new light on habitat characterization and modeling. Frontiers in Ecology and the Environment 6:.90-98.

Vogelmann, J.E., Howard, S.M., Larson, C,R., Wylie, B.K., and Van Driel, N. 2001. Completion of the 1990s national land cover data set for the conterminous United States from Landsat Thematic Mapper data and ancillary data sources. Photogrammetric Engineering and Remote Sensing 67:650–662.

Whittaker, R.H. 1956. Vegetation of the Great Smoky Mountains. Ecological Monographs 26:1-80.

Wagner, C.E., Keller, I., Wittwer, S., Selz, O.M., Mwaiko, S., Greuter, L., Sivasundar, A. and Seehausen, O. 2013. Genome-wide RAD sequence data provide unprecedented resolution of species boundaries and relationships in the Lake Victoria cichlid adaptive radiation. Molecular Ecology 22: 787-798.

Waits, L. P., Cushman, S. A., and Spear, S. F. 2016. Applications of landscape genetics to connectivity research in terrestrial animals. In: Landscape Genetics: Concepts, Methods, Applications, First Edition. John Wiley and Sons Ltd., p. 199-219.

Weiss, A. 2001. Topographic positions and landforms analysis. ESRI International

User Conference, San Diego, CA. (http://www.jennessent.com/downloads/tpi-poster-tnc_18x22.pdf)

Weyer, J., Jørgensen, D., Schmitt, T., Maxwell, T. J., and Anderson, C. D. 2014. Lack of detectable genetic differentiation between den populations of the Prairie Rattlesnake (*Crotalus viridis*) in a fragmented landscape. Canadian Journal of Zoology 92: 837-846.

Whittaker, R.H. 1956. Vegetation of the Great Smoky Mountains. Ecological Monographs 26:1-80.

Wickham, J. D., Riitters, K. H., Wade, T. G., Coan, M., and C. Homer 2007. The effect of Appalachian mountaintop mining on interior forest. Landscape Ecology 22: 179-187.

Wickham J., Wood, P.B., Nicholson, M,C., Jenkins, W., Druckenbrod, D., Suter, G.W., Mazzarella, C., Gallow, W., Amos, J. 2013. The overlooked terrestrial impacts of mountaintop mining. BioScience 63: 335-348.

Wilcove, D. S., Rothstein, D., Dubow, J., Phillips, A., and Losos, E. 1998. Quantifying threats to imperiled species in the United States. BioScience 48: 607-615.

Willi, Y., Van Buskirk, J., and Hoffmann, A. A. 2006. Limits to the adaptive potential of small populations. Annual Review of Ecology, Evolution, and Systematics 37: 433-458.

Willing, E. M., Dreyer, C., and Van Oosterhout, C. 2012. Estimates of genetic differentiation measured by FST do not necessarily require large sample sizes when using many SNP markers. PloS one 7:e42649.

Witt, E.L. 2012. Evaluating streamside management zone effectiveness in forested

watersheds of the Cumberland Plateau. Ph.D. Thesis, University of Kentucky, Lexington, KY, USA.

Wittenberg, R. D. 2012. Foraging ecology of the timber rattlesnake (*Crotalus horridus*) in a fragmented agricultural landscape. Herpetological Conservation and Biology 7: 449-461.

Wood, P.B., Bosworth, S.B., Dettmers, R. 2006. Cerulean warbler abundance and occurrence relative to large-scale edge and habitat characteristics. Condor 108: 154–165.

Wood, P.B., Williams, J.M. 2013. Terrestrial salamander abundance on reclaimed mountaintop removal mines. Wildlife Society Bulletin 37: 815-823.

Wood, P.B., Larkin, J., Mizel, J., Zipper, C., Angel, P. 2017. Reforestation to enhance Appalachian mined lands as habitat for terrestrial wildlife. US Office of Surface Mining, Appalachian Regional Reforestation Initiative, Forest Reclamation Advisory Number 10

Yang, X.J., Lin, A., Li, X.L., Wu, Y., Zhou, W., Chen, Z. 2013. China's ion-adsorption rare earth resources, mining consequences and preservation. Environmental Development 8: 131-136.

Yu, L., Xu, Y., Xue, Y., Li, X., Cheng, Y., Liu, X., Porwal, A., Holden, E.J., Yang, J. and Gong, P., 2018. Monitoring surface mining belts using multiple remote sensing datasets: A global perspective. Ore Geology Reviews 101: 675-687.

Zeng, X., Liu, Z., He, C., Ma, Q., and J. Wu. 2018. Quantifying surface coal-mining patterns to promote regional sustainability in Ordos, Inner Mongolia. Sustainability 10: 1135.

Zipper, C.E., Burger, J.A., Skousen, J.G., Angel, P.N., Barton, C.D., Davis, V., Franklin, J.A. 2011.Restoring forests and associated ecosystem services on Appalachian coal surface mines. Environmental Management 47: 751-765.

VITA

Thomas Arthur Maigret

Education

B.S., Conservation Biology, 2011, SUNY College of Environmental Science and Forestry
M.S., Forestry, 2013, University of Kentucky, Department of Forestry

Publications

Maigret, T.A., Cox, J.J., and D.W. Weisrock. 2020. A spatial genomic approach identifies time lags and historic barriers to gene flow in a rapidly fragmenting Appalachian landscape. Molecular Ecology 29: 673-685.

Maigret, T.A., Cox, J.J., and J. Yang. 2019. Persistent geophysical effects of mining threaten ridgetop biota of Appalachian forests. Frontiers in Ecology and the Environment 17: 85-91 (cover article).

Maigret, T.A. 2019. Snake scale clips as a source of high quality DNA suitable for RAD sequencing. Conservation Genetics Resources 11: 373-375.

Spaulding, S.H., Cox, J.J., **Maigret, T.A.**, Drayer, A.N., Richards, J.M., and J. Treanor. 2018. Low-level Batrachochytrium dendrobatidis detection persists in plethodontid salamanders following timber harvests in Kentucky, USA. Herpetological Review 49: 258-262.

Dillard, J.R., and **T.A. Maigret**. 2017. Delayed dispersal and prolonged brood care in a family-living beetle. Journal of Evolutionary Biology 30: 2230-2243.

Murphy, M.O., Agha, M., **Maigret, T.A.**, M.E. Dorcas, and S.J. Price. 2016. The effects of urbanization on body size of larval stream salamanders. Urban Ecosystems 18: 1-12.

Maigret, T.A., Cox, J.J., Schneider, D.R., Barton, C.D., Price, S.J., and J.L. Larkin. 2014. Effects of timber harvest within streamside management zones on salamander populations in ephemeral streams of southeastern Kentucky. Forest Ecology and Management 324:46-51.

Recognition

2017 Tracy Farmer Institute for Sustainability, Appalachian Research Award, $300
2017 UK Appalachian Center Eller and Billings Research Award, $1,000
2015 Kerri Casner Environmental Sciences Fellowship, $2,550
2015 American Museum of Natural History Theodore Roosevelt Memorial Grant, $3,500
2014 Association of Southeast Biologists, Brooks/Cole Cengage Learning Student Research Award in Aquatic Biology, $200
2013 University of Kentucky, Department of Forestry, Graduate Student Excellence Award, $250
2012 KY Chapter of The Wildlife Society, Outstanding Student Paper Award, $150